What Cause an Enzyme to degrade during biocatalysis?

A thesis submitted to University College London

For the degree of
DOCTOR OF PHILOSOPHY

By

Phattaraporn Morris

The Advanced Centre for Biochemical Engineering
Department of Biochemical Engineering
University College London
Torrington Place
London
WC1E 7JE

2011

Abstract

Biocatalysis continues to be a powerful tool for the efficient synthesis of optically pure pharmaceuticals that are difficult to access via conventional chemistry. The efficient application of biocatalysis requires the availability of suitable enzymes with high activity and stability under process conditions. However, the borderline stability of biocatalysts in many types of reaction media has often prevented or delayed their implementation for industrial-scale syntheses of fine chemicals and pharmaceuticals. Consequently, there is great interest in understanding the effects of solution conditions on protein stability, as well as in developing strategies to improve enzyme stability and activity in desired reaction media. The enzyme transketolase (TK; E.C. 2.2.1.1) from *Escherichia coli* is an important biocatalyst in stereo-specific carbon-carbon bond synethesis. The power of transketolase is further augmented when the bioconversion takes place in a multi-step biotransformation in which transketolase and transaminases are employed in series to create chiral amino alcohols from achiral substrates. These compounds are synthetically very useful in the production of a range of compounds with pharmaceutical application.

Although many useful reactions have been reported for TK, many of the substrates and products are unstable or insoluble at the pH or temperature range for which the enzyme has optimum activity in aqueous media. Understanding the activity and structural stability of transketolase under bioprocess conditions will

improve our capacity to comprehend and ultimately to engineer it to make it work at a broader range of pHs and temperatures, and also in the presence of organic co-solvents. This will potentially help to reduce process development times and also increase the stability and solubility of substrates and products.

To provide further insight into the underlying causes of TK deactivation in process conditions, the effects of temperature, pH and organic solvents on the structure, stability, aggregation and activity of *Escherichia coli* transketolase were characterized in Chapters 3 and 4. The results provided useful information for the engineering of TK enzymes with improved thermostability or extreme pH tolerance and in organic solvent mixtures. For thermostability and tolerance to low pH, mutations may be usefully targeted towards regions of protein sequence predicted to have a high propensity for aggregation. For the retention of biocatalytic activity at high pH or temperatures, stabilisation of the cofactor binding loops were found to be an attractive target. By contrast, the results in aqueous-solvent mixtures instead implied that the solvent dependence of catalytic activity cannot be simply explained by only one mechanism such as active-site binding or the replacement of water molecules, and that the effect of different solvents on protein structure penetration, denaturation and aggregation must also be considered.

In the final Chapter, mutagenesis was targeted to the cofactor binding loops to further evaluate their impact on thermal stability. one mutant was found that successfully improved the stability of *E. coli* transketolase at elevated temperatures, giving a 3 fold specific activity increase at 60 ^{o}C compared to wild-type TK.

Acknowledgements

To all those people who have assisted me in the course of my PhD, thank you. In particular I would like to thank my supervisor Dr Paul Dalby whom gave me extensive advice and support throughout my period at UCL, namely when this project went through a difficult period. He always remained confident in my work and in a positive outcome. In our regular meetings there were often new insights to guide me onto the next steps. His comments were very valuable for me.

I also would like to thank all those people within the Deapartment of Biochemical Engineering at UCL who help me during my research. Particulary, I would like to thank, Andrea, Adriana, Raha, Maria, Panwajee, CJ, Dawid, Amana and Murni, has made get to this point a decidedly and more pleasant and joyful journey. A big thank you for the past student, especially in Foster Court group who gave me advices and motivation-Julio, Subhas, Sandro and Micheal.

The big thank you for Leo and Homam, my best friends. There were an outstanding source of motivation, support and friendship and of lots and lots of help in all experimental issues faced, a constant presence at late hours and weekends. Thank you, Leo who inspires me for travelling, collaborative, and learns more about the culture and the history. Thank you Homam who always support me sad or happy. You always with me.

A very big and special thank you goes to my family, for their support, love and believing in me.

.

In particular, I recognise that this research would not have been possible without the financial assistance of Royal Thai Government Scholarships fund, and express my gratitude to this agency.

I, Phattaraporn Morris, declare that the dissertation, submitted in partial fulfilment of the requirements for the degree of Doctorate of Philosophy represents my own work and has not been previously submitted to this or any other institution for any degree, diploma or other qualification.

Signature_____

Content

Lists of Figures

List of Tables

Abbreviations

Ala	Alanine
AcCN	Acetonitrile
Amp+	ampicilin resistance
Apo-TK	Apo-transketolase
Arg	arginine
Asn	asparagine
Asp	aspartic acid
CD	Circular dichroism
Cys	cysteine
ddH2O	d destilate H2O
DLS	dynamic light scattering
DNA	deoxyribonucleic acid
dNTP	deoxynucleotide A/C/G/T triphosphate
DTT	dithiothreitol
EC	Enzyme commision
EDTA	ethylenediaminetetraacetic acid
EtoAc	ethyl acetate
GA	glycoaldehyde
Gln	glutamine
Glu	glutamic acid
Gly	Glycine
HCL	hydrochloric acid

His	histidine
Holo-TK	Holo-transketolase
HPA	hydroxypyruvate
HPLC	high performance liquid chromatography
Ile	isoleucine
iPrOH	Isopropanol
Leu	Leucine
Li	Lithium
Lys	lysine
Met	methionine
Mg	magnesium
$MgCl_2$	magnesium chloride
MRE	mean residue ellipticity
MW	molecular weights
NaCl	Sodium chloride
nBuOH	*n*-butanol
NaOH	Sodium hydroxide
NCBI	National Center for Biotechnology Information
Ni	Nickel
NTA	nitrilotriacetic acid
PCR	polymerase chain reaction
PDB	proteine data bank
Phe	phenylalanine
PP	pyrophosphate-binding domain
Pro	Proline

Pyr	pyridinium-binding domain
QCM	QuickChange™ Site-Directed Mutagenesis System
r	Pearson's correlation coefficient
SDS	Sodium dodecyl sulfate
SDS PAGE	sodium dodecyl sulfate polyacrylamide gel electrophoresis
Ser	serine
Taq	Thermos Aquaticus
TBE	Tris/Borate/EDTA
TPSA	Topical Polar Surface
TFA	trifluoroacetic acid
THF	tetrahydrofuran
Thr	threonine
TK	transketolase
TPP	thiamine pyrophosphate
Tris	hydroxymethylaminomethane
Trp	tryptophan
Tyr	tyrosine
Val	valine
wt	wild-type

Chapter 1

1. Introduction

1.1 Biocatalysis

Biocatalysis has increased becoming a major tool in the industrial application synthesis such as main chemicals, agrochemical intermediates, pharmaceuticals, and food ingredients. (Morris et al., 1996; Schmid et al., 2001, Zaks, 2001, Nestl et al., 2011). For example, lipases have been exploited in many biotechnology applications, including for the manufacture of pharmaceuticals and pesticides, single cell protein production, biosensor preparation and in waste management (Torossian et al., 1991, Gandhi, 1997; Saxena et al 1999). This success has been mainly due to their ability to utilize a variety of substrates, while exhibiting high stability towards extremes of temperature, pH and organic solvents, and significant chemo-, regio- and enantioselectivity.

While enzymes have been the major focus of biocatalysis research (Walsh, 2001), All research in lysate , purified enzymes or whole cell biocatalysts have shown their extraordinary catalytic potential. (Matsuyama et al., 2002; Schoemaker et al., 2003;Ishige et al., 2005; Pollard and Woodley, 2006; Nestl et al., 2011,) . Enzymes can often accept different verities of complex molecules as substrates, and are typically very selective, catalyzing reactions with incomparable both chiral (enantio-) and positional (regio-) selectivities. As a result, biocatalysts can be used in both simple and complex transformations in enantio- and regioselective chemical

syntheses, as well as providing a clean processing alternative to organic synthesis (Schmid et al., 2001).

The application of biocatalysis has been extended by research that has focussed on understanding their potential in terms of activity and stability, and also by successfully improving their ability using directed evolution (Liebeton et al., 2000, Nakagawa et al., 2007). Understanding the potential advantages of biocatalysts, relative to many chemical catalysts, in terms of their specificity, structure, and activity under mild or extreme conditions, as well as their biodegradability, is important for advancement (Polastro, 1989). This is particularly useful for identifying the factors that currently limit the number and diversity of biocatalytic applications, such as limited enzyme availability, substrate scope, and operational stability. In the past 10 years, the rapid growth of biocatalysis is a direct result of research and development in enzyme engineering technologies, including molecular evolution and associated high-throughput screening methods (Aucamp et al., 2005, Dalby, 2007; Hibbert et al., 2008)

Figure1-1 shows the development programme for a typical biocatalytic process. It is important in industry to identify and develop a biocatalytic process that is economically feasible. The development of such a process therefore requires the input of many different specialists. To improve the economic efficiency of a biocatalytic process, it is important to characterise the biocatalyst in terms of its activity and structure in relevant bioprocess conditions, to inform enzyme and process engineers who can then implement an appropriate strategy for improvement. An additional requirement for the development of a successful biocatalytic process is

to obtain a good knowledge base for process design in terms of biocatalyst performance under a range of conditions that might benefit for example the stability or solubility of reactants or products. A major disadvantage of biocatalysts from natural sources is that they often operate in aqueous media under moderate conditions *in vivo*, and therefore they are not usually tolerant to extreme conditions of pH or temperature, or in the presence of organic solvents.

The increasing interest and rapid growth in terms of apply using enzymes in industrial processes has urged the research into their characterisation and the exploration of a wider range of biocatalysts. A particularly interesting biocatalytic conversion is the formation of C-C bonds, such as that catalysed by transketolase (TK), which has been utilized in various asymmetric carbon-carbon bond synthesis reactions *in vitro* (Woodley et al., 1996). TK has an important potential role in industrial applications (Turner, 2000), particularly for the asymmetric synthesis of complex multifunctional molecules such as sugar molecules and their analogues (Brocklebank et al., 1999). In the Department of Biochemical engineering at University College London, a significant body of previous work has characterised transketolase for the development and optimisation of a biocatalytic process, improved its activity and substrate range by directed evolution, and coupled it to the transaminase (TAm) enzyme *in vitro* and *in vivo* for the synthesis of high value chiral compounds such as amino-alcohols (Rios-Solis et al., 2011), as described in more detail below. In this thesis the stability and activity of TK under biocatalytic process conditions of extreme pH, temperature and organic solvents, is characterised

in detail to inform process and enzyme engineering strategies that aim to improve biocatalytic process performance and efficiency.

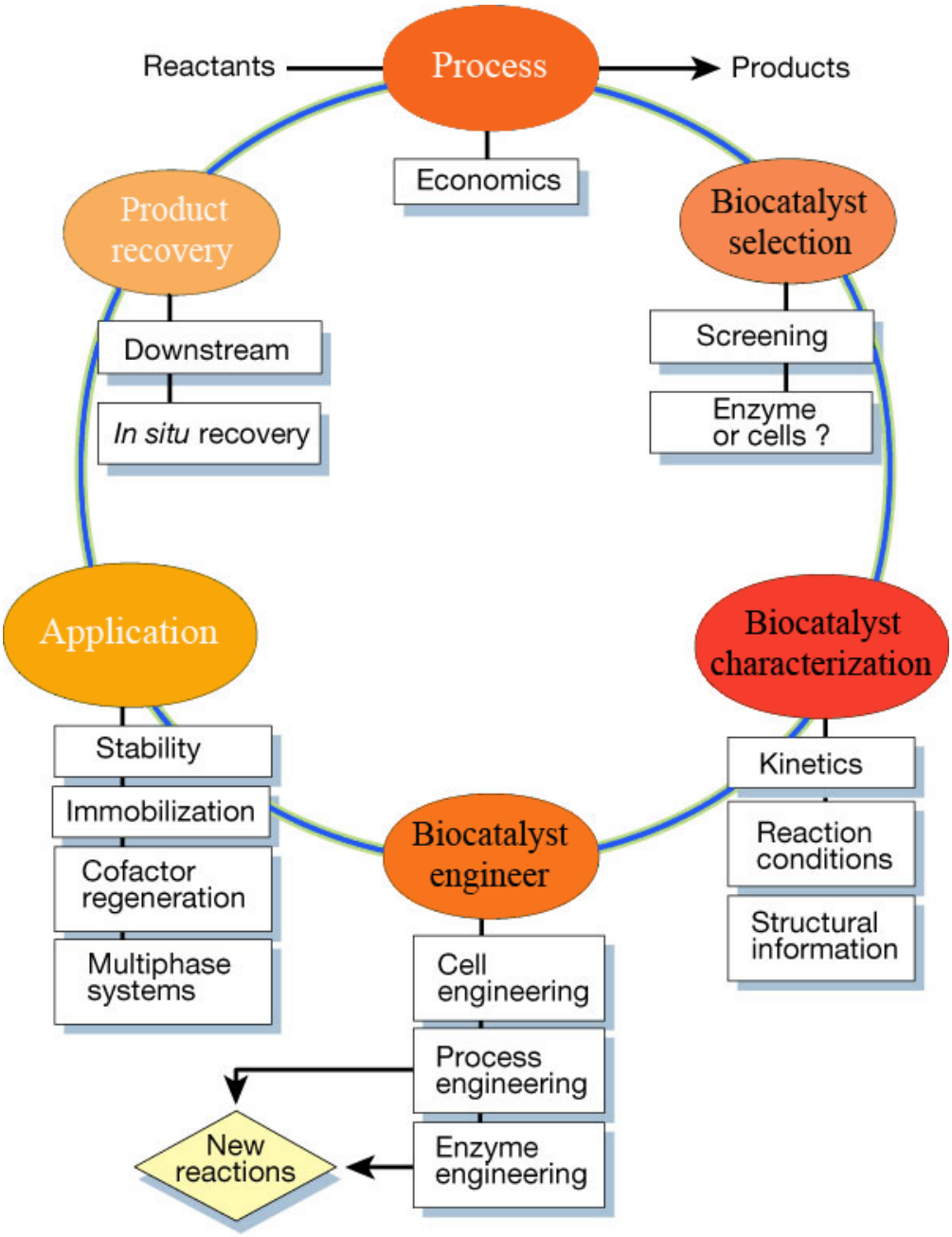

Figure 1-1 Biocatalysis development cycle. (Adapted from Schmid et, al 2001).

1.2 Enzyme stability

Naturally most of the enzymes which are normally used in the industry are not suited in many industrial application conditions due to their loss of stability during the operation of a process. The poor stability of enzymes in many types of reaction media has often prevented or delayed their implementation for industrial-scale synthesis of fine chemicals and pharmaceuticals (Brocklebank et al., 1999). However, using enzymes at more extreme, non-physiological conditions is often desirable and beneficial such as the use of high process temperature or organic solvents that increase substrate and product solubility, and process speed, and decrease the likelihood of microbial contamination (Dordick, 1991)

Temperature, pH, Oxidative stress, the presence of solvents, chemical inactivation, and the binding of metal ions or co-factors are the factors that has an effect on enzyme stability. However, there is great outcome in understanding the effects of solution conditions in enzyme stability, as well as in expand the strategies of directed evolution that improve their stability in desired reaction media (Aucamp et al., 2005; Eijsink et al., 2005; Hibbert et al., 2007; Martinez-Torres et al., 2007; Jahromi et al., 2011).

1.2.1 pH stability

pH is one of the most important factors in the stability of enzymes. The point where the enzyme is most active is known as the optimum pH. However, the optimum is not the same for each enzyme, as with activity, for each enzyme there is also a region of pH optimal stability. Extremely high or low pH values generally

result in complete loss of activity for most enzymes (D'Souza et al., 1987; Jahromi et al., 2011). The pH of the environment of an enzyme may affect the activity of an enzyme in one or more of several possible ways. Consequently, it is of importance to know the effect of pH upon both enzyme activity and structure to elucidate the mechanism(s) by which pH affects enzyme stability for each specific case. Changes in pH may not only affect the structure, conformation and ionisation of an enzyme, but it may also change the structure or charge state of the substrate so that either the substrate cannot bind to the active site or it cannot undergo catalysis.

In the physiological range, pH primarily affects the state of ionization of acidic (Asp, Glu) or basic (Lys, Arg, His) side chains in enzymes, as well as the N- and C-termini. Acidic amino acids have carboxyl functional groups in their side chains, whereas some basic amino acids have amine functional groups in their side chains. At more extreme pH values, eg. <pH 5 or >pH 9, additional side chains can become ionised, such as by the deprotonation of serine OH, cysteine SH or tyrosine OH at high pH. At low pH, the mainchain amides can also become protonated.

Ionization of residues that are directly involved in catalysis can have an immediate impact upon activity by slowing down the rate of critical proton transfers in general acid and general base catalysis (Illanes, 2008). These events are the most common explanation for the classical "bell shaped" pH profile for the activity of enzymes. The addition or removal of charges can also affect the binding affinity and productive orientation of substrates. If the state of ionization of amino acids in a protein is altered then the surrounding bonds and non-covalent interactions that

contribute to the overall secondary and tertiary structure of the protein can also be altered. This can lead to altered protein recognition or enzyme inactivation due to structural disruption (Schaefer et al., 1997). Understanding the effects of pH on enzyme stability, in terms of mechanism of deactivation in biocatalysis, has received little attention. However, the directed evolution of improved pH tolerance and pH-optima for activity has received considerable recent attention (Richardson et al., 2002; Boer and Koivula., 2003; Jahromi et al; 2011), and the results of such work can potentially provide more detail to understand the stability of enzymes in extreme pH conditions.

1.2.2 Solvent stability

Many advantages has been found by using the organic solvents as media for biocatalytic reactions either in terms of the fundamental or practical areas, and also increasing in synthetic organic chemistry (Arnold et al., 1990; Dordick, 1991; Gupta et al., 1992 Klibanov, 1997). The use of enzymes in organic solvents has been reviewed several times (Butler, 1979, Lilly and Woodley, 1985 Klibanov, 1997). It is well known that the catalytic activity of enzymes in organic solvents is typically far lower than in water (Kibanov, 1997). Information on enzyme stability in organic solvents has appeared in many articles, although it has seldom been the main issue in the past. Most of the work in organic solvents has been previously carried out using Lipase (Zaks and Klibanov, 1985), α-Chymotrypsin (Dong et al., 1996, Li et al. 2010) and Subtilisin Carsberg (Pasta et al., 1988). Catalytic activity is chosen as the main tool for testing enzyme stability in organic solvent. However, structural conformation and the aggregation state of the biocatalytic system provide additional methods for the

analysis of enzyme stability in organic solvent systems. As there has been no previous study of the use of TK enzymes in the presence of organic solvent, it has been explored in this thesis in terms of their impact upon catalytic activity, structure, stability and aggregation.

1.2.3 Thermal stability

A past few years many of works on protein stability are focusing on the improvement of the stability at elevated temperatures. At high temperatures many of the enzymes loss their ability to perform the reaction by losing of their activity which can be cause from not in the optimum temperature condition and also can be explain as become all or partly unfolding. This could relate to the intrinsic stability of the enzymes to thermal unfolding (Danson et al., 1996; Daniel et al., 2001; Peterson et al., 2004). It is often assumed that enzymes with improved thermal stability also become more tolerance to other denaturing factors, such as organic co-solvents (Wang et al., 2000). However, this correlation is still unclear, especially not when it comes to denaturation processes which do not, or only marginally, depend on global folding stability.

The activity and structure of *E. coli* transketolase at elevated temperatures has been studied recently and part of this work was carried out and describe in this thesis (Jahromi et al., 2011). The study shows that moderately elevated temperatures initially promoted the partial disordering of secondary structure, and subsequent re-annealing or cofactor activation upon re-cooling, to form a more active native holo-TK state. Whether the partial denaturation is also an obligate pre-cursor to

aggregation remains unclear. However, these results provided useful information for the potential engineering of TK enzymes with improved thermostability. Further study of wild-type and mutant transketolases for thermostability has been carried out in this present work to provide important additional insights and to increase the stability of the enzyme at elevated temperatures.

1.3 Transketolase (TK) as a biocatalyst.

Transketolase (TK; E.C.2.2.1.1) is a homodimeric enzyme and has served as a model system to study the involvement of the cofactor thiamine diphosphate (TPP) in enzymatic catalysis (Littlechild et al, 1995; Nikkola et al, 1994). There are many natural sources of TK and the first purified TK was from the yeast *Saccharomyces cerevisiae* (de la Haba et al., 1955). Subsequently TK has been isolated from other sources such as rat liver (Horecker et al., 1956), spinach (Horecker et al., 1956), pig liver (Simpson, 1960), the bacterium *Lactobacillus pentosus* (Racker, 1961), the fungus *Torula sp.* (Racker, 1961), rabbit liver (Racker, 1961), the yeast *Saccharomyces carlsbergensis* (Racker, 1961), the bacterium *Alcaligenes faecalis* (Domagk and Horecker, 1965), the yeast *Candida utilis* (Kiely et al., 1969), human erythrocytes (Heinrich and Wiss, 1971), mouse brain (Blass et al., 1982), wheat (Murphy and Walker, 1982), human leukocytes (Mocali and Paoletti, 1989), and the bacterium *Escherichia coli* (Sprenger, 1991). Most of the recent work on TK in the Department of Biochemical Engineering, at University College London has been

carried out using *Escherichia coli* TK (Aucamp et al 2005; Martinez-Torres et al., 2007; Hibbert et al., 2007; Jahromi et al., 2011).

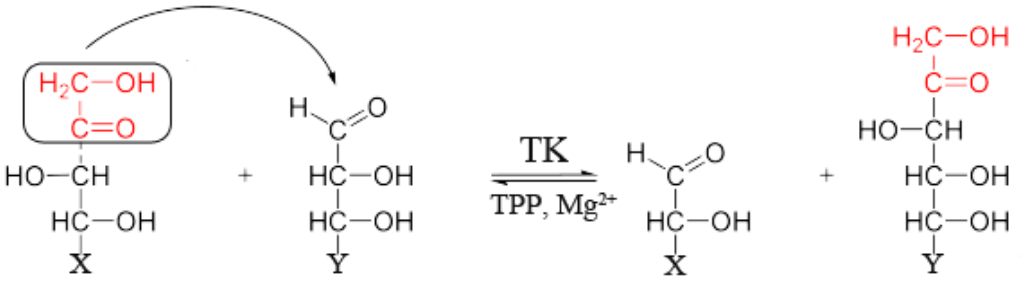

Figure 1-2. Scheme of the transketolase reaction show in Fischer projection. A 1,2-dihydroxyethyl group is transferred between a ketose (red carbon skeleton) to an aldose. X and Y are variable (R groups).

TK catalyses the stereoselective transfer of a two-carbon ketol donor group to an aldose acceptor sugar (Figure 1-2) producing a new asymmetric carbon-carbon bond (Daltta and Racker, 1961). This makes the enzyme attractive for the biocatalytic synthesis of complex carbohydrates and their analogues (Hecquet et al., 1994; Hecquet et al., 1996, Liqvist et al, 1992). *In vitro*, TK can accept a wide range of substrates (Table 1-1) such as xylulose 5-phosphate, fructose 6-phosphate, sedoheptulose 7-phosphate, hydroxypyruvate (HPA), as the donor substrate, and ribose 5-phosphate, erythrose 4-phosphate, glyceraldehydes 3-phosphate, glyceraldehyde (GA), as the acceptor substrate. The TK reaction is reversible, though

the donor substrate of choice is hydroxypyruvate, due to the release of CO_2 which renders the process irreversible, and therefore more attractive for industrial biocatalysis (Datta and Racker, 1961; Schenk et al., 1998; Kochetov, 2001).

Substrate		**Product**	**Reference**
Donor	**Acceptor**		
β-HPA	Glycolaldehyde	L-Erythrulose	Bolte et al., 1987
[2,3-$^{13}C_2$]hydroxy-pyruvate	D-Glyceraldehyde	D-[1,2-$^{13}C_2$]xylulose	Demuynck et al., 1990
β-HPA	D/L- 3-hydroxy-4-oxobutyronitrile	2-Deoxy-L-threo-5-hexulosonitrile	Effenberger and Null, 1992
β-HPA	D-Ribose	D-Sedoheptulose	Dalmas and Demuynck, 1993
β-HPA	4-Deoxy-L-threose	6-Deoxy-L-sorbose	Hecquet et al., 1996
L-Erythrulose	2-Deoxy-D-erythrose-4-phosphate	4-Deoxy-D-fructose-6-phosphate	Guérard et al., 1999
Xylulose-5-phosphate	D-[5-^{14}C, 5-^{3}H] ribose-5-phosphate	[7-^{14}C, 7-^{3}H]sedo heptulose-7-phosphate	Lee et al., 1999
β-HPA	D-Glyceraldehyde-3-phosphate	D-Xylulose-5-phosphate	Zimmermann et al., 1999
β-HPA	3-*O*-benzyl-glyceraldehyde	5-*O*-benzyl-D-xylulose	Humphrey et al., 2000

Table 1-1 A selection of fine chemicals and drug precursors that have been synthesised using transketolases.

1.3.1 Transketolase structure

According to X-ray studies of *S. cerevisae* (Nikkola et al., 1994) and *E. coli* (Littlechild et al., 1995) transketolases, TK is homodimeric with each subunit of the dimeric transketolase molecule consisting of three domains: pyrophosphate-binding (PP-domain; residues 3-322), pyridinium-binding (Pyr domain; residues 323-538), and the C-terminal domain (residues 539-680) (Figure 1-3). Two molecules of TPP and a bivalent metal-ion (Ca^{2+} or Mg^{2+}) cofactor bind in two identical deep clefts located between the PP-domains of one subunit and the Pyr-domains of the other, to form the active holoenzyme. This binding is completely inaccessible from solvent, except for the thiazolium ring of TPP which is presented at the base of each active site. In contrast to the PP-domain and Pyr domain, the biological function of the C-terminal domain is still unclear (Schneider and Lindqvist, 1992) because this domain is not involved in the active dimer formation or in TPP binding. Truncation of the C-terminal domain also did not loss to significant loss of activity, although purificaiton of a stable enzyme became difficult (Costelloe al., 2008).

Comparative structural studies of yeast apo-TK and holo-TK showed that the conformation of the cofactor binding loops 187-198 and 384-394 were different, in that they were disordered in the apo-TK (Sundstrom et al., 1992). These two loops interact with one another and with TPP in holo-TK to form the active center in which the loops become more ordered (Nikkola et al., 1994). The enzyme requires both divalent magnesium ions and thiamine diphosphate for activity.

The molecular properties of the enzyme from baker's yeast have been studied in significant detail (Kochetov and Philippov, 1969). Its amino acid sequence, some functional groups of the apo-protein and the coenzyme, as well as the enzyme's crystal structure and organization of its active site, are already known. Some progress has been made towards the understanding of the mechanism of TK, particularly from studies which combine NMR with the use of TPP analogues (Tittmann et al., 2003). However, the existence of any mechanism of regulation of the enzyme's catalytic activity remains unclear.

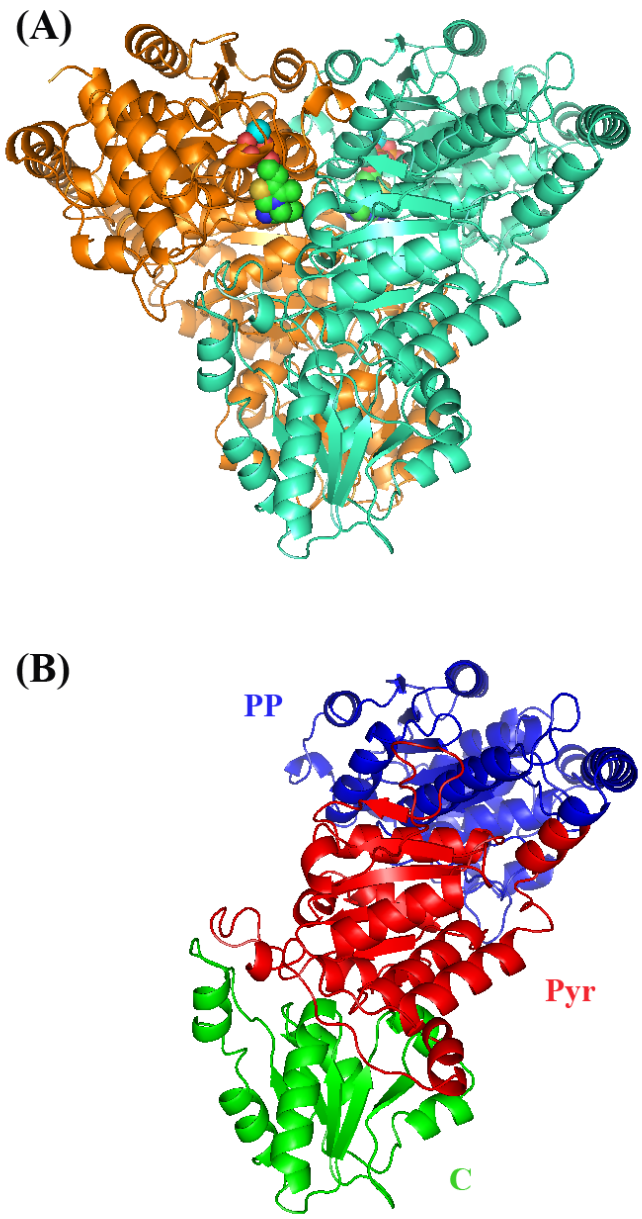

Figure1-3. (A) Structure and (B) Subunit domains *E. Coli* transketolase obtain from 1qgd.pdb (Littlechild et al, 1995), a subunit are shaded differently from top to bottom **PP-domain**, **Pyr-domain**, and **C-terminal**. Ribbon structure showing the subunit arrangement in the dimeric holoenzyme; for the active site, the two TPP cofactors is highlight as CPK sphere and the metal ion cofactor is highlight as a cyan spheres. PDB file was obtained from 1qgd.pdb (Littlechild et al., 1995). Figure generated with Pymol (DeLano, W.L. (2002), The PyMOL Molecular Graphics System on World Wide Web http://www.pymol.org).

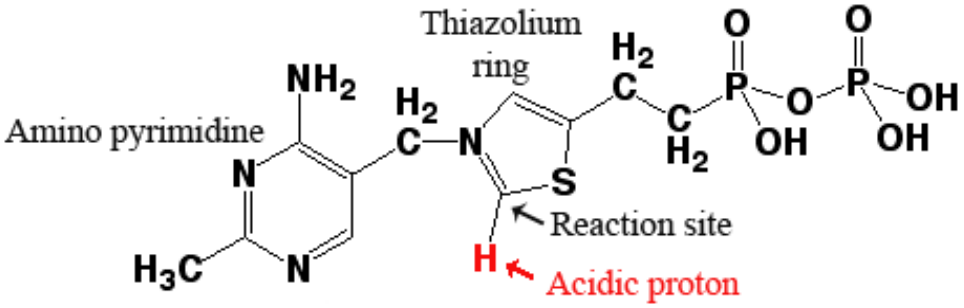

Figure 1-4. Chemical structure of thiamin pyrophosphate (TPP). The aminopyrimidine ring is linked via a methylene bridge to the thiazolium ring. The reaction center of TPP is Carbon 2 of the thiazole moiety, and its acidic proton (red).

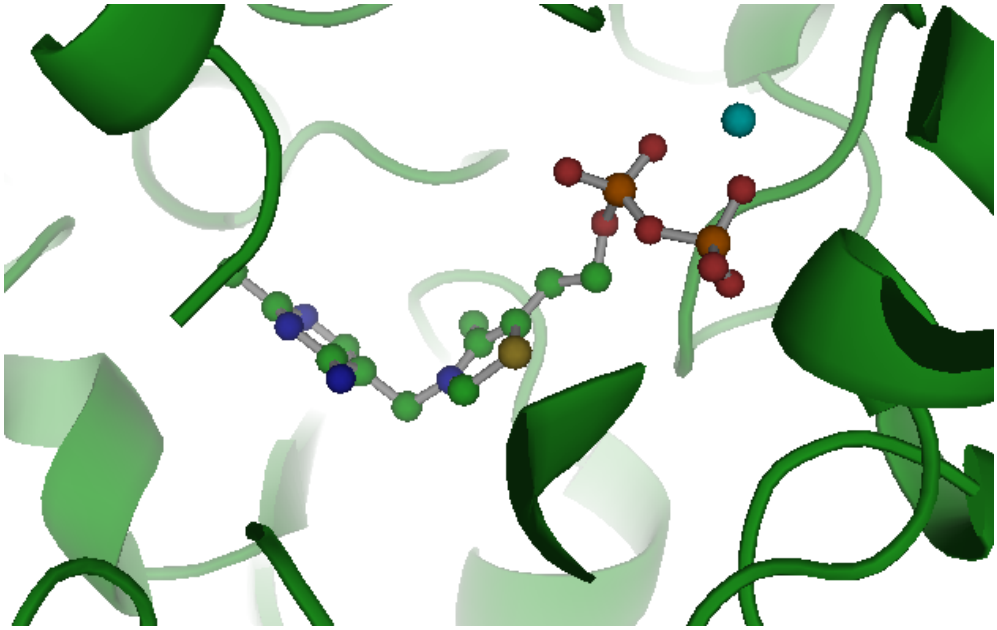

Figure 1-5 The structures of TPP has shown in a "V conformation" which provides a direct contact between the amino group of the pyrimidine ring and the C^2-H bond of the thiazolium ring. The metal ion cofactor is highlight as a cyan spheres. Figure generated with Pymol (DeLano, W.L. (2002), The PyMOL Molecular Graphics System on World Wide Web http://www.pymol.org).

1.3.2 TPP binding of TK

A major biologically active form of thiamine is thiamine pyrophosphate (TPP), sometimes called thiamine diphosphate (ThDP). In thiamine pyrophosphate the hydroxyl group of thiamine is replaced by a diphosphate ester group (Figure1-4). TPP binds to transketolase through several interactions. Its diphosphate group is bound at the switchpoint between neighbouring strands 1 and 3 at the amino-terminus of a small α-helix in the PP-domain of one subunit (Figure1-3). Firstly, there are direct interactions through hydrogen bonds to His69, His263, and Gly158 (His66, His261, and Gly156 in *E. coli*). Secondly, there are indirect interactions through the divalent metal ion bound to the phosphate groups in TPP.

The reactive site of TPP is in the thiazolium ring, for which the C-2 proton is unusually acidic due to stabilisation of the resulting negative charge as an Ylide. This site is set in the cleft between the PP-domain of one subunit and the Pyr-domain of the second subunit, while the rest of the thiazolium interacts hydrophobically with residues from both subunits. The conserved aspartate residue Asp382 (Asp381 in *E. coli*) is probably involved in compensating for and hence stabilising the positive charge of the thiazolium ring. The pyrimidine ring of TPP binds in a hydrophobic pocket, formed by residues from the Pyr-domain of the second subunit. The pocket is made up of a number of aromatic side chains belonging to Phe442, Phe445, and Tyr448 (Phe434, Phe437, and Tyr440 in *E. coli*). A hydrogen bond between the N1' atom of the pyrimidine ring and the side chain of a conserved glutamate residue (Glu418 in *S. cerevisiae* and Glu411 in *E. coli*) is significant since it is observed in all TPP-dependent enzymes.

TPP binds at the interface between subunits and interacts with residues from both subunits (Kovina et al, 2002). The comparison of the 3 D structures of some thiamine diphosphate holoenzymes has shown that the enzyme-bound TPP has a so called “V conformation” (Figure 1-5) which provides a direct hydrogen bond contact between the amino group of the pyrimidine ring and the C2 proton of the thiazolium ring. Since both subunits are involved in active site formation the dimer may be considered as a catalytically competent unit.

1.3.3 TK in industry application

Transketolase has been utilized in various asymmetric carbon-carbon bond synthesis reactions *in vitro* (Woodley et al., 1996), displaying an important role in many potential industrial applications (Turner, 2000). The enzyme has also been used commercially for the synthesis of xylulose 5-phosphate (Shaeri et al., 2006). Moreover, there is currently great interest in the use of biocatalysis for preparing flavour and fragrance components because of the desire to produce 'natural' molecules that can command a premium price as food additives. TK from spinach (Villafranca and Axelrod, 1971) has been employed in a chemo-enzymatic synthesis of 6-deoxy-L-sorbose, which is a known precursor of furaneol, a compound with caramel-like flavour, this compound has been found as an important industrial aromatic product used in the food industry (Schenk et al., 1998; Turner, 2000).

The power of transketolase is augmented when the bioconversion takes place in a multi-step biotransformation within a single whole cell that contains a *de-novo* pathway (Figure 1-6). TK catalyses the asymmetric carbon-carbon bond formation,

and then transaminase (TAm) catalyses the enantioselective amination of the resulting ketone group. The combined utilisation of TK+ TAm can be illustrated in the production of a single diastereoisomer of 2-amino-1, 3, 4-butanetriol (ABT). In this two step synthesis L-erythrulose is irreversibly produced by TK from the achiral substrates glycolaldehyde (GA) and β-hydroxypyruvate (β-HPA). TAm is then used to convert the L-erythrulose into ABT using an amine donor such as L-methylbenzylamine. The original 2-step process gave an overall yield of 21% (Ingram et al., 2007) whereby the biocatalysis could take place within the whole cell, or within the cell lysate. Amino diols are excellent synthons for many pharmaceuticals syntheses, so for this reason, TK+TAm bioconversions are of consequence, and using TK mutants and an alternative transaminase, the yield for ABT was significantly increased (Rios-Solis et al., 2011)

Methods applied to facilitate the use of transketolase include scale up procedures (Woodley et al., 1996), improvement of enzyme stability such as by immobilisation to a support matrix (Broklebank et al., 1999), and the improvement of activity by directed evolution (Dalby, 2007; Hibbert et al., 2007). Despite the progress made to date, studies aimed at further understanding the stability of TK, have the potential to guide modifications that improve enzyme function during biocatalysis, and hence would have significant benefit for various enzymatic syntheses using TK.

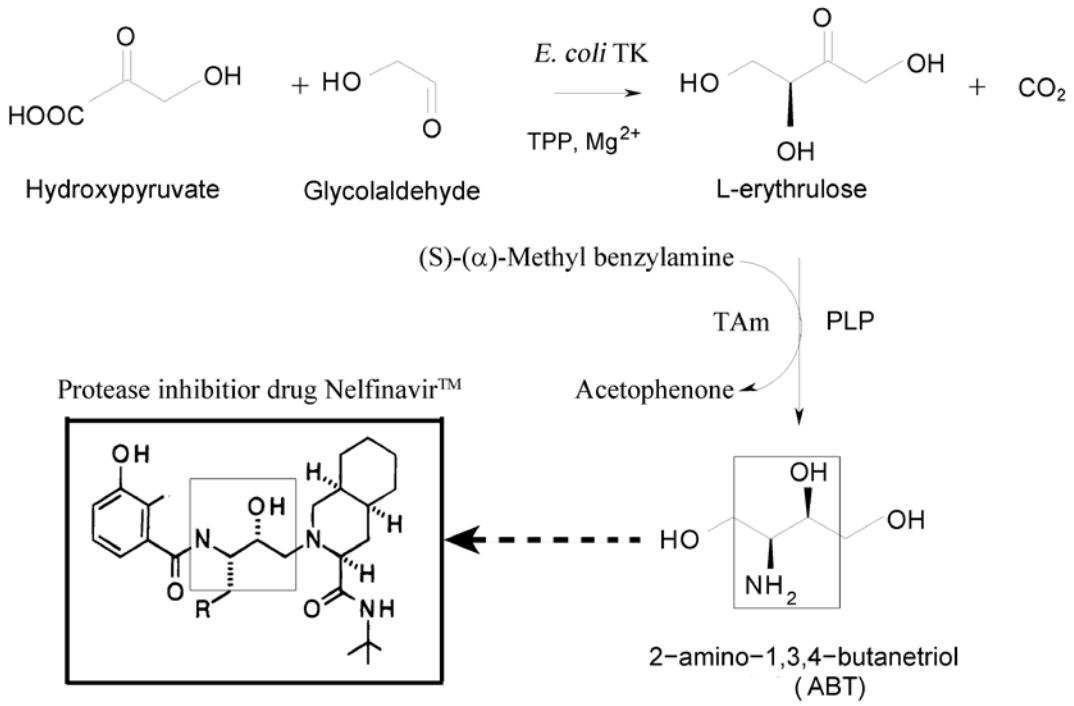

Figure1-6. TK+TAm enzymatic pathway to produce 2-amino- 1, 3, 4-butanetriol (ABT, also referred to as EAT). TK produced L-erythrulose as a precursor substrate for TAm.

1.3.4 Gradual deactivation of *E. coli* TK during biocatalytic processes

E. coli TK was found to be denatured at equilibrium by urea under reducing conditions at pH 7.5 (Martinez-Torres et al, 2007). Also it was found that transketolase is susceptible to superoxide damage in a superoxide dimutase (SOD) deficient strain (Benov and Fridovich, 1999). The inactivation of transketolase by superoxide is believed to occur through oxidation of the enamine intermediate, 1,2-dihydroxyethyl thiamine pyrophosphate. This occurs in the presence of both O_2^- and a donor substrate such as X5P or HPA. However, neither urea nor the presence of superoxide species are expected to be present in biocatalytic reactions with TK.

It was reported previously that TK from *E. coli*, covalently linked to a support matrix, undergoes inactivation when stored in the presence of air as opposed to storage under nitrogen (Brocklebank et al., 1999). Although the authors suggested that an active site cysteine may be responsible, this has not been confirmed. It has also been suggested that *E. coli* TK in both apo- and holo- form, is susceptible to inactivation by the oxidation of essential amino acid residues involved in catalysis (Mitra et al, 1998).

The stability of an enzyme is affected by many factors, such as temperature, pH, oxidative stress, and the presence of organic solvents. *E. coli* TK is gradually deactivated during prolonged biocatalytic processes. Previous studies have highlighted oxidation (Brocklebank et al., 1999), deactivation by aldehyde substrates (Bong et al., 1997), irreversible denaturation at pH values below 6.5 (Mitra et al., 1998; Jahromi et al., 2011), and the loss of TPP cofactor (Mitra et al.,1998) as

potential causes for deactivation of TK during biocatalysis. However, none of these mechanisms have been confirmed by biophysical analysis of the resulting protein. In this thesis, the effect of pH, and organic co-solvents upon the stability, catalytic activity, protein structure and aggregation of *E. coli* TK has been investigated using biophysical analysis methods. Mutants of TK based upon the sequence of TK from the thermostable organism *Thermus thermophilus* were also designed and examined for their impact upon stability and activity at elevated temperatures.

Chapter 2

2. Materials and Methods

2.1 General notes

All chemicals were obtained from Sigma–Aldrich UK unless otherwise stated.

2.2 Media, buffers and reagents preparation

2.2.1 Luria Bertani (LB) media

All the fermentations were performed using a LB medium. LB media was prepared by dissolving, 10 g/L NaCl, 10g/L tryptone and 5g/L yeast extract in Deionised H_2O. Media pH was adjusted to 7.0 with 1.0 M NaOH. The medium was then sterilised by autoclaving.

2.2.2 LB-Ampicillin Agar

LB agar was prepared by adding 15 $g{\cdot}L^{-1}$ select agar to LB medium. The agar preparation was then autoclaved. Autoclaved LB agar was allowed cooled to approximately 55 ^{o}C and ampicillin was used at a final concentration of 150 µg mL^{-1}. Approximate 15-20 ml LB agar were poured into each standard- sized petri dishes and allowed to set. The remainder of the ampicillin stock was stored at -20 ^{o}C.

2.2.3 Ampicillin

Ampicillin was dissolved in pure water to a concentration of 150 g L^{-1}. Stocks were sterilized by filtration passing slowly through a 0.2 µm filter (Fisher Scientific, UK) and aseptically aliquoted in previously sterilized 1.5 ml Eppendorfs and stored at -20 °C. Ampicillin was used at a final concentration of 150 µg mL^{-1} and added to either LB medium or LB agar before it was set to select bacteria carrying the plasmid pQR791.

2.2.4 50 mM and 25 mM Tris HCL buffer (pH 7.0)

50 mM and 25 mM Tris (hydroxymethylaminomethane) buffers with a pH of 7.0 were prepared by dissolving 7.88 or 3.94 mg mL^{-1} in RO water. The pH was adjusted to pH 7.0 by adding a small volume of concentrated solutions of either sodium hydroxide or hydrochloric acid.

2.2.5 Standard transketolase cofactor solution

Standard cofactor solutions were prepared on the day by dissolving 2.5 mg mL^{-1} (27 mM) of $MgCl_2$ and 3.3 mg mL^{-1} (7.2 mM) TPP in 50 mM Tris-buffer, pH 7.0. The pH was adjusted back to pH 7.0 by adding a small volume of concentrated solutions of either sodium hydroxide or hydrochloric acid.

2.2.6 Standard transketolase substrate solution

Standard substrate solution was prepared on the day by dissolving 16.5 mg mL^{-1} (50 mM) of Li-HPA and 9.0 mg mL^{-1} (50 mM) of GA in 50 mM Tris-

buffer, pH 7.0. The pH was adjusted back to pH 7.0 by adding a small volume of concentrated solutions of either sodium hydroxide or hydrochloric acid.

2.2.7 Standard *E. coli* Transketolase reaction

0.1 mg mL^{-1} (1.38 µM) of pure enzyme was mixed with 100 µL of standard cofactor solution (section 2.2.5) by pipetting it up and down in a 96 microwell plate, and incubating for 30 minutes to allow full reconstitution of holo-TK from apo-TK. The reaction was started by adding 100 µL of substrate solution (section 2.2.6). Aliquots of 20 µl were taken at various time intervals and quenched with 180 µL of a 0.2% v/v trifluoroacetic acid (TFA) solution. The concentration of erythrulose reaction product in this quenched sample was determined by HPLC (section 2.2.8). Reactions were performed at 21 °C and pH 7.0 unless otherwise stated. The initial rate of the reactions were calculated by SigmaPlot programme using the equation of the exponential rise to maximum $y = a\ 1\text{-}e^{-bx}$ (y = product concentration and x = time point) to allow the full conversion of the reaction to be fitted. Then the linear regression y = ax+b were then fitted to the graph and calculate for the initial rate in the range of the product and time that fit to the linear regression.

2.2.8 HPLC method to estimate L-Erythrulose concentration

This method was developed by Christine Ingram (Department of Biochemical Engineering, UCL). 10 µL samples of reactions (section 2.2.7) were analysed by HPLC (Dionex, CA, USA) with UV detection at 210 nm. Samples were injected onto a 300 mm Aminex HPX387H ion-exchange column (Bio-Rad Laboratories) and maintained at 60 °C using a LC30 chromatography oven (Dionex

Corp.) for a 16 min high accuracy measurement. The components Li-HPA (substrate) and L-erythrulose (product), were resolved with a 0.1% (v/v) TFA mobile phase at a flow rate of 0.6 mL min^{-1}.

2.2.9 Retention time and calibration curve

The retention times of Li-HPA and L-erythrulose products were 8.5 and 11.5 minutes respectively. The progress of the reaction was followed by the appearance of L-erythrulose product, the peak area of which was used in subsequent analysis. Standard curve of 1.5–45 mM of L-erythrulose in the same conditions reaction was used to obtain the L-erythrulose concentrations. Figure 2-1 below illustrates the standard calibration curve of L-erythrulose using HPLC method (section 2.2.8).

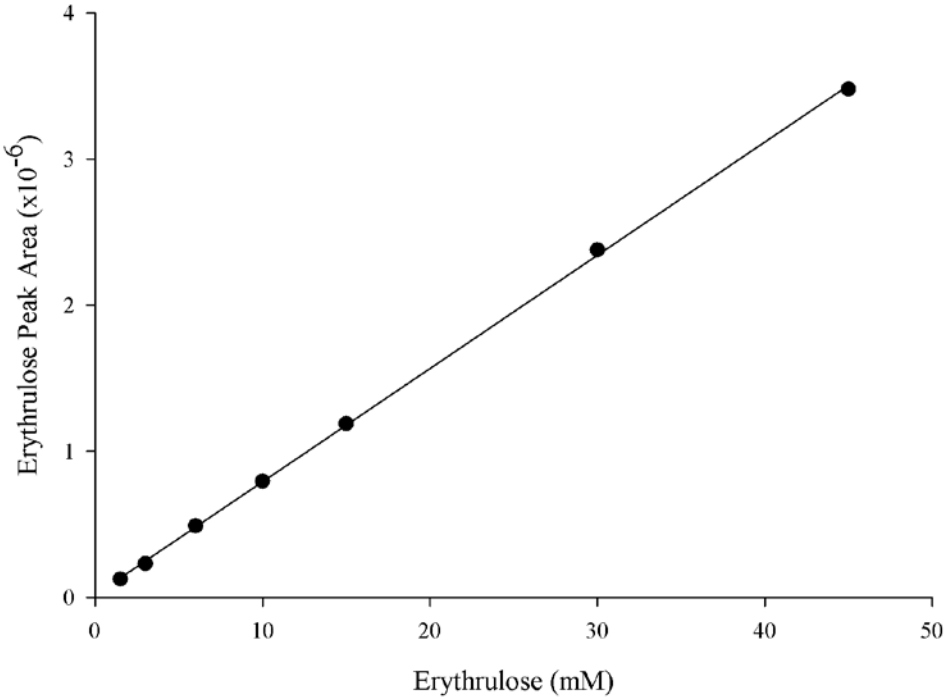

Figure 2-1 Standard calibration curve of L-Erythrulose determined on the 300 mm Aminex HPX-87H ion-exclusion column. L-erythrulose was prepared in 0.2% TFA. Figure shows a linear relationship between peak area and L-erythrulose concentration (mM) with a R^2 of 0.9997. The ranges of the erythrulose concentration in the reaction are normally 0-60 mM in 1:10 dilution.

2.2.10 Hydroxypyruvate synthesis

Li-Hydroxypyruvate (HPA) was synthesized by reacting bromopyruvic acid with LiOH following a previously described method (Morris *et al.*, 1996). The details of the synthesis were the following: bromopyruvic acid (0.06 mol) was dissolved in 100 ml water followed by careful addition of aq. LiOH (1 M) until a stable pH of 9 was reached. At no time during the addition was the pH allowed to exceed 9. The reaction mixture was then adjusted to pH 5.0 by addition of glacial

acetic acid and concentrated under vacuum to approximately 20 ml. Following refrigeration at -20 ^{o}C overnight, the crude product was washed with ethanol and then suspended in 50 ml ethanol at 25 ^{o}C for 30 min. After filtration the solid product was dried under vacuum to give a white or slightly yellowish powder (expected yield is 2-4 grams) which was stored at -20 ^{o}C. A standard curve of 6–45 mM of HPA in the same conditions as the reaction was used to obtain the HPA concentrations by HPLC. Figure 2-1 illustrates the standard calibration curve of HPA using HPLC method (section 2.2.8).

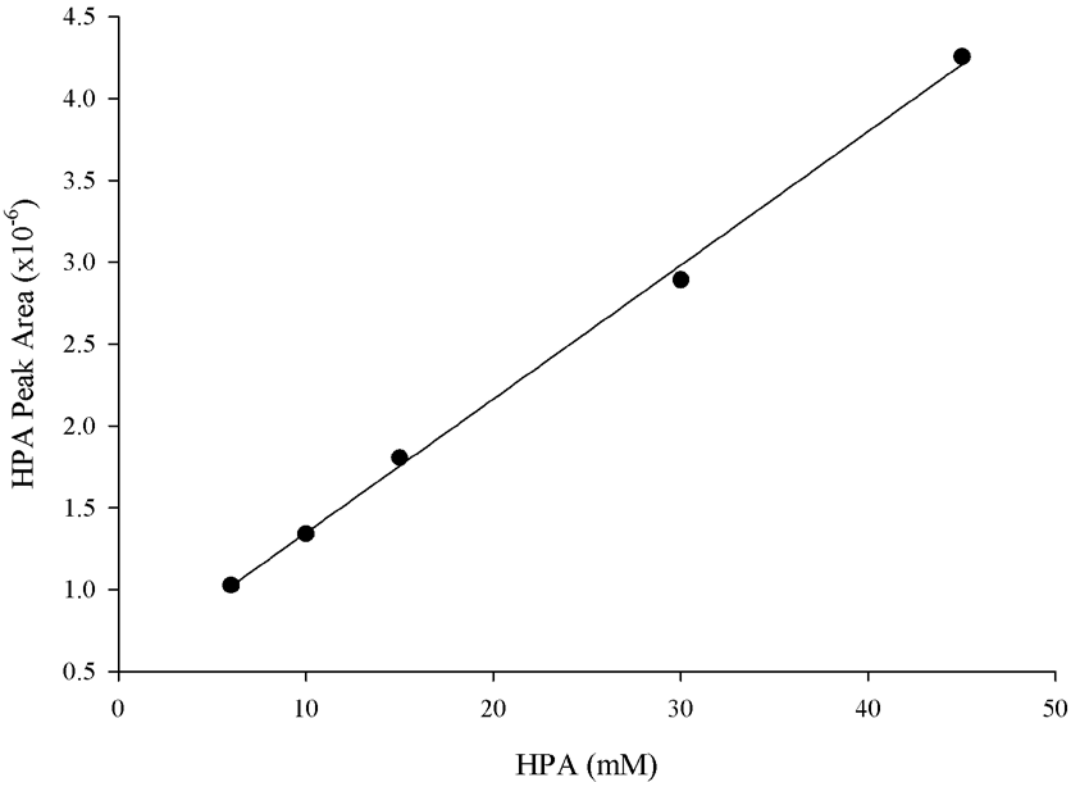

Figure 2.2 Standard calibration curve of HPA determined on the 300 mm Aminex HPX-87H ion-exclusion column. HPA was prepared in 0.2% TFA. Figure shows a linear relationship between peak area and HPAconcentration (mM) with a R^2 of 0.9975. The concentration of HPA as a substrate using for each reactions is 50 mM.

2.3 Molecular Biology procedures

2.3.1 Shake flask fermentations

A culture from a frozen glycerol stock was streaked out onto a Petri dish of LB agar (Amp+) using a flame sterilized wire loop. The plate was incubated overnight at 37 °C. A single *E. coli* colony was picked from the agar plate and transferred into 20 mL of LB medium contained in a 250 mL shake flask. The flask was incubated for 12-16 h at 37 ^{o}C with orbital shaking 250 rpm using an SI 50 orbital shaker (Stuart Scientific, Redhill, UK). Then 20 mL of an overnight culture was transferred to 180 mL LB medium (Amp+) in a sterile 1 L shake flask and was incubated at 37 ^{o}C for 6-8 h with orbital shaking 250 rpm. The cells were harvested and removed the broth by centrifugation for 10 min at 2370g (Hettich zentrifugen, universal 320R, Germany). The cells were then kept at -20 ^{o}C if not used on that day.

2.3.2 Master glycerol stocks

A 20% (v/v) glycerol stock was prepared by adding an overnight culture in a one to one (1:1) ratio volume with filter-sterilized 40% (v/v) glycerol in a 0.75 mL sterilized eppendorf. The aliquots were stored at -80 °C. The master glycerol stocks were used throughout this project.

2.3.3 DNA plasmid extraction and quantification

A QIAprep spin miniprep kit (Qiagen, Crawley, UK) was used to obtain plasmid DNA from host *E. coli* cells, and the method was carried out following the

techniques described by the supplier. The concentration of plasmid DNA was determined by spectrophotometric quantification at 260 nm absorbance (A260) (UV/Vis2, Unicam Ltd Cambridge, UK) using a quartz microcuvette (Hellma UK Ltd, Essex, UK) and a dilution of 1:10. The plasmid DNA concentrations were calculated by considering that 1.0 A260 unit of double-stranded DNA was equivalent to 50 ng μl^{-1}. Readings were blanked with the same buffer solution as that used for DNA elution from miniprep columns, and also for subsequent dilutions. The DNA purity was assessed by using A260/A280 ratio, and was expected to be in the range 1.85-2.0. All plasmids were partially commercially sequenced to verify their sequences by the service available at the Wolfson Institute for Biomedical Research, UCL. The construction of pQR791 and all mutations generated were verified using the TKN, TK 250^{+}, TK 400^{+} sequencing DNA-oligomers.

2.3.4 Plasmid pQR791

Plasmid pQR791 was used as a template for production of wild-type transketolase and mutants through this project. The pQR791 plasmid was modified previously from pQR790 plasmid (Aucamp, 2005) in which a BglII restriction site was introduced into the tkt gene promoter region within the pQR711 plasmid (French & Ward, 1995). An N-terminal His6-tag was introduced into the transketolase gene within pQR790 to create pQR791, resulting in a plasmid that allowed purification of TK by using Ni-affinity columns.

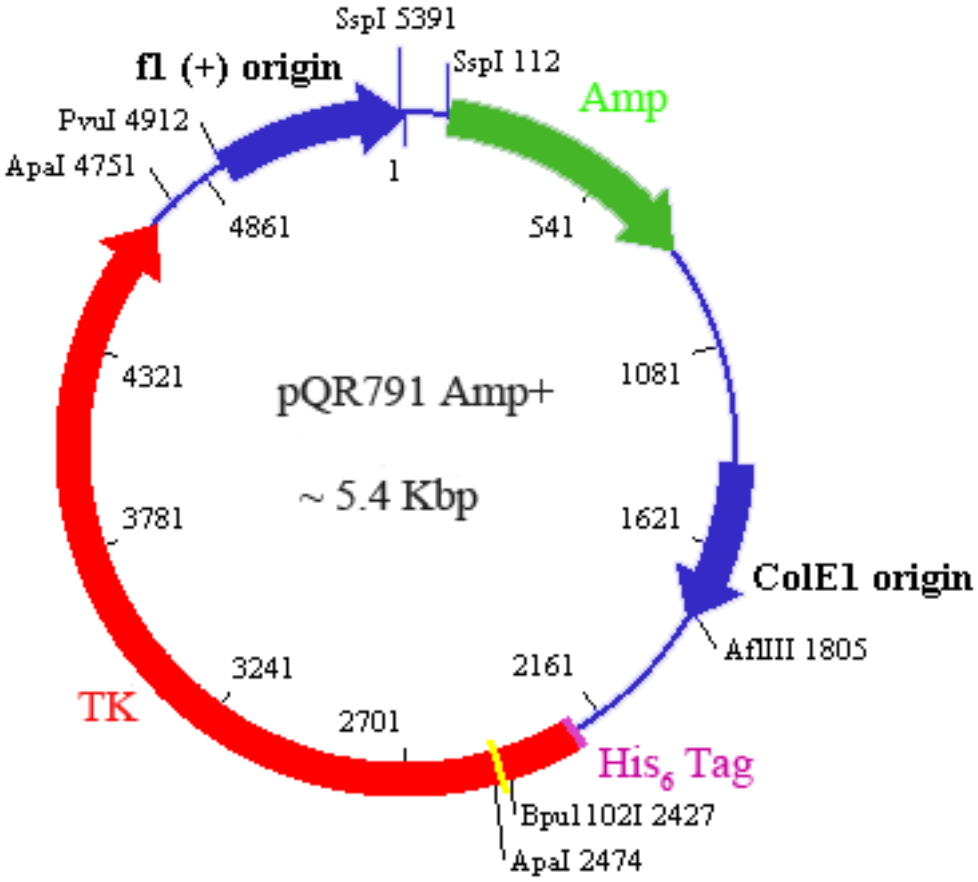

Figure 2-3 Schematic representation of plasmid pQR791. The ampicilin resistance (Amp+) is represented in green; the tkt gene is represented in red, and the poli His_6 -tag tail is coloured in purple. The total plasmid size is 5.4 kbp.

2.3.5 QuickChange™ site-directed mutagenesis

The TK-MutF and TK-MutR DNA-primers were obtained from operon biotechnologies GmbH (Cologne, Germany). These DNA-primers were used to create mutants using the pQR791 plasmid as template. The PfuTurbo DNA-polymerase, Pfu reaction buffer and dNTP's were obtained from Stratagene, (La Jolla, CA, USA). A PCR cocktail was prepared containing both the forward and reverse primers as shown in Table 2-1. The polymerase chain reaction (PCR) was performed with the temperature cycling profile depicted in Figure 2-1 for 15 cycles with an annealing temperature of 55 ^{o}C in a Techgene thermal cycler (Techne Limited, Cambridge, UK).

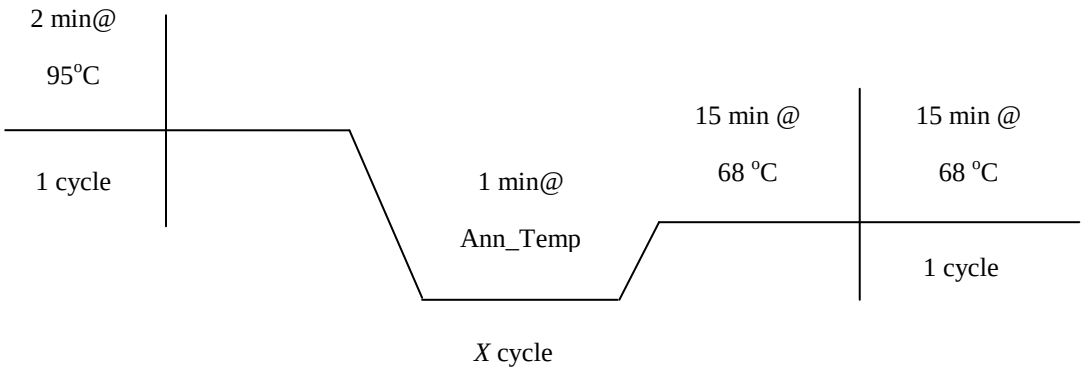

Figure 2-4. Generic thermocycler profile used for PCR reactions

Volume (µL)	Reagent
5	10X reaction buffer
1	ds DNA template (10 ng)
2	mutant primer forward (125 ng)
2	mutant primer reverse (125 ng)
1	dNTP mix
3	quick solution
36	H_2O (sterile deionised)
1	pfuTurbo DNA polymerase (2.5 $U.\mu L^{-1}$)

Table 2-1 Components of the PCR reactions.

2.3.6 Restriction digestion reactions

Restriction digests were carried out by adding 1 µl of the DpnI restriction enzyme (10 $U \cdot ml^{-1}$) directly to each PCR product and incubated in a water bath at 37 ^{o}C for 1 hr to remove methylated parental plasmid DNA. The remaining plasmid product was used for cell transformation.

2.3.7 Transformation of *E. coli* strains using XL10-Gold

XL10-Gold ultracompetent cells (Stratagene) were thawed on ice and 50 µl aliquots transferred into a pre-chilled Falcon tube. 2 µl of the PCR product from Section 2.3.6 was added to cell aliquots and incubated on ice for 30 minutes. The XL10-Gold cells were then heat shocked in a 42 ^{o}C water bath for 45 seconds and transferred back onto ice for 2 minutes. 0.5 ml of SOC broth (Sigma Chemical Co.) was added and cells incubated at 37 ^{o}C for 1 hr with orbital shaking at 250 rpm. Between 50 ml and 100 ml transformed cells were plated out on LB (Amp+) agar. Colonies were picked from plates and incubated overnight in 5 mL LB media containing 150 µg mL^{-1} ampicillin. The overnight culture was used to produce master stocks and also used for extracting plasmid DNA for mutant sequencing. Master cultures were preserved in 40% sterile glycerol and stored at -80 ^{o}C.

2.3.8 Agarose gel electrophoresis

Double-stranded DNA fragments were separated by gel electrophoresis in agarose gels 0.6-1% (w/v) depending on the size of fragments to be analysed. Agarose was suspended in 1x TAE buffer (diluted from 10xTAE buffer, pH 8) and heated in a microwave oven. When agarose was dissolved and solution cooled to less than 45 ^{o}C, Sybr® safe DNA gel stain (Invitrogen, UK) was added and the agarose poured into an electrophoresis tray. When the gel had hardened, it was placed horizontally in a gel electrophoresis tank containing enough 1x TAE buffer to cover the surface of the gel to a depth of 1 mm. DNA samples were mixed with

0.2 volumes of the 6X gel loading buffer (Invitrogen, UK) before loading into the wells in the gel. Electrophoresis was carried out for 1 hour at a constant voltage of 75 V. Fragment sizes were estimated by comparison with tracks of a standard super-coiled DNA ladder (Invitrogen, UK) (Figure 2-4).

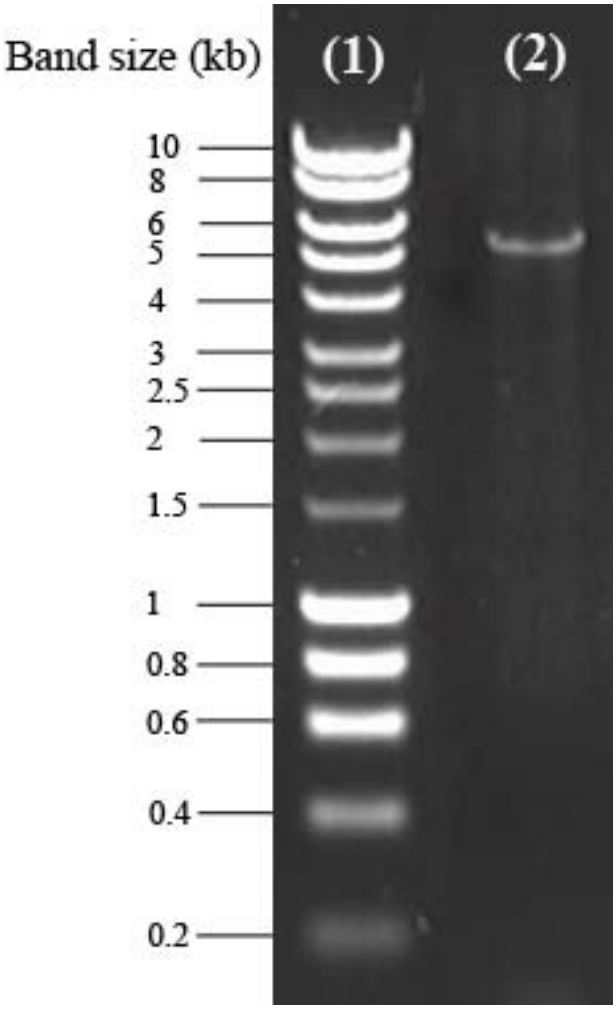

Figure 2-5 Digital image of plasmid pQR791 in a 0.6% (w/v) agarose gel.
Lanes are as follow: lane (1) corresponds to the DNA marker lanes (2) corresponds to ~5.4 Kbp super-coiled plasmid pQR791.

2.4 Enzyme preparation

2.4.1 Sonication

The cells paste from section 2.3.1 was re-suspended in 50 mM Tris-HCl, pH 7 then lysed with an ultrasonication protocol of 10 cycles of 10 seconds at 8 μ pulses with 10 seconds interval (Soniprep150, Sanyo, UK). Cell-free extract was clarified by centrifugation at 17,700g for 20 minutes in a bench microcentrifuge (Kendro Laboratory,UK). Cells were placed on ice during the sonication to stop overheating.

2.4.2 His_6-tag enzyme purification

The cell lysate extract from section 2.4.1 was used for the TK purification process. Columns packed with Ni-NTA agarose beads for his-tag protein were equilibrated using 10 volumes of equilibration buffer (Table 2-2). Cell lysate was loaded and the column shaken at 175 rpm for 30 min, then washed with 5 column volumes of wash buffer (Table 2-2) to remove non-specifically bound protein. Transketolase was then recovered using the elution buffer (Table 2-2), and extensively dialysed against 50 mM Tris-HCl, pH 7.0 at 4 ^{o}C.

buffer	composition
Equilibration	50 mM (NaH_2PO_4), 300 mM NaCl, 10 mM Imidazole
Wash	50 mM (NaH_2PO_4), 300 mM NaCl, 25 mM Imidazole
Elution	50 mM (NaH_2PO_4), 300 mM NaCl, 150 mM Imidazole

Table 2-2 Compositions of Equilibration, Wash and Elution buffers for His_6-Tag TK purification (section 2.4.2).

2.4.3 SDS-PAGE

SDS-Page analysis in Figure 2-5 was performed following the manufacturer's instructions. SDS-PAGE for protein analysis was carried out on a Mini-Protean II system (Bio-Rad Laboratories Inc., Hemel Hempstead, UK) using 10% w/v Tris-Glycine comercial gels (1.5 mm, 10 well, Invitrogen, Paisley, UK). 5 µl of standard molecular weight marker (Fermentas PageRuler^{TM} prestained protein ladder) was inserted into the first lane, and subsequent lanes were filled with 20 µl of the protein samples. Protein samples were first mixed (1:1) with 2X blue sample buffer, Laemmli from Sigma, then heated to 99 ^{o}C and held there for 10 mins using a

Techgene thermal cycler (Techne Limited, Cambridge, UK) before loading 20 µL sample per well. Protein separation was achieved by applying a constant voltage of 120V for 150 mins.

2.4.3 Protein Dialysis

Purified protein was usually transferred to SnakeSkin dialysis tubing with a 10,000 Da molecular-mass cutoff (Pierce Biotechnology Inc., USA) and dialysed for 24 h against 50 mM Tris–HCl, pH 7.0, at 4 °C.

2.4.4 Protein Concentration

Protein concentration was determined by absorbance at 280 nm spectrophotometer assuming a monomeric molecular weight (MW) of 72260.82 g mol^{-1} and an extinction coefficient (ε) of 93905 L mol^{-1} cm^{-1} (Pace et al., 1995). Pure transketolase was stored in 50 mM Tris–HCl, pH 7.0, at 4 °C for a maximum of 2 weeks without loss of activity, and with no precipitation visible.

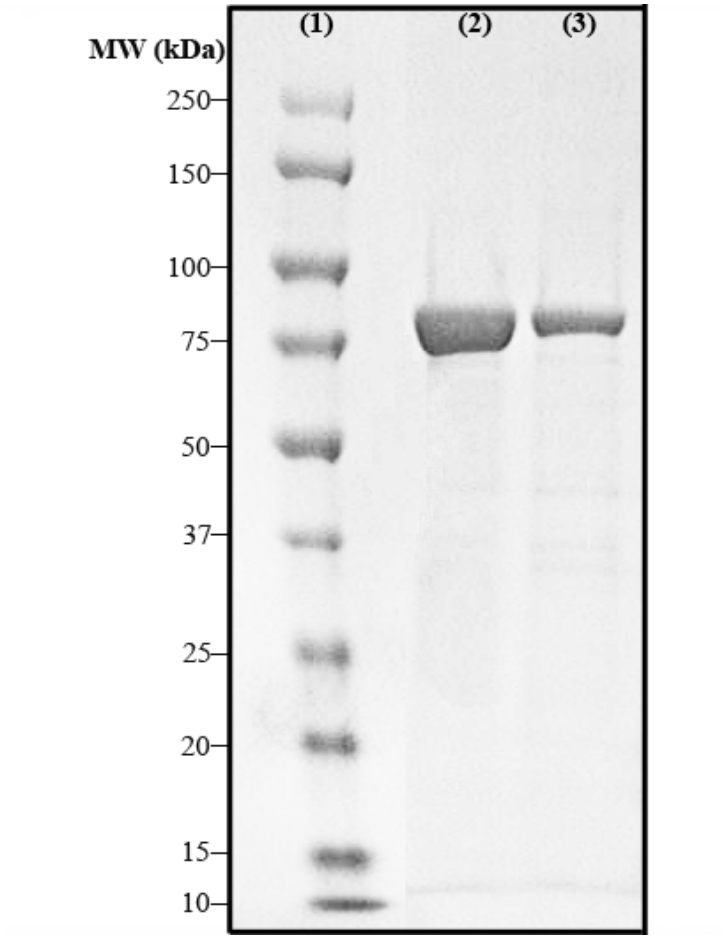

Figure 2-6 Top view of a 10% SDS-page gel of purified wild-type transketolase. Enzyme was purified by using a Ni-column. Sample lines are as follow: (1) Protein standard marker; (2) Purified transketolase; (3) A 1:30 purified transketolase. The darkest band at ~75KD corresponds to the transketolase monomer.

Chapter 3

3. Stability and Activity of *E. coli* transketolase at different pH and temperature

3.1 Aims and Introduction

The aims of this thesis are to explore the factors that lead to transketolase inactivation during biocatalysis. Understanding these would then inform enzyme engineering strategies to improve the application of transketolase at a wider range of pH, temperature and solvent conditions. The study of conformational changes and the stability of native holo-TK is very important in order to improve it use in industrial processing. Thus, understanding the inactivation mechanisms linking it to denaturation phenomena is a major objective from both technical and scientific points of view. For example, they can be exploited for the engineering of new enzymes for important bioengineering applications and for the improvements of industrial processes. Indeed, improving stability may also prolong the half-life of transketolase under mild reaction conditions to increase its reusability in a process.

The need to explore the use of TK at more extreme pH, temperature and solvent conditions has arisen recently as the enzyme potential has increased for conversion of a broader range of substrates using directed evolution and pathway engineering. TK has long been an attractive catalyst for the synthesis of high value compounds in industry such as complex carbohydrates, sugar analogs (Hecquet et al, 1994; Hecquet et al, 1996, Liqvist et al, 1992; Turner 2000). Recently, TK has

also been utilized in a one pot synthesis (Ingram et al., 2007; Rios-Solis et al., 2011) and a two-step bioconversion of chiral amino alcohols (Smith et al., 2010), which act as precursors for the synthesis of protein inhibitors and antibiotics. However, the range of substrates was previously limited to sugars and related highly polar hydroxylated aldehydes.

Recent applications of directed evolution have successfully modified the substrate specificity of TK to better accept non-phosphorylated substrates (Hibbert et al., 2007), aliphatic aldehydes (Hibbert et al., 2008), of increasing size (Cazares et al., 2010) or with enhanced and reversed enantioselectivity (Smith et al., 2008), and also the acceptance of hetero aromatic aldehyde substrates (Galman et al., 2010). These results have addressed the need for improved stereo chemical control in carbon-carbon bond formation, to meet the increasing demand for enantiopure pharmaceuticals (Dalby et al., 2009; Koeller and Wong, 2001). However, they have also created a need for TK variants that can tolerate the conditions of pH, temperature and solvent, used to improve the stability and solubility of the increasingly organic and aromatic substrates. The development of TK enzymes with higher stability under these conditions, coupled with the modifications to substrate acceptance, will enhance the adoption of TK for the stereoselective biocatalytic syntheses of carbon-carbon bonds in the industrial production of pharmaceutical intermediates.

The first step towards this is to improve our understanding of TK inactivation, which begins from previous observations that *E. coli* transketolase (TK) was susceptible to inactivation at low pH, where frustratingly, the HPA

substrate is most stable to degradation (Mitra et al., 1998). Overall, the stability of *E. coli* TK is also limited by the fact that it retains a high catalytic activity in only a relatively narrow pH range (6.5-9.5) (Mitra et al., 1998), and temperature range (20-40^{o}C) (Sprenger and Pohl, 1999).

The optimum pH of TKs from difference sources have been previously reported to be quite similar (Datta & Racker, 1961; Himmo et al., 1988; Masri et al., 1988; Sprenger et al., 1995). By contrast, the optimum temperature for activity varies across different sources of TK. For example, for rabbit liver TK the optimum temperature for activity is around 40 ^{o}C (Masri et al., 1988). For human erythrocyte TK, after incubation at 55 ^{o}C for 5 min it retained 50% activity (Takeuchi et al., 1986), whereas porcine liver TK showed no activity loss after 1 hour 50 ^{o}C in the presence of thiamine pyrophosphate (TPP) (Philippov et al., 1980). However, there have been no reports that have determined deactivation mechanism for holo-TK at higher temperatures. Similarly, the inactivation of TK at low and high pH has only been speculated upon (Mitra et al., 1998), and not previously characterised.

As the structure and the catalytic mechanism of *E. coli* TK has been well characterised under physiological conditions (Littlechild et al., 1995; Nikkola et al., 1994; Datta and Racker, 1961; de la Haba et al., 1955; Nilsson et al., 1997; Schorken and Sprenger, 1998), there is a solid structural basis from which to begin to elucidate the mechanisms of TK inactivation at extremes of pH, temperature and solvents. TK is a homodimeric enzyme which needs TPP and a bivalent metal-ion

as a cofactor bound within each of the two identical active-sites formed at the dimer interface, to form the active holo-TK.

Previous cofactor binding studies indicated that both TPP and Mg^{2+} easily dissociate from *E. coli* holo-TK at high pH, and that irreversible denaturation of TK may cause inactivation at pH below 6.5 (Mitra et al., 1998). TK may also become partially inactivated by misfolding or aggregation during biocatalysis at pH 7.5 where a significant degree of denaturation can occur in the bioreactor, due for example to a high concentration of chemical denaturant (Martinez-Torres et al., 2007).

A previous study at UCL (Martinez-Torres et al., 2007), has shown that the denaturation of TK with urea follows a non-aggregating but irreversible unfolding and dimer dissociation pathway in which the cofactor binding appears to become altered but without dissociating, followed at higher urea by partial denaturation of the homodimer prior to any further unfolding or dissociation of the two monomers. That study provides useful knowledge of the potential of TK to form intermediate but inactive and dimeric states in the unfolding pathway. However, urea itself can suppress aggregation, and is also not generally present in biocatalysis, and so further analysis is necessary to probe the inactivation, denaturation and potential aggregate formation of TK under other denaturing conditions present in biocatalysis.

This Chapter describes my contributions towards a publication describing a larger body of work on the impact of pH and temperature upon TK structure and function, carried out collaboratively with other members of the Department of

Biochemical Engineering at UCL (Jahromi et al., 2011). This paper is presented in Appendix I of this Thesis. TK inactivation in harsh conditions such as high temperature and various pH was measured in terms of its activity, but also changes to structure or aggregation propensity as determined by circular dichroism and dynamic light scattering.

3.2 Materials and Methods

All chemicals were obtained from Sigma-Aldrich UK.

3.2.1 Over-expression and purification of His-tagged wild-type transketolase

Transketolase was expressed with an N-terminal His_6 tag from *E. coli* XL10-Gold (Stratagene, La Jolla, CA) containing the engineered plasmid pQR791, purified as described previously (Martinez-Torres et al., 2007), dialysed for 24 hours against 25 mM Tris-HCl, pH 7.0, at 4 °C then stored at 4 °C for a maximum of two weeks without loss of activity, and with no precipitation visible. Protein concentration was determined by absorbance at 280 nm, assuming a monomeric molecular weight (MW) of 72260.82 g mol^{-1} and an extinction coefficient (ε) of 93905 L mol^{-1} cm^{-1} (Pace et al., 1995).

3.2.2 pH dependence of holo-TK activity

Samples of 30 µL purified holo-transketolase at 0.5 mg mL^{-1} (6.9µM) were incubated (2.4 mM $MgCl_2$, 9 mM TPP) at a range of pH from 3.0-11.0 for 180 minutes. 50 mM Tris-HCl was used for pH 3-7, and 50 mM Tris-Base for pH 9-11. Enzyme reactions were initiated by addition of 100 µL of a substrate solution containing 50 mM Li-HPA and 50 mM GA in the appropriate buffer (Tris-HCl for pH3-7 and Tris-Base for pH 9-11) and the erythrulose production over 180 mins determined as above by HPLC (Dionex, CA, USA) with 210 nm absorbance detection, a 50mm PL Hi-Plex H guard column (Polymer Laboratories Ltd, UK), 0.1 % (v/v) TFA mobile phase, and a flow rate of 0.6 mL min^{-1}. Standard curves of L-erythrulose in the same conditions were used to obtain the final L-erythrulose concentrations.

3.2.3 pH dependence of apo-TK and holo-TK circular dichroism (CD) spectra

Purified wild-type apo- or holo-transketolase (with 2.5 mM $MgCl_2$, 0.25 mM TPP) was prepared at 0.08 mg mL^{-1} enzyme and the appropriate 50 mM buffer for each pH as above, and incubated for two hours prior to recording CD spectra as above in a 1 mm path length quartz precision cell cuvette. CD spectra were also recorded over time and showed no observable change in signal at any wavelength between 45 and 120 mins.

3.2.4 Temperature inactivation of holo-TK

Wild-type *E. coli* transketolase was obtained purified enzyme 0.1 mg mL^{-1} (1.38 μM) enzyme, containing 2.4 mM TPP, 9 mM $MgCl_2$ and in 25 mM Tris-HCl, pH 7.0 and pre-incubated at 25 °C for 30 minutes. Temperature inactivation was initiated by placing the 100 μL samples into a water bath pre-heated at 55 °C. Sample temperatures were monitored using a digital wired-thermometer (Topac, USA). Samples were removed after 1 h, immediately cooled on ice then equilibrated to 25 °C. Reactions were initiated with 50 μL of 50 mM Li-HPA and 50 mM GA in 25 mM Tris-HCl, pH 7.0, then quenched at various times over 180 minutes with 1 vol. 0.2 % (v/v) trifluoroacetic acid (TFA). Purified TK standard condition was also measuring at 25^{o}C as a control. Samples were analysed as above by HPLC.

3.2.5 Dynamic light scattering (DLS)

The thermal denaturation of purified transketolase was measured with a Zetasizer Nano S (Malvern Instruments Ltd., UK). Apo-TK or holo-TK at

0.1 mg mL^{-1} (1.38 μM) was prepared in 25 mM Tris-HCl pH 7.0 (with 0.5 mM TPP, 5 mM $MgCl_2$ for holo-TK). The temperature was raised from 4 to 70 °C at 1.0 °C intervals per minute between measurements. A control sample of buffers with or without cofactors was subtracted from each recording. Data were acquired in triplicate with a low volume disposable sizing cuvette with a path length of 1 cm. The hydrodynamic diameters of each sample were calculated from the averaged-measurements using the Zetasizer Nano Series software V.4.20 (Malvern Instruments Ltd., Worcestershire, UK).

3.3 Results and Discussion

3.3.1 Investigation of the effect of pH on holo-TK catalytic activity.

The optimum enzyme activity of TK has been previously reported at pH 8-8.5 (Sprenger and Pohl, 1999), but also at pH 7.0-7.5 (Mitra et al., 1998) indicating an additional effect of buffer composition. The effect of pH on the activity of 0.5 mg mL^{-1} of holo-TK (2.4 mM $MgCl_2$, 9 mM TPP) in purified TK is shown in Figure 3-1. Samples were incubated at the relevant pH for 45 mins before reactions. Incubating for up to 90 and 120 mins produced no noticible further change (data not shown). At pH 7 the TK bioconversion was completed within 3 h while at pH 9, 80% bioconversion was achieved in 3 h. No difference was observed between the pH profile from purified enzyme shown here, and the same enzyme concentration in clarified lysate presented in (Jahromi et al., 2011), although the clarified lysate had a marginally higher activity than the purified protein at pH 6 only. This indicated that if there are any as yet unobserved stabilising effects due to retaining the enzyme in the cell lysate, then these do not noticeably affect the pH-activity profile.

The pH profile in Figure 3-2 shows that the optimal pH for TK is 7.0 as observed previously (Mitra et al., 1998), while TK was completely inactivated at pH 3.0. However, this is the first report of a complete pH profile for TK, and it can be seen to be asymmetrical rather than the classical "bell-shaped" curve expected from the simple titration of catalytically important residue pK_as. Enzyme activity of greater than 80% was maintained at between pH 6.0-8.0, with 50% activity at

approximately pH 4.5 and pH 9. Each transition could potentially result from either a degree of protein denaturation or aggregation, in addition to the titration of key catalytic residues in the enzyme active site.

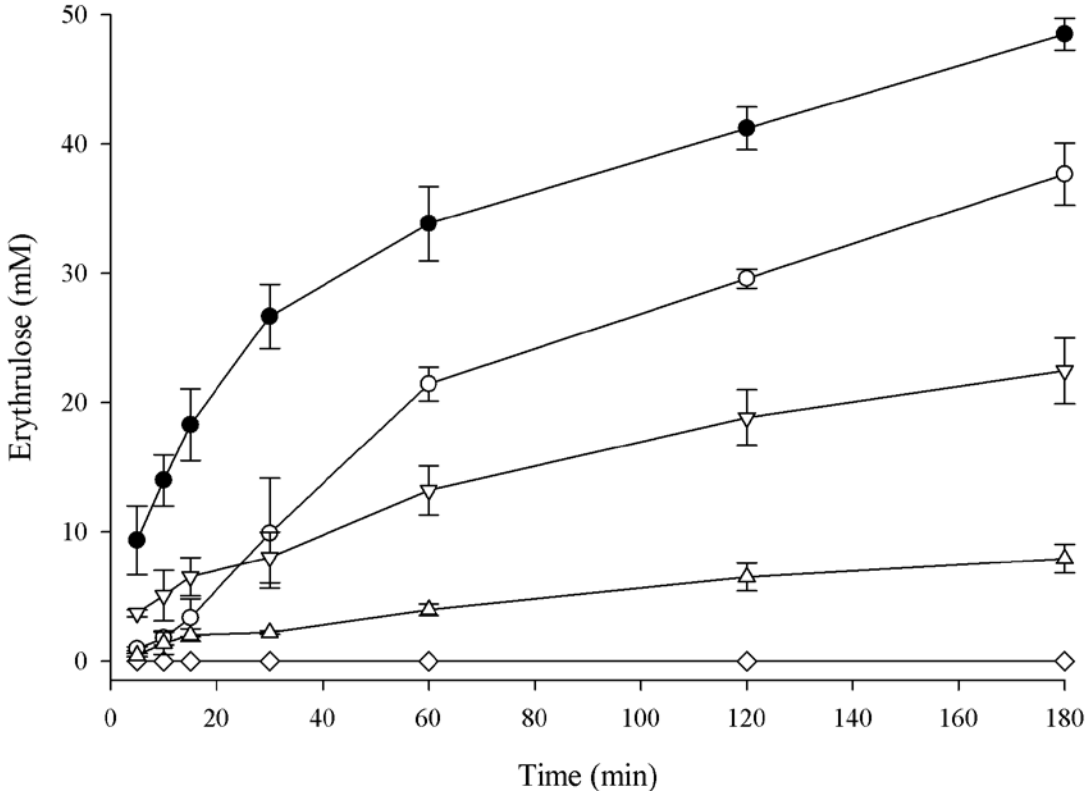

Figure 3-1 Catalytic activity of holo-transketolase in a range of pH. The catalytic activity of pure wild-type was measured in triplicate over a range of pH from 3.0 to 11.0 in 50 mM Tris-HCl for pH 3-7 and 50 mM Tris-base for pH 11. (◊) pH3, (∇) pH 5, (●) pH7, (○) pH9 and (Δ) pH 11. Specific activity was measured using 50 mM GA and 50 mM HPA as substrates and L-erythrulose as a product, in their respective buffers, at 25 ^{o}C.

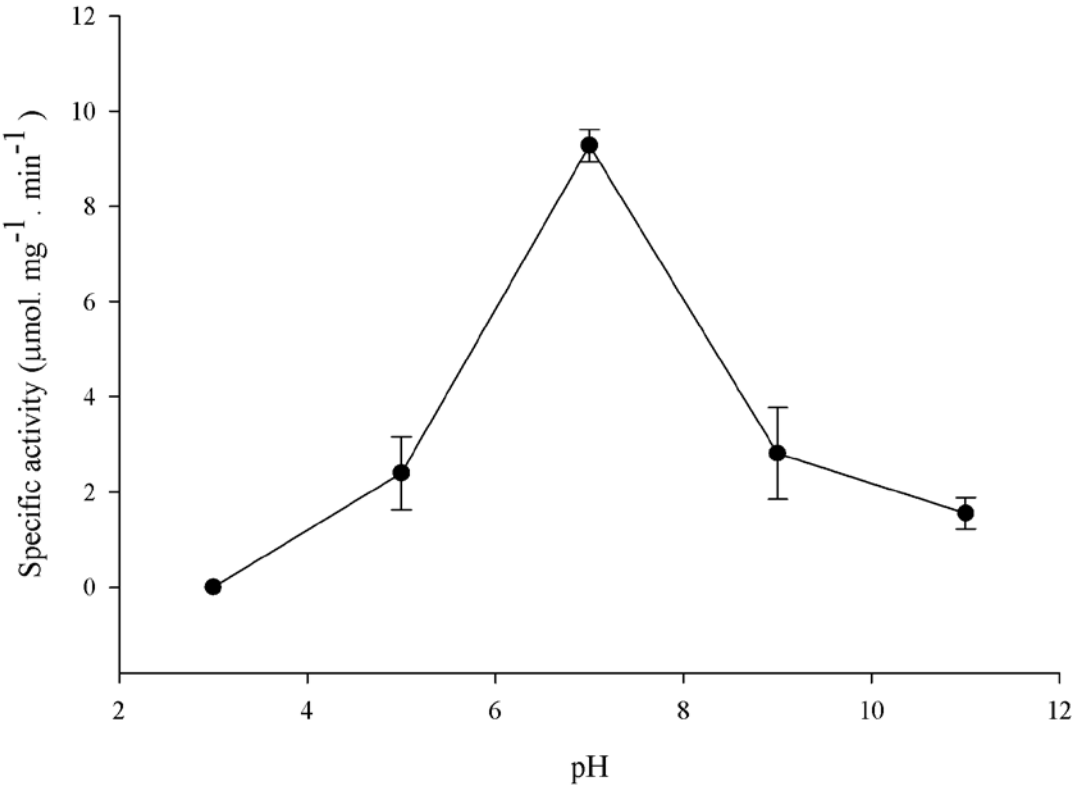

Figure 3-2 Effect of pH on holo-transketolase activity. Specific activity of pure wild-type were measured in triplicate over a range of pH from 3.0 to 11.0 in 100 mM Bis-Tris for pH 4-5; 50 mM Tris-HCl for pH 6-9, and 50 mM Tris Base for pH 10-11. Specific activity was measured using GA and HPA as a substrates, in their respective buffers, at 25 ^{o}C.

Previous work has observed that exposure to pH below 6.5 results in a decrease in activity of holo-TK, and this was assumed to be due to irreversible denaturation of the protein (Mitra et al., 1998). The same study also observed that high pH (above 7.5) led to the dissociation of TPP from the enzyme when the cofactor was not present in excess in solution (Mitra et al., 1998). To clarify these

potential mechanisms further at both pH extremes, the effects of pH on the secondary structure holo-TK by CD were determined.

3.3.2 Effect of pH on the structure and solubility of apo-TK and holo-TK

The secondary structure content for both apo-TK and holo-TK was measured by CD at different pHs ranging from 3 to 11 (Figures 3-3,3-4). The effect of pH on secondary structure content as measured by the ellipticity at 222 nm, is shown in Figure 3-5. The structure of holo-TK remained mostly α-helical and stable across the pH range of 5 to 11, and the CD spectra did not change significantly between 45 mins and 120 mins incubation at any wavelength. At pH 3 and 4, the secondary structure content decreased to 81 and 79% respectively, relative to that at pH 5 and above, indicating partial acid denaturation of the holo-TK structure. The data of the effect of pH upon fluorescence intensity of holo-TK (Jahromi et al., 2011) (data not shown) is consistent with the CD data, with a distinct transition observed at pH 4. The holo-TK fluorescence intensity did not change significantly beyond the first two hours at any pH. The most likely cause of the transitions observed by CD and fluorescence was revealed by DLS at various pH (Jahromi et al., 2011), which shows that holo-TK at 25 ^{o}C was slightly larger at pH 11 compared to pH 7-9 (9-10 nm) and was aggregated at pH 4, whereas at pH 5 the average particle size was 19 nm, indicating a degree of denaturation and perhaps the formation of some small oligomers at pH 5.0.

Apo-TK is less resistant to aggregation at pH 11 than holo-TK (Jahromi et al., 2011). The gradual and only partial loss of activity at Aggregation was also not observed for either holo-TK or apo-TK at 25 °C and pH 6-9. Comparison of the

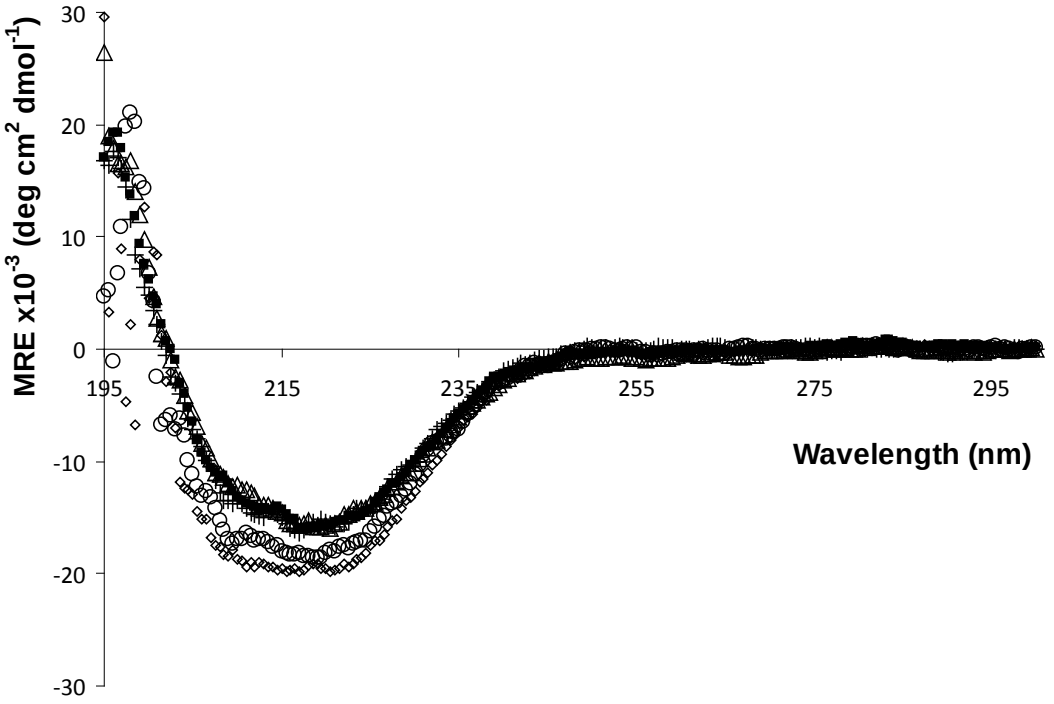

Figure 3-3 pH dependence of circular dichroism spectra for apo-TK. Samples of 0.08 mg mL^{-1} apo-TK were incubated in 50 mM buffer at each pH (3-11) for 45 min at 25 °C before full spectra (190-300 nm) were acquired. Spectra are shown for both apo-TK at (+) pH 3, (Δ) pH 6 (■) pH 7, (○) pH 9,(◊) pH 11.

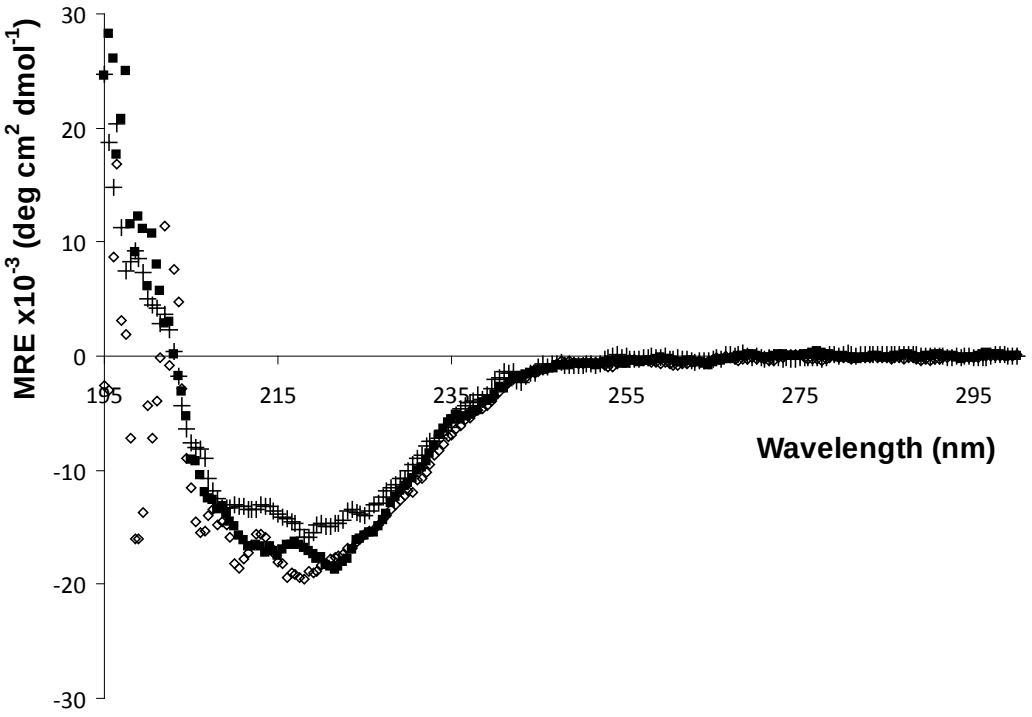

Figure 3-4 pH dependence of circular dichroism spectra for holo-TK. Samples of 0.08 mg mL^{-1} holo-TK (with 2.5 mM $MgCl_2$, 0.25 mM TPP) were incubated in 50 mM buffer at each pH (3-11) for 45 min at 25 °C before full spectra (190-300 nm) were acquired. Spectra are shown for holo-TK at (+) pH 3, (■) pH 7, (◊) pH 11. For clarity, not all spectra obtained are shown.

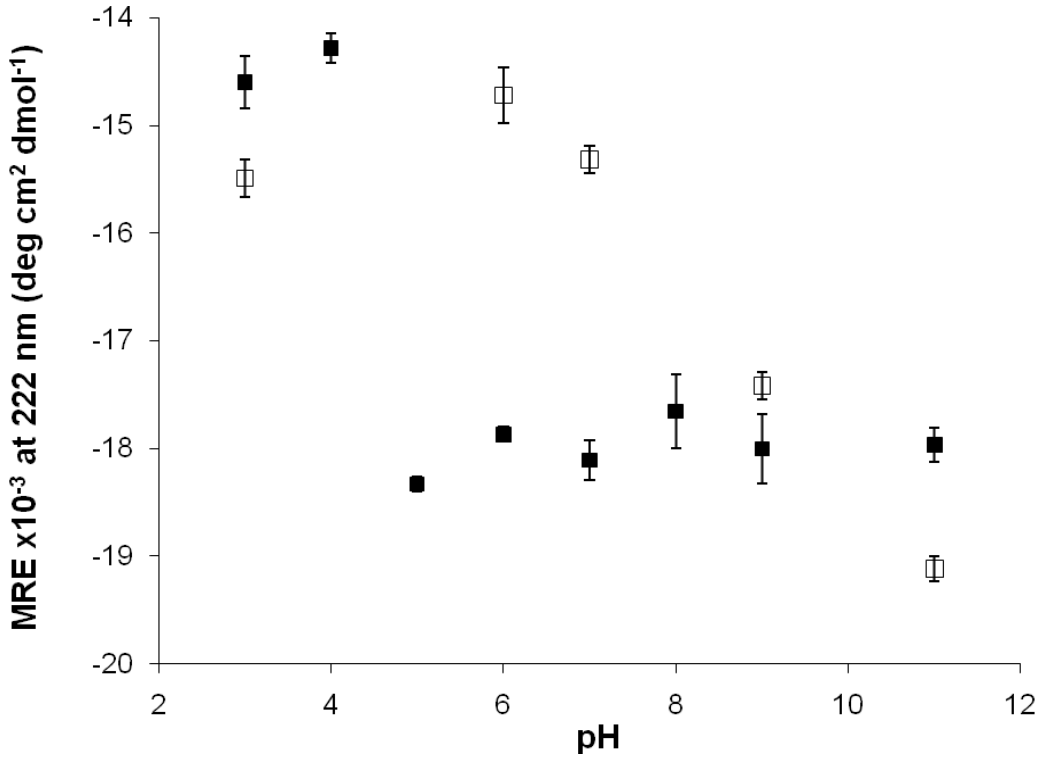

Figure 3-5. Effect of pH on *E. coli* TK far-UV CD signal at 222 nm. Samples of 0.08 mg mL^{-1} (□) apo-TK or (■) holo -TK (with 2.5 mM $MgCl_2$, 0.25 mM TPP) were incubated at a range of pH from 3.0-11.0 in 50 mM Tris-HCl for pH 3-7.5 and 50 mM Tris-Base for pH 8-11. Samples were incubated for 45 min at 25 °C before spectra were acquired.

222 nm CD signals in Figure 3-5 indicate that apo-TK contained up to 20% less secondary structure than holo-TK at both pH 6 and pH 7, which was presumed previously to be due to ordering of the cofactor-binding loops in the holo-TK

structure (Martinez-Torres et al., 2007). However, the CD signal for apo-TK at pH 9 increased in magnitude and converged onto that of holo-TK which remained the same at pH 5-11. This suggests that at pH 9 the cofactor-binding loops become more structured in apo-TK, though it cannot be determined by CD alone whether these loops in apo-TK at pH 9 formed the same structure as that observed in the active holo-TK structure at pH 5-8.

Dissociation of TPP (and Mg^{2+}) at high pH was previously proposed as the possible cause of inactivation when excess cofactor was removed (Mitra et al., 1998). However, the formation of increased structure in apo-TK indicates a more complex mechanism than simple loss of cofactor affinity due to pH titration of active site residues. More recent studies suggested that the cofactor remained associated in an inactive form of the enzyme that was stabilised at 2 M urea (Martinez-Torres et al., 2007). In this state the fluorescence signals of apo-TK and holo-TK converged, and yet the secondary structure content of the holo-TK remained unaltered from that at 0 M urea, and also remained more structured than that of apo-TK, indicating a local structural change had affected the polarising environment of the bound TPP cofactor. It was speculated that this inactive, yet cofactor associated intermediate form may be the same or similar to that observed during the kinetic reconstitution of holo-TK from apo-TK. By contrast, secondary structure content of apo-TK and holo-TK also converge at pH 9 suggesting that the structure of apo-TK may now also influence the association of cofactors. The structural observations could therefore be linked to partial enzyme inactivation by various possible mechanisms.

Increased structure in the cofactor-binding loops of apo-TK could simply have hindered access to the cofactor binding site and therefore shifted the equilibrium more towards cofactor dissociation. Alternatively, the cofactor binding loops of apo-TK may have adopted a non-native conformation to which cofactors have access but cannot bind. Finally, it is also possible that the cofactor-binding loops reorganised into an alternatively stabilised structure that is the same for both apo-TK and holo-TK, and to which the cofactors may bind but only in a catalytically inactive form. Distinguishing these possibilities will require a more detailed analysis of the specific cofactor binding loop conformation and structure.

TK enzyme inactivation at low pH appears to be directly linked to denaturation and subsequent aggregation of the enzyme, and this difference leads to the asymmetry observed in the pH-dependent activity profile. Holo-TK was clearly less stable at pH 5 than at pH 7-8 resulting in the lower aggregation temperature observed by DLS, and the marginally increased fluorescence intensity which suggests partial loss of tertiary structure (Jahromi et al., 2011). At pH 4, this destabilisation led rapidly to aggregation, which was seen for both holo-TK and apo-TK. Though the specific structural cause of aggregation at pH 4 cannot be directly determined from these data, it does suggest that protein engineering could be usefully aimed at stabilising the enzyme to denaturation at low pH. However, an underlying contribution to deactivation at low pH by simple active-site residue titration cannot be completely ruled out.

3.3.3 Thermal inactivation of holo-TK

The optimum enzyme activity of TK has been previously reported as 20-40 °C (Sprenger and Pohl, 1999). In this Chapter, the thermal inactivation of holo-TK at 55 °C was characterised. At 55 °C the catalytic activity was measured after re-cooling samples to 25 °C. The catalytic activity of wild-type TK at 55 °C, obtained after re-cooling to 25 °C, shows complete bioconversion, and at a faster rate than for a control at 25°C (Figure 3-6).

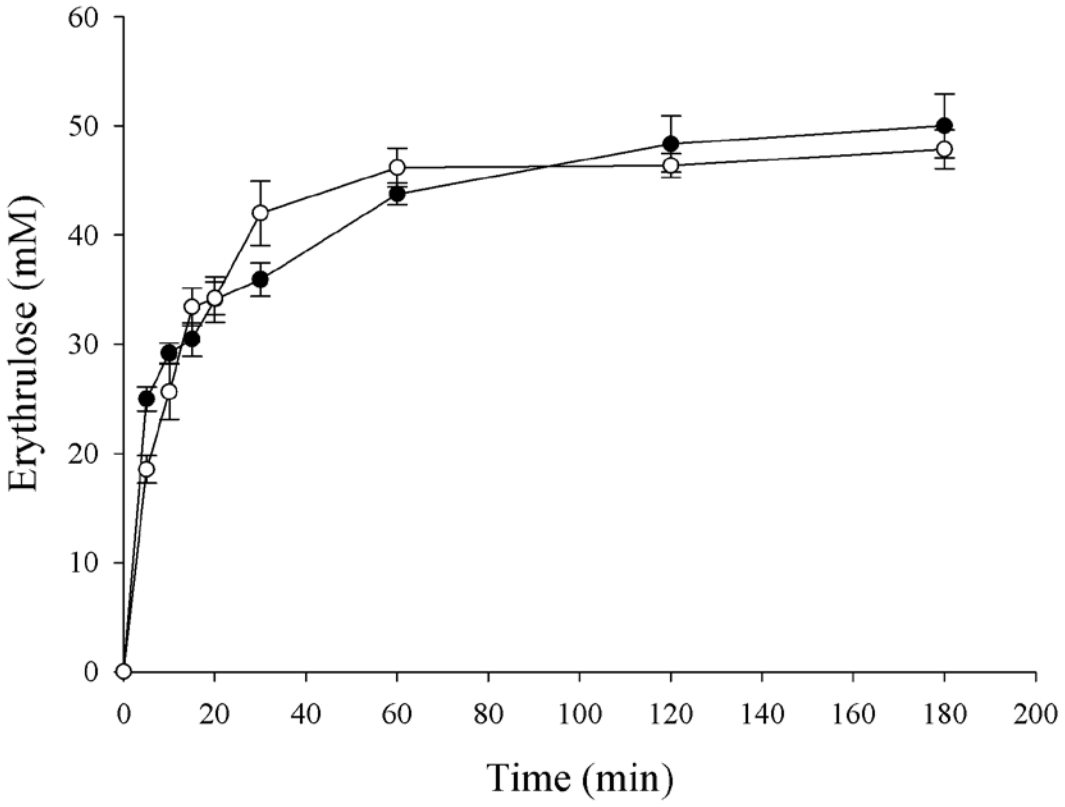

Figure 3-6 Catalytic activity of holo-transketolase at 25 and 55°C. The catalytic activity of pure wild-type was measured in triplicate at 25°C (●) as a control and after pre-incubation at 55 °C for 1 hour and re-cooling sample at 25 °C (○) 50 mM Tris-HCl. The enzyme catalytic activity was measured using 50 mM GA and 50 mM HPA as substrates and L-erythrulose as a product.

The residual activity of holo-TK measured at 25 °C, after a pre-incubation at elevated temperatures, was characterised in more detail subsequently, and found to increase initially with the incubation temperature (Jahromi et al., 2011). At above 55 °C, the residual enzyme activity then rapidly decreased, indicating irreversible protein denaturation or the formation of aggregates.

CD measurements at increasing temperatures also showed a sharp cooperative transition to zero signal at 58 °C, and was potentially due to aggregation rather than simple protein denaturation (Jahromi et al., 2011). The unusual thermal behaviour of TK activity indicated that the protein undergoes an irreversible annealing, such that inactive forms of the enzyme are physically altered or activated by temperature. No aggregates were observed at <55 °C, and yet the temperature dependent CD signal showed a strongly sloped initial baseline, suggesting a gradual alteration of secondary structure (Jahromi et al., 2011). Therefore, the CD data could be consistent with either the "shuffling" of incorrectly formed dimers into the correct form, or structural re-annealing of for example the cofactor binding loops, cofactor conformation, or other active site elements, leading to a more active enzyme. DLS was required to fully characterise the presence of aggregates at each temperature.

3.3.4 Particle-size distribution of apo- and holo-TK during thermal denaturation

The effect of temperature on the Z-average hydrodynamic radius of apo-TK and holo-TK was determined by DLS from the particle size distributions as measured by % volume (Figure 3-7,3-8). The expected Z-average of 9-10 nm for the TK homodimer remained constant above 20 °C for both apo-TK and holo-TK until they increased at above 50^{o}C, reflecting the known lower stability of the apo-TK (Martinez-Torres et al., 2007). Cooling of the samples from 57 °C back to 25 °C did not return the protein to the smaller particle size, but remained at >1000 nm confirming the irreversible formation of aggregates (Jahromi et al., 2011). Although the particle size base line of holo-TK shows higher than apo-TK in even lower temperature, these might be due to the cleaning of the cuvette.

Although the size of the holo-TK peak started to increase from 45-55 ^{o}C, significant denaturation was not observed by CD prior to the aggregate formation at 58 °C (Jahromi et al., 2011). However, a gradual non-cooperative loss of secondary structure observed by CD as the temperature was increased to 58 °C may have eventually induced the aggregation, even though it initially also improved the enzyme activity. The denaturation of holo-TK previously began at 2 M urea with a convergence of the intrinsic fluorescence to that of the apo-TK form, yet no change in the holo-TK CD signal or convergence with that of apo-TK (Martinez-Torres et al., 2007). The apo-TK and holo-TK protein structures differ only in the formation of two cofactor binding loops in the active site (Nikkola et al., 1994; Sundstrom et al., 1992). This suggested that the cofactor-binding conformation changed initially

without significantly disrupting the enzyme secondary structure. The gradual non-cooperative loss of secondary structure at increasing temperatures prior to aggregation suggests a different effect on structure to that observed previously in the early urea-induced denaturation. Presumably, a number of weakly stabilised structural elements such as ordered loops become partially denatured as temperature increases, and eventually induce the formation of aggregates. The 10% non-cooperative loss of secondary structure is relatively significant so the denatured regions could easily, though not necessarily, have included the cofactor-binding loops. That the enzyme activity actually increases initially is at least consistent with the suggestion that the cofactor loops may be involved. Further studies with specific cofactor-loop mutations of the active site or detailed structural studies will be required to resolve this issue. Such mutations were carried out and presented later in Chapter 5 of this thesis.

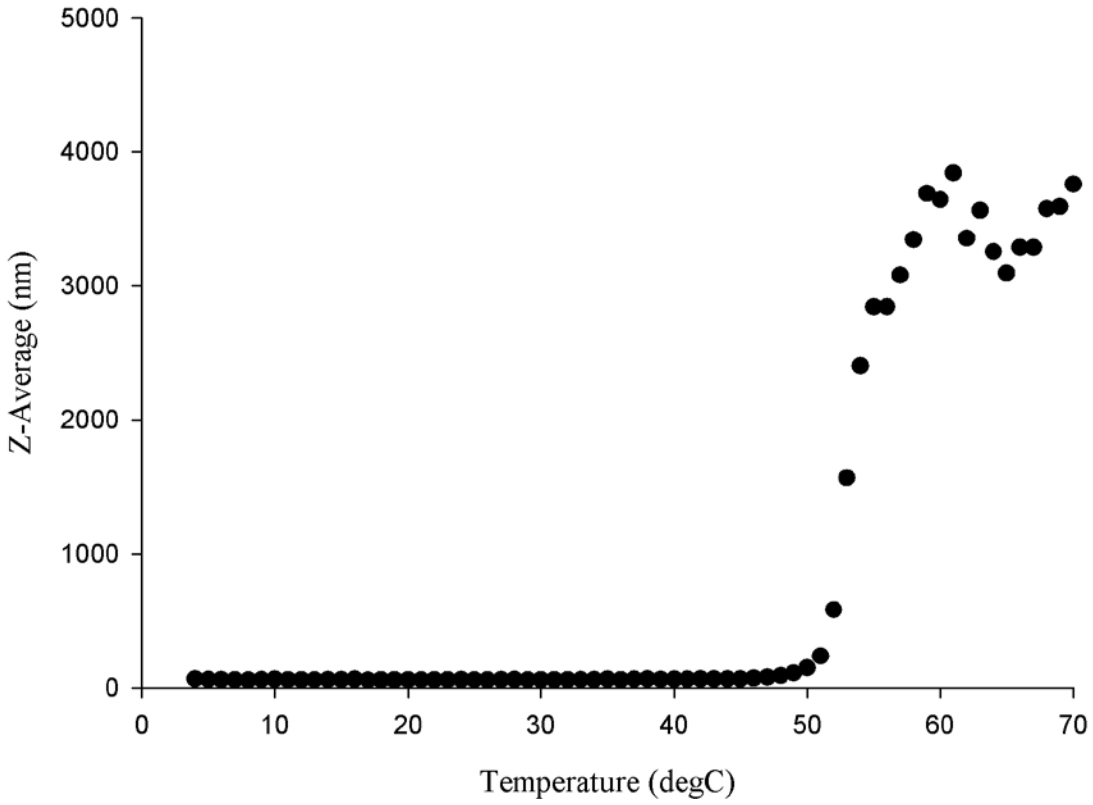

Figure 3-7. Average particle size in temperatures for apo-TK by dynamic light scattering. Aggregation temperature (T_{agg}) particle size of aggregates for apo-TK at 0.1 mg mL^{-1} (1.38 μM). Temperature was increased at 1.0 °C per minute from 4-70 °C for each measurement of particle size distribution. Mean diameter (Z-average) was calculated from the % volume distribution.

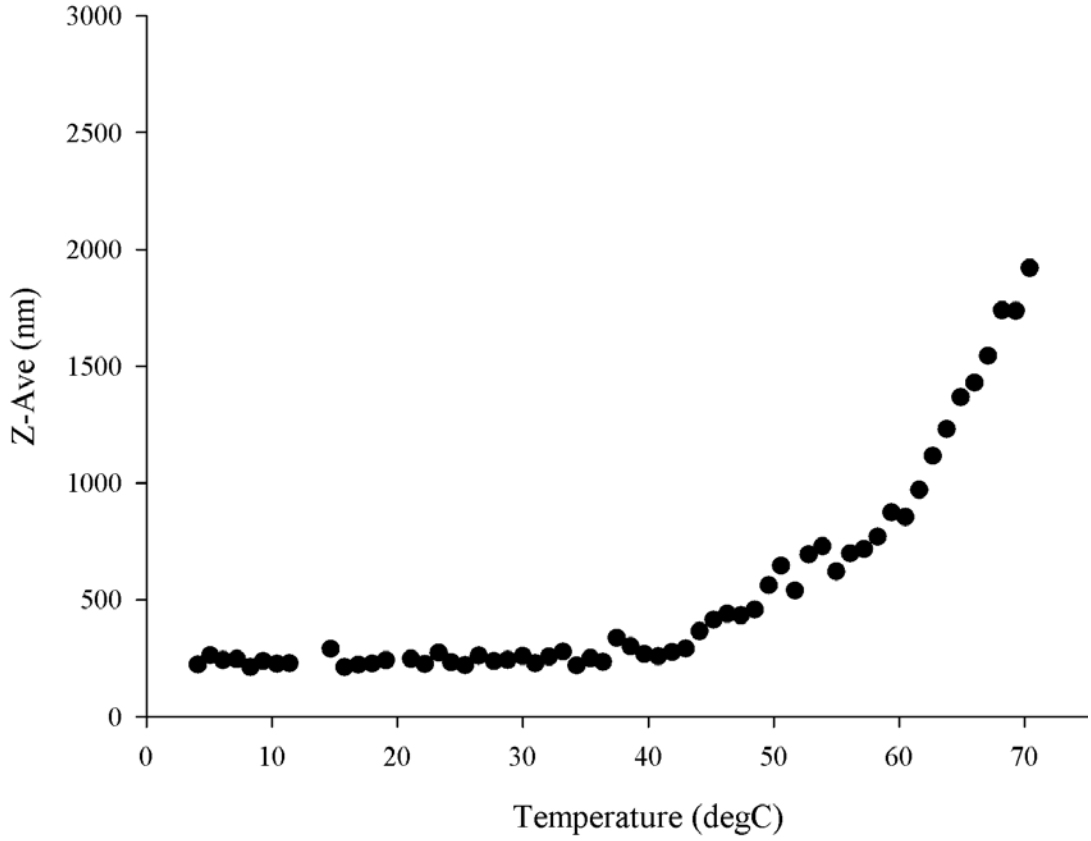

Figure 3-8. Average particle size in temperatures for holo-TK by dynamic light scattering. Aggregation temperature (T_{agg}) particle size of aggregates for holo-TK at 0.1 mg mL^{-1} (1.38 μM). Temperature was increased at 1.0 °C per minute from 4-70 °C for each measurement of particle size distribution. Mean diameter (Z-average) was calculated from the % volume distribution.

3.4 Conclusions

Holo-TK loses activity at above 55 °C due to irreversible aggregation which occurs at 58 °C. Surprisingly, heating at 55 °C and re-cooling of the enzyme progressively increased the enzyme activity due to annealing at 55 °C for 1 hour. DLS indicated that the protein remained as a soluble compact homodimer prior to aggregation at >58 °C.

The pH profile of holo-TK activity is asymmetric, and the optimum enzyme activity was confirmed to occur at pH 7. The enzyme was more tolerant to deactivation at high pH than at low pH, with 50% activity remaining even at pH 11. No loss of secondary or tertiary structure was apparent at pH 9, although apo-TK appeared to become more structured by CD. Simple dissociation of cofactors as proposed previously does not fully explain the partial inactivation at pH 9. Reorganisation of the cofactor binding loops in at least the apo-TK form may hinder cofactor access. Alternatively, they may have formed a non-native structure form that either has no affinity for cofactors, or that binds them in an inactive state. At low pH, denaturation and subsequent aggregation of holo-TK was the predominant cause of enzyme inactivation, both confirming and extending the previous suggestion from Mitra and coworkers that irreversible denaturation was the cause.

These results provide useful information for the engineering of TK enzymes with improved thermostability or extreme pH tolerance. For thermostability and tolerance to low pH, mutations may be usefully targeted towards regions of protein

sequence predicted to have a high propensity for aggregation. For retention of biocatalytic activity at high pH, stabilisation of the cofactor binding loops in their native holo-TK structure would be an attractive target. The mutagenesis targetted to cofactor binding loops for thermal stability is further studied here in Chapter 5.

Chapter 4

4. Impact of various co-solvents on Transketolase activity in their activity and structure

4.1 Introduction

Biocatalysis has become increasingly important for the synthesis of pharmaceuticals and agrochemicals, where the need for optically pure molecules is critical but also for food ingredients, neutraceuticals and fragrances (Schmid et al., 2001;Zaks 2001;Nestl et al., 2011). While biocatalysts are often limited in terms of their stability under industrial process conditions, directed evolution and rational enzyme engineering can potentially be used to address many of these issues, which include poor stability at extremes of pH, temperature and under oxidative stress (Dordick 1991;Brocklebank et al., 1999;Klibanov 2001;Eijsink et al., 2004;Eijsink et al., 2005).

Many syntheses involve organic substrates or products that are not soluble in water, resulting in a need for enzymes that operate efficiently in organic media or aqueous-organic mixtures. Furthermore, the use of organic solvents can decrease the degradation or re-arrangement of water sensitive compounds, and in some cases improve enzyme stability or even alter its enantioselectivity (Dordick 1991; Bryan et al., 1979). Many enzymes are already known to be able to function in both organic and aqueous media (Klibanov et al., 1994; Krishna et al, 2000). However, many

become rapidly inactive, even at low concentrations of organic co-solvents, and yet the mechanisms of their activity loss remain unclear. Activity loss is typically solvent concentration dependent, but is also found to vary with different organic solvents, potentially depending on their hydrophobicity (Cooney et al., 1974; Klibanov et al., 2001).

Enzymes typically have lower reaction rates in organic media relative to those in aqueous solutions, and yet they are also often found to retain their overall native structure (Pasta et al., 1988, Dong et al., 1996). However, direct structural investigations of enzymes that are either suspended or solubilized into organic media are difficult, and so in the past, activity assays have been relied upon to give an indirect probe of protein structure and function. As a result, the mechanism of partial inactivation of enzymes in organic solvents is still unclear and not well established for a wide range of enzymes, in particular the relative roles of surface or active-site dehydration, structural denaturation, partial unfolding or enzyme aggregation.

To take advantage of the benefits of organic solvents in biocatalysis, many efforts have been made to enhance enzyme activity and stability in organic solvents, particularly using enzyme immobilisation (Kreiner et al.,2005; Kvittingen et al., 1994; Shuge et al., 2008). Directed evolution has also successfully increased the tolerance of some enzymes to organic co-solvents (Moore and Arnold 1996, Moore and Arnold 1997; Badoei-Dalfard et al., 2010). However, rational or computational design of novel organic solvent tolerant enzymes, and their directed evolution, could be significantly improved if the mechanisms by which organic solvents cause enzyme inactivation were better understood.

The synthetic potential of TK has already been significantly improved by directed evolution, using a combination of structural inspection and phylogenetic analysis (Costelloe et al., 2008) to target saturation mutagenesis to selected active-site residues. Variants have been found from these libraries with enhanced and revered enantioselectivity (Smith et al., 2008), and improved activity towards various substrates including glycolaldehyde (Hibbert et al., 2007), propanal (Hibbert et al., 2008), and a range of other aliphatic (Cazares et al., 2010) and aromatic (Galman et al., 2010) aldehydes. However, many of these new substrates are poorly water soluble which has increased the need to explore the use of TK variants in the presence of organic co-solvents.

The performance of transketolases in the presence of organic solvents has not been studied to date, and the aim of this Chapter was to characterise the impact of various types of solvent on TK activity as well as to deduce any activity-structure relationships that might be used to guide future enzyme engineering efforts. It is important to understanding the mechanisms of enzyme inactivation as well as reversibility or irreversibility of the reactions therefore will give more informations in enzyme stability characterization leading to improve the controlling of the deactivation process . Organic co-solvents could mediate their effects on TK activity via one or more of several potential mechanisms that include: i) protein denaturation; ii) aggregation; iii) altering the flexibility or stability of local structure and domains; and iv) modulating the accessibility of water molecules or substrates into the active site.

Here we have used a range of biophysical studies to measure the response of both TK activity and structure to a range of commonly used organic solvents: acetonitrile (AcCN); *n*-butanol; ethyl acetate; isopropanol; and tetrahydrofuran (THF). Their impact on both the apo- and the more stable holo-enzyme was studied to examine the role of protein conformational stability in deactivation by organic solvents. We found that several factors contribute to the loss of TK activity in organic media, including changes in protein structure and the onset of aggregation. However, the more stable holo-TK form did not always retain more activity than the apo-TK form after exposure to organic solvents, indicating that solvent tolerance was not simply correlated to conformational stability.

4.2. Materials and Methods

All chemicals and solvents were obtained from Sigma-Aldrich UK.

4.2.1 pQR791 purification

N-terminally His6-tagged wild type *E. coli* transketolase was expressed from *E. coli* XL10-Gold (Stratagene, La Jolla, CA) containing the engineered plasmid pQR791, purified as described previously (Martinez-Torres et al., 2007), and in Section 2.4, then dialysed at 4 °C for 24 hours against 25 mM Tris-HCl, pH 7.0, and stored at 4 °C for a maximum of two weeks without loss of activity, and with no precipitation visible. Protein concentration was determined as described in Section 2.4.4.

4.2.2 Residual activities after incubation with organic solvents

Samples were divided into two groups. The first aimed to determine the impact of solvents on Apo-TK. Apo-TK 0.1 mg mL^{-1} (1.38 μM), was incubated with different % (v/v) of a range of solvents, for 3 h at 25 °C with 1000 rpm shaking, then incubated with 50 μL of cofactors (2.4 mM TPP, 9 mM $MgCl_2$) in 50 mM Tris-HCl, pH 7.0 for 20 minutes to form holo-TK before adding the 50 μL of substrates (50 mM HPA, 50 mM Glycoladehyde in 50 mM Tris HCl) to assay for residual activity. The second group aimed to determine the impact of organic solvents upon Holo-TK directly. Holo-TK 0.1 mg mL^{-1} (1.38 μM), was obtained by incubating Apo-TK with 50 μL of cofactor in 50 mM Tris-HCl, pH 7.0 (and 2.4 mM TPP, 9 mM $MgCl_2$) for 20 minutes at 25 °C with 1000 rpm shaking, and then incubated with different %

(v/v) solvents 3 h at 25 °C 1000 rpm. prior to dilution by addition of the 50 µL of substrate solutions. A 0% solvent control was included in both groups. All the incubations and reactions of both apo- and holo-TK were carried out in glass vials with a total final volume of reaction of 300 µL after adding substarte. Reaction samples were diluted 1:10 into 0.1% TFA (20µL of reaction and 180µL of 0.1% TFA) to stop the reactions, and then transferred into 96 micro-well plates for measuring of products by HPLC (Section 2.2.8). The final solvent dilution in % (v/v) is presented in the data as that obtained after adding the substrates.

4.2.3 Secondary structure monitored by circular dichroism (CD).

CD spectra (190-300 nm) were recorded on an AVIV 202 SF spectrometer (AVIV Associates, Lakewood, NJ) at 25 °C using a 1 mm path length quartz precision cell cuvette. One volume of wild-type transketolase at 0.5 and 0.1 mg mL^{-1} with/without 2.5 mM $MgCl_2$ and 0.25 mM TPP for holo-TK and apo-TK respectively, in 25 mM Tris-HCl, pH 7.0, and then solvent added to% (v/v). CD spectra were recorded at 0.5 nm intervals and averaged for 4 seconds at each wavelength for 3 h. Reducing agents were not included as this is typically not used in biocatalytic reactions with TK. A spectrum for 25 mM Tris-HCl, pH 7.0 buffer was subtracted from each recording.

4.2.4 Intrinsic fluorescence intensities

Purified wild-type holo- and apo-transketolase, with /with 0.5 mM TPP and 5 mM $MgCl_2$, respectively was prepared at 0.1 mg mL^{-1} in 25 mM Tris–HCl, pH 7.0. Samples were incubated at 25 °C in UV transparent 96-well microplates (Costar, Corning Incorporated, NY, USA). Fluorescence intensity was measured every 30

minutes for 6 hours from below the plate at 340 nm emission and 280 nm excitation using a FLUOstar microplate reader (BMG Labtechnologies Ltd., Aylesbury, UK). Due to the interference with measurements by an incompatibility of ethyl acetate with the sample plates that appears after longer incubations, the ethyl acetate incubations were carried out in glass vials before transferring samples to UV transparent 96-well microplates immediately prior to measurements.

4.2.5 Dynamic light scattering (DLS)

The particle size distributions of transketolase in the presence and absence of solvent was measured at 25 °C with a Zetasizer Nano S (Malvern Instruments Ltd., UK). Holo-TK at 0.1 mg mL^{-1} was prepared in 25 mM Tris-HCl, pH 7.0, with 0.5 mM TPP and 5 mM $MgCl_2$. Samples were incubated for 1, 2 and 3 hrs prior to data acquisition. Data were acquired in triplicate, with a 1 cm path length low volume disposable sizing cuvette. A control sample of buffers with or without cofactors was subtracted from each recording. The hydrodynamic diameters of each sample were calculated from the averaged-measurements using the Zetasizer Nano Series software V.4.20 (Malvern Instruments Ltd., Worcestershire, UK).

4.3 Results and Dicussion

4.3.1 Transketolase activity in organic solvents

To understand the effect of polar organic co-solvents upon TK stability, as well as the stabilising influence of cofactors upon the retained activity of TK after incubation with the solvents, we carried out experiments for both the apo- and holo-TK forms. Apo-TK was incubated with the organic solvents for 3 h and then incubated with the cofactor to form the holo-TK before adding the substrates. To test holo-TK, the apo-TK was first incubated with cofactors to form the holo-TK then incubated with organic solvents for 3 h before adding the substrates. The results shown in Figure 4-1 compare the effect of increasing final solvent concentrations upon the retained activity for apo-TK and holo-TK. In nearly all cases, the increased concentration of co-solvents eventually reduced the remaining activity to zero. It is also apparent from Figure 4-1 that apo-TK was apparently more stable to all of the solvents tested, except for *n*-butanol where apo-TK was less stable, and for isopropanol where the two forms had similar stability. For example, acetonitrile inactivated apo-TK and holo-TK by 50% at critical concentrations of 20% and 12% (v/v) respectively. Similarly, the activity of holo-TK reached 50% at approximately 3% (v/v) ethyl acetate whereas for apo-TK 50% inactivation occurred at approximately 6% (v/v) ethyl acetate. Nevertheless, apo-TK was always able to

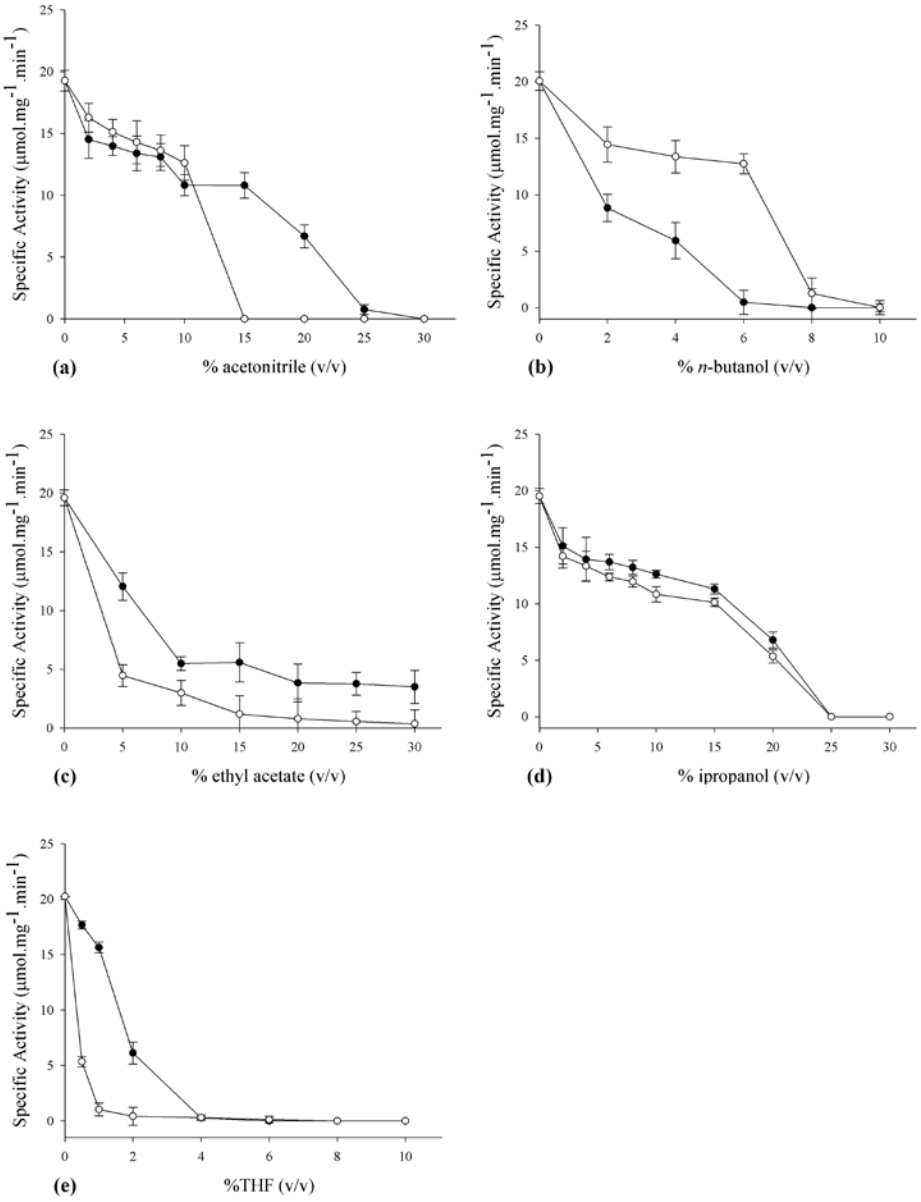

Figure. 4-1 Tolerance of transketolase to pre-incubation with solvents as measured by the retention of catalytic activity. Both (◖) Apo - and (○) HoloTK were compared for varying percentage by volume of (a) acetonitrile (b) *n*-butanol (c) ethyl acetate (d) isopropanol (e) THF. The activity were measure Samples were incubated with solvent in 50 mM Tris-HCl, pH 7.0 (and 2.4 mM TPP, 9 mM $MgCl_2$ for holo-TK) for 3 h at 25°C with 1000 rpm shaking. Enzyme activity was measured after a 1:10 dilution into 2.4 mM TPP, 9 mM $MgCl_2$, 50 mM Tris-HCl, pH 7.0, incubation for 20 minutes and then further 1:10 dilution by adding substrates to 50mM HPA and 50 mM GA in 2.4 mM TPP, 9 mM $MgCl_2$, 50 mM Tris-HCl, pH 7.0. The final solvent dilutions were % (v/v) after adding substrate.

retain a residual activity of at least 20%, even up to 30% ethyl acetate, whereas holo-TK activity tended to zero. This result can be partly explained in terms of the 8.3 g solvent/100 g water solubility of ethylacetate which is equivalent to 9.3% v/v (www.trimen.pl/witek/ciecze/old_liquids.html). Above this volume ratio the remaining solvent would simply form a separate organic layer. Therefore, the decrease in activity would be less effective above 9.3% v/v as observed for the apo-TK in particular. The slight decrease for both forms at above 9.3% v/v may be explained by the presence of the solvent-water interface with increasing surface area, where the protein could potentially be deactivated by denaturation at the surface.

In isopropanol, both apo and holo-TK behaved similarly with a gradual drop in activity until there was no activity in either case at 25% (v/v) isopropanol. THF was the most effective at deactivation with lower concentrations. Holo-TK was completely inactive by just 2% (v/v) THF and apo-TK by 4% (v/v) THF. By contrast, apo-TK was less stable to *n*-butanol than holo-TK with critical concentrations of 2% and 7% respectively giving rise to 50% activity. For both apo-TK and holo-TK in *n*-butanol the residual activity tended to zero before the solubility limit for *n*-butanol of (8.3 g solvent/100 g water, or 10.3% v/v) was reached.

The generally lower tolerance of holo-TK to co-solvents compared to apo-TK is counterintuitive given that holo-TK is thermodynamically more stable than apo-TK (Martinez-Torres et al., 2007; Esakova et al., 2005). The dependence on solvent concentration is also clearly not a simple one as can be seen when the inactivation profiles are considered more closely. For example with acetonitrile, apo-TK deactivated continuously but gradually as the solvent concentration was increased

from zero, and actually inactivated more than holo-TK initially. Holo-TK then inactivated with a sharp transition between 10% and 15% v/v solvent whereas the apo-TK continued to inactivate more gradually. A sharper transition for holo-TK also occurred with *n*-butanol and to a lesser degree with THF and ethylacetate. It may be that the sharp loss of holo-TK results from cooperative protein denaturation or a cooperative partial unfolding event, for example unfolding of the cofactor binding loops. However, the cause of inactivation for all solvents does not appear to simply relate to the thermodynamic stability of protein structure elements. Indeed, binding of solvent to the active site, dehydration of the active site, or aggregation of the protein could also play a role. Furthermore, it is possible that partial unfolding from the holo-TK could result in a native-like structure that is still different to, and more aggregation prone than that of the apo-TK form in most of the solvents.

4.3.2 Correlation of TK activity to calculated organic solvent properties

Although, all the organic-solvents in these experiments are polar, they show considerable variability in their impact on retained TK activity, including the critical concentrations for inactivation, the sharpness of the deactivation curves, and the relative effects upon the apo-TK and holo-TK forms. Previous work has suggested that the loss of enzyme activity in polar solvents is primarily due to the stripping of water from the protein surface and from the active site of the enzyme, where enzymes require water for the maintenance of the correct active-site geometry and hence the catalytic function and stability of enzyme (Prasad et al., 2002; Simon et al., 2007). The effectiveness of a polar solvent for dehydration of proteins might

therefore be expected to depend upon the polarity or hydrophobicity of the solvent, and the ability to form hydrogen bonds in place of water. The characteristics of each solvent used in terms of various theoretically calculated and experimentally determined physicochemical properties, is shown in Table 4-1.

The polar solvents can be categorized as either aprotic (acetonitrile, ethyl acetate and THF), or protic (*n*-butanol and isopropanol). This simple categorization appeared to have no obvious correlation to the amounts of the co-solvents required for either half or complete enzyme inactivation. In fact as seen in Figure 4-2 the topological polar surface area (TPSA) calculated for each co-solvent molecule gave the best correlation to the volume fraction of solvent required for complete inactivation of the enzyme activity (R^2=0.53). Only isopropanol deviated signficantly from this correlation, and omitting this solvent increased the correlation to R^2 = 0.92 (Figure 4-2). By contrast, other calculated solvent properties correlated very poorly to the fraction of co-solvent required for inactivation, such as log *P* (R^2=0.25), the number of potential hydrogen bonding sites (R^2=0.07), the solvent dipole moment (R^2=0.002), and the dielectric constant of the co-solvent (R^2=0.045). Similar correlations to the enzyme half-inactivation points were also generally poor. Clearly the correlation with TPSA is oversimplified, but a linear combination with other factors in Table 4-1 may be able to explain the trend though this will require a linear regression to data from a much greater number of co-solvents.

As the co-solvent properties were not simply correlated to loss of enzyme activity, we sought to determine whether activity loss with each solvent resulted from one or more additional underlying mechanisms which could potentially include

protein denaturation, aggregation, active-site binding and inhibition, altered conformational dynamics, or altered cofactor binding, among other more subtle effects.

Table 4-1. Physicochemical properties of the polar organic solvents.

Solvent	$[S_{100}]$[a] (%v/v)	$[S_{50}]$[a] (%v/v)	TPSA[b] ($Å^2$)	logP[b]	Vol[b] ($Å^3$)	MW[b] (Da)	HB[c]	Dielectric constant[d]	Dipole[d] (D)
iPrOH	25	15	20.2	0.42	70.6	60	2	19.9	1.66
AcCN	15	12	23.8	0.47	46.1	41	1	37.5	3.44
THF	2	0.4	9.23	0.70	78	72	2	7.58	1.75
EtoAc	20	3	26.3	0.76	90.5	88	4	6.02	1.88
nBuOH	9	6.5	20.2	1.12	87.6	74	2	17.5	1.75
R^2 [e]			**0.53**	**0.25**	**0.02**	**0.01**	**0.07**	**0.045**	**0.002**

[a]Concentration of solvent required for complete $[S_{100}]$, and half $[S_{50}]$, enzyme inactivation. [b]Calculated using the Molinsky online software tool (www.molinspiration.com). [c]Number of potential hydrogen bond acceptor and donor sites. [d]Obtained from the Louisiana State University Macromolecular Studies Group Server (http://macro.lsu.edu/). [d]R^2 values are for linear Pearson correlations to $[S_{100}]$.

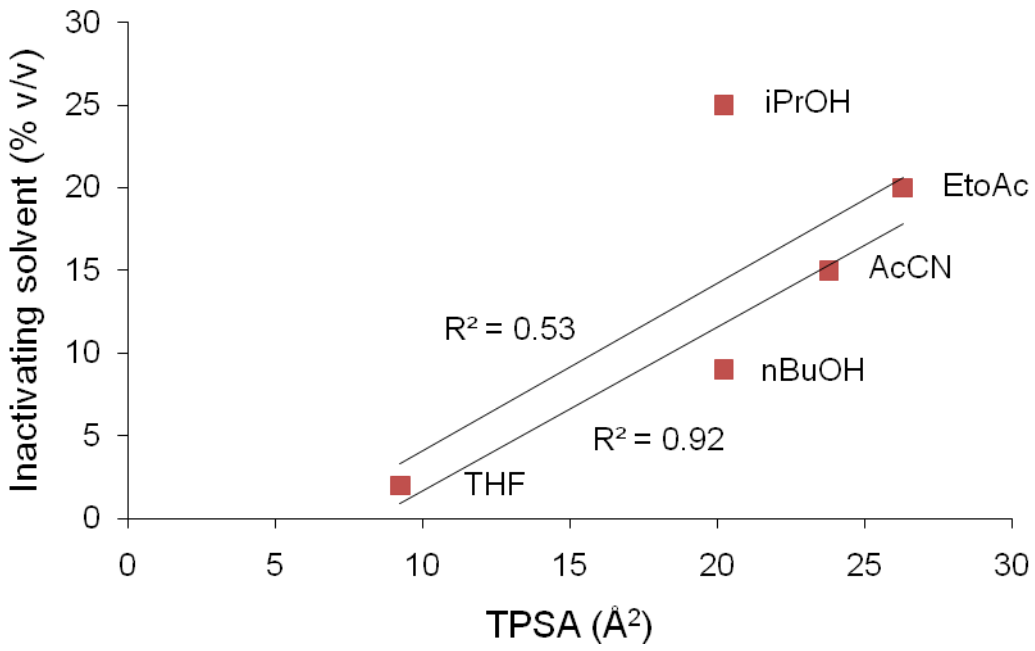

Figure 4-2 Correlations between topical polar surface area (TPSA) of the solvent and the concentration of solvent required to completely inactivate holo-TK, both including (R^2=0.53) and excluding (R^2=0.92) isopropanol (iPrOH).

4.3.3 Secondary structure of apo-TK and holo-TK in polar co-solvents.

To determine the impact of co-solvents on the secondary structure content of TK, and also whether the enzyme was denaturing or aggregating, far-UV circular dichroism (CD) spectra were obtained for both apo-TK and holo-TK, using a volume fraction of solvent that results in at least 50% inactivation of the enzyme. It was already known from yeast apo-TK and holo-TK crystal structures (Sundstrom et al., 1992) and from previous CD spectra in aqueous buffers (Martinez-Torres et al., 2007), that apo-TK contains marginally less secondary structure content than holo-TK as a result of the increased flexibility of the two cofactor-binding loops.

The far-UV CD spectra of apo-TK indicated that the protein retained native-like secondary structure in 20% acetonitrile, 8% *n*-butanol, 10% ethyl acetate or 20% isopropanol, whereas approximately half of the secondary structure was lost in 2% THF (Figure 4-3A). By comparison, holo-TK became almost completely denatured in both acetonitrile and THF. These data suggested that global protein denaturation was the primary cause of enzyme inactivation by THF, where the degree of inactivation is linked to the degree of denaturation for both apo-TK and holo-TK. However, the stability to THF is greater for apo-TK relative to holo-TK, opposite to that observed for stability to thermal or urea unfolding, implying that the denaturation pathway is different, and that the structured cofactor loops, or presence of cofactors in holo-TK play a role in promoting the unfolding by THF.

Acetonitrile at 20% v/v only appeared to denature the holo-TK form, which was consistent with the complete loss of holo-TK activity after a sharp cooperative transition at 10-15% v/v acetonitrile. The retention of secondary structure for apo-TK at 20% v/v is also consistent with the gradual non-cooperative deactivation leading to half-inactivation of apo-TK after incubation for 3 hours in the same conditions. Given that apo-TK has a lower conformational stability than holo-TK when denatured by urea (Martinez-Torres et al., 2007), simple denaturation by acetonitrile is again unlikely to be the sole mechanism of inactivation by acetonitrile. The gradual loss of activity for apo-TK points to a non-structural mechanism of deactivation, whereas the structured cofactor loops or binding of cofactors in holo-TK promotes an additional structural unfolding mechanism, similar to that observed for THF.

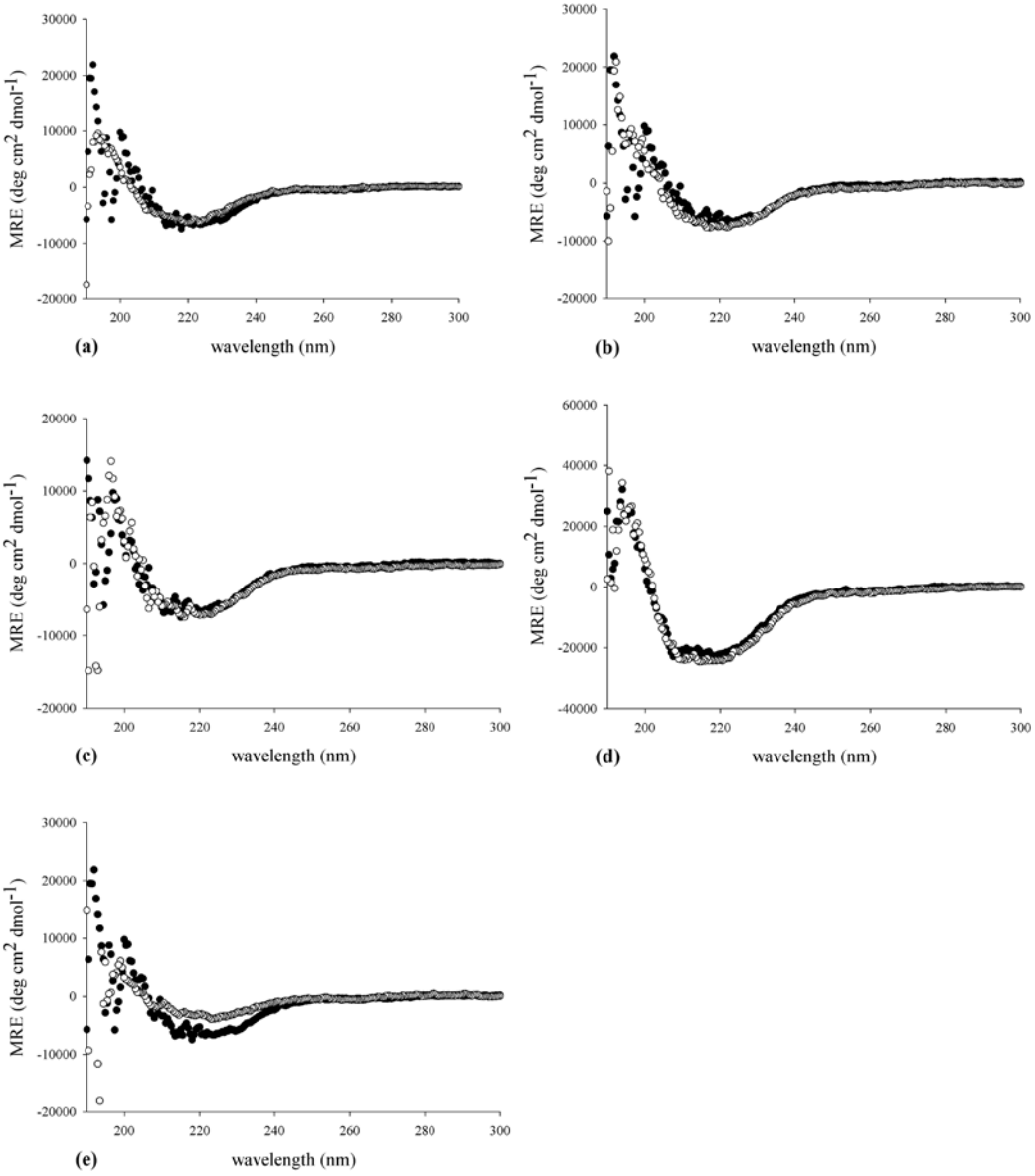

Figure 4-3 A. Circular dichroism spectra of apo-transketolase in the presence of organic solvents. Apo-TK (0.1 mg mL^{-1}) in 25 mM Tris-HCl, pH 7.0: (●) without solvent; and (○) with solvent at (a) 20% acetonitrile (b) 8% *n*-butanol (c) 10% ethyl acetate (d) 20% isopropanol (e) 2% THF, was incubated for 3 h at 25 °C before full spectra (195–300 nm) were acquired.

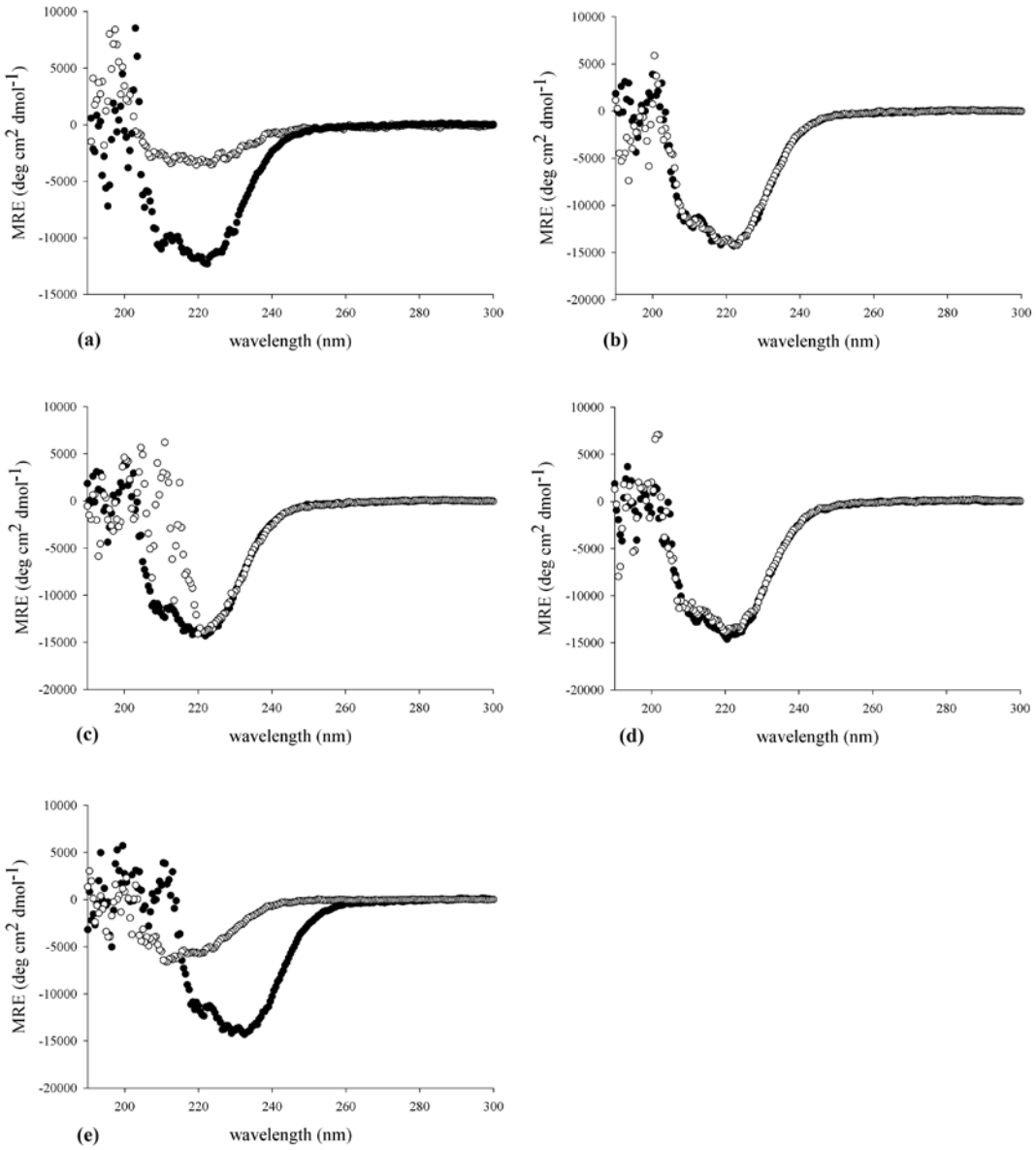

Figure 4-3 B. Circular dichroism spectra of holo-transketolase in the presence of organic solvents. Holo-TK (0.5 mg mL^{-1}) in 25 mM Tris-HCl, pH 7.0, 2.5 mM $MgCl_2$, 0.25 mM TPP: (●) without solvent; and (○) with solvent at (a) 20% acetonitrile (b) 8% *n*-butanol (c) 10% ethyl acetate (d) 20% isopropanol (e) 2% THF, was incubated for 3 h at 25 °C before full spectra (195–300 nm) were acquired.

Denaturation of protein secondary structure did not occur at all for apo-TK or holo-TK in 8% *n*-butanol, 10% ethyl acetate or 20% isopropanol. However, for ethyl acetate, a fully native-like spectrum of the holo-TK form was obtained at 220-300 nm, whereas the solvent appeared to interfere with the CD spectrum below 220 nm. This was due to saturating absorption of light by ethyl acetate at below 220 nm when combined with the higher holo-TK concentration (0.5 mg/ml) compared to that used for apo-TK (0.1 mg/ml). The differences signal between control spectra, in apo-TK was found due to using a different batch of enzyme.

For all solvents tested, perturbation of the active site structure, loss of cofactor binding or the formation of aggregates could not yet be ruled out as these can potentially occur without significantly affecting the CD spectra. Further analysis by intrinsic fluorescence intensity and dynamic light scattering was therefore carried out.

4.3.4 Tertiary structure of apo-TK and holo-TK in polar co-solvents

The change in intrinsic fluorescence intensity of *E. coli* TK as it is denatured is already known to be complex. For example, urea denaturation shows an initial increase in fluorescence intensity followed by a decrease at higher urea concentrations (Martines-Torres., et al 2007). The addition of co-solvents led to an increase in the intrinsic fluorescence of both apo-TK and holo-TK in acetonitrile, *n*-butanol and isopropanol (Figure. 4-5 and 4-6). For apo-TK, the increases were monotonic from 0% v/v with acetonitrile and *n*-butanol, but occurred monotonically at above 10% for isopropanol. These curves all mirrored the gradual inactivation for

apo-TK with acetonitrile or *n*-butanol, and also the sharper inactivation transition at above 10% isopropanol. By contrast, holo-TK gave abrupt fluorescence intensity transitions at 15% acetonitrile, 8% *n*-butanol and 20% isopropanol, which coincided with the sharper transition points for inactivation of the holo-TK.

For acetonitrile (apo-TK only), *n*-butanol and isopropanol, the increases in fluorescence intensity coupled with the retention of secondary structure as observed by CD, suggested either the gradual weakening of tertiary structure to form an inactive molten globule-like species, an indirect effect of aggregate formation upon fluorescence intensity, or a simple de-quenching of solvent exposed tryptophan and tyrosine residues with an increasingly non-polar solvent. The generally monotonic increases in fluorescence intensity for apo-TK in acetonitrile and *n*-butanol indicated that these changes were non-cooperative, and therefore not linked to any cooperative protein unfolding events.

By contrast, for holo-TK the transitions with acetonitrile, *n*-butanol and isopropanol were sharper which suggested that more cooperative structural changes occurred. The sharp transition at 15% acetonitrile for holo-TK but not for apo-TK was consistent with the significant loss of secondary structure that was observed for holo-TK only at 20% acetonitrile. Acetonitrile at 15% v/v therefore appeared to denature both the secondary and tertiary structure of holo-TK, whereas for apo-TK the formation of an inactive native-like, molten globule-like, or aggregate species was gradual, and also protective in some way whereby the activity retained by the apo-TK was greater than for holo-TK at above 10% acetonitrile. The sharp transitions with *n*-butanol and isopropanol for holo-TK fluorescence intensity,

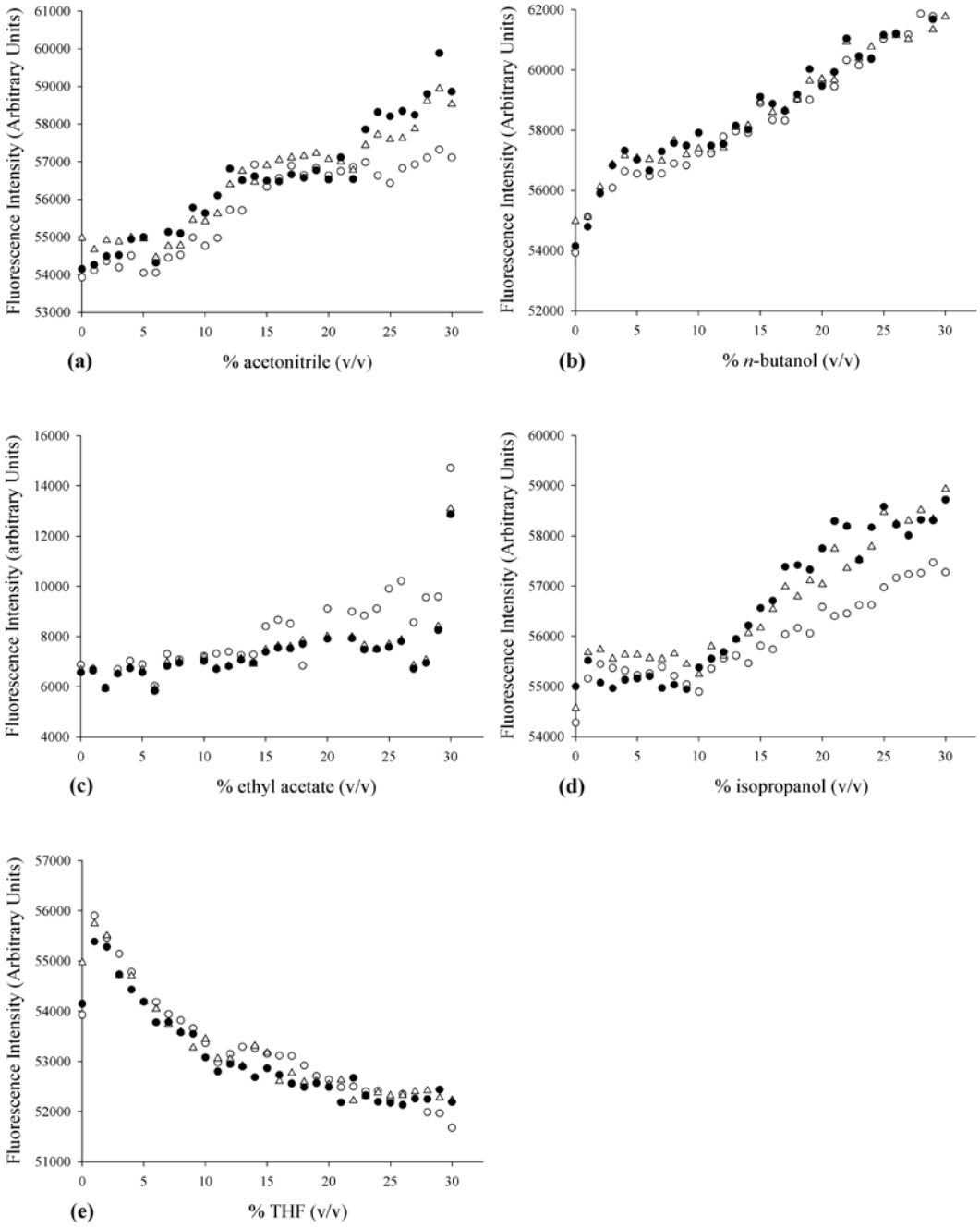

Figure 4-5. Fluorescence intensity measurements of apo-transketolase in the presence of organic solvents. Fluorescence intensity was measured at 340 nm with excitation at 280 nm. Apo-TK at 0.1 mg mL^{-1} in 25 mM Tris-HCl, pH 7.0 was incubated with (a) acetonitrile (b) *n*-butanol, (c) ethyl acetate (d) isopropanol (e) THF for (○) 1 hr, (Δ) 2 hr ,(●) 3 hr at 25 °C prior to measurements.

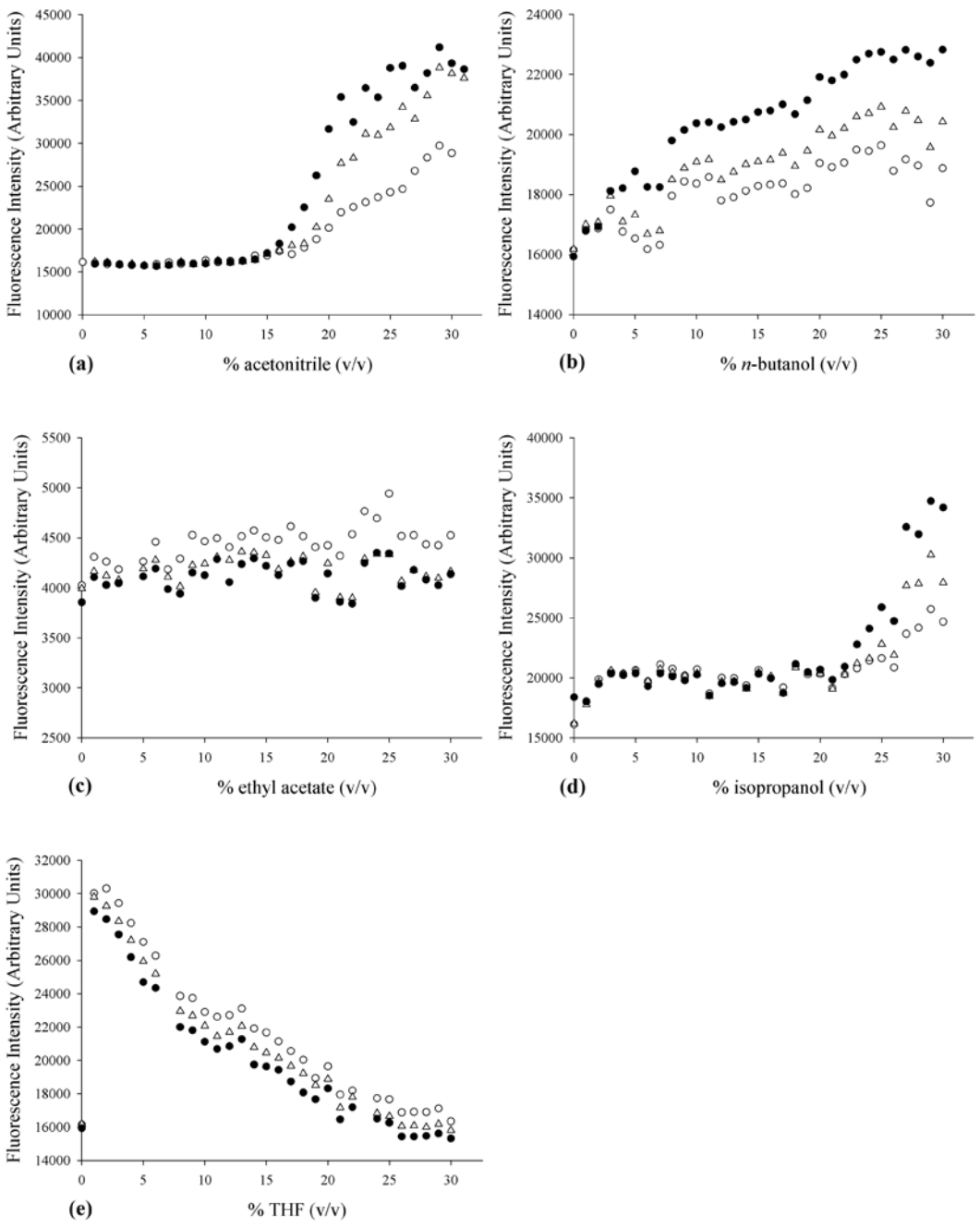

Figure 4-6 Fluorescence intensity measurements of holo-transketolase in the presence of organic solvents. Fluorescence intensity was measured at 340 nm with excitation at 280 nm. Holo-TK at 0.1 mg mL^{-1} in 5 mM $MgCl_2$, 0.5 mM TPP, 25 mM Tris-HCl, pH 7.0, was incubated with (a) acetonitrile (b) *n*-butanol (c) ethyl acetate (d) Isopropanol (e) THF for (○) 1 hr, (Δ) 2 hr ,(●) 3 hr at 25 °C prior to measurements.

coupled to the retention of secondary structure suggested the cooperative formation of inactive molten globule-like species and/or aggregates.

For ethyl acetate, there was no significant change in fluorescence intensity for either apo-TK or holo-TK, although for apo-TK, the intensity increased sharply at 30% ethyl acetate. As the CD spectra also showed no loss of secondary structure for apo-TK or holo-TK in ethyl acetate, it appeared that the loss of TK activity by more than 50% at 10% ethyl acetate was due to mechanisms other than a major change in structural conformation of enzyme. For example, aggregation of native-like proteins, active site replacement of water molecules, or gradual modification of the pK_as of key catalytic residues could not yet be ruled out.

For THF, the fluorescence intensity for both apo-TK and holo-TK initially increased sharply to a maximum at just 1% v/v THF, and then gradually decreased until levelling off at approximately 30% v/v. This increase in fluorescence intensity followed by a decrease at higher co-solvent concentrations, was consistent with the formation of an intermediate state and then subsequent denaturation, similar to the denaturation pathway observed previously with urea (Martinez-Torres et al., 2007). Partial loss of apo-TK secondary structure, and complete loss of holo-TK secondary structure at 2% THF was also observed by CD, and so the initial increase and subsequent decrease in fluorescence intensity was consistent with a concomitant loss of both tertiary and secondary structure. When compared with the inactivation profiles in Figure 4-1, these data suggest that population of the intermediate state that produces a maximum fluorescence intensity at 1-2% v/v THF, also coincides with

significant loss of activity. Indeed the intermediate state observed in the urea denaturation pathway (Martinez-Torres et al., 2007), was similarly inactive.

Apo-TK and holo-TK were both completely inactive by 4% v/v THF (Figure 4-1), and holo-TK was fully denatured at 2% v/v THF (Figure 4-3B). The continued monotonic decrease in fluorescence intensity at above 5% v/v THF therefore suggested an additional underlying influence of THF upon the fluorescence of the denatured state.

The time dependence of fluorescence intensity changes for holo-TK at critical solvent concentrations is shown more clearly in Figure 4-7. Denaturation with THF was essentially equilibrated within 1 hour as very little additional change occurred beyond that (Figure 4-5, 4-6 and 4-7). By contrast, the change in fluorescence intensity was much slower for acetonitrile, *n*-butanol and isopropanol, indicating that there was either a slower diffusive process for these solvents into the protein core, or a slow accumulation of aggregates (Figure 4-7), or both. There was also some evidence of solvent concentration-dependent lag phases in the time-dependent fluorescence intensities with these solvents, and was particularly apparent for acetonitrile, but less so for isopropanol and *n*-butanol. This is typical of the formation of aggregates which accelerates when a critical concentration of nucleating oligomer, partially unfolded species or molten-globule state is reached (Li et al., 2010).

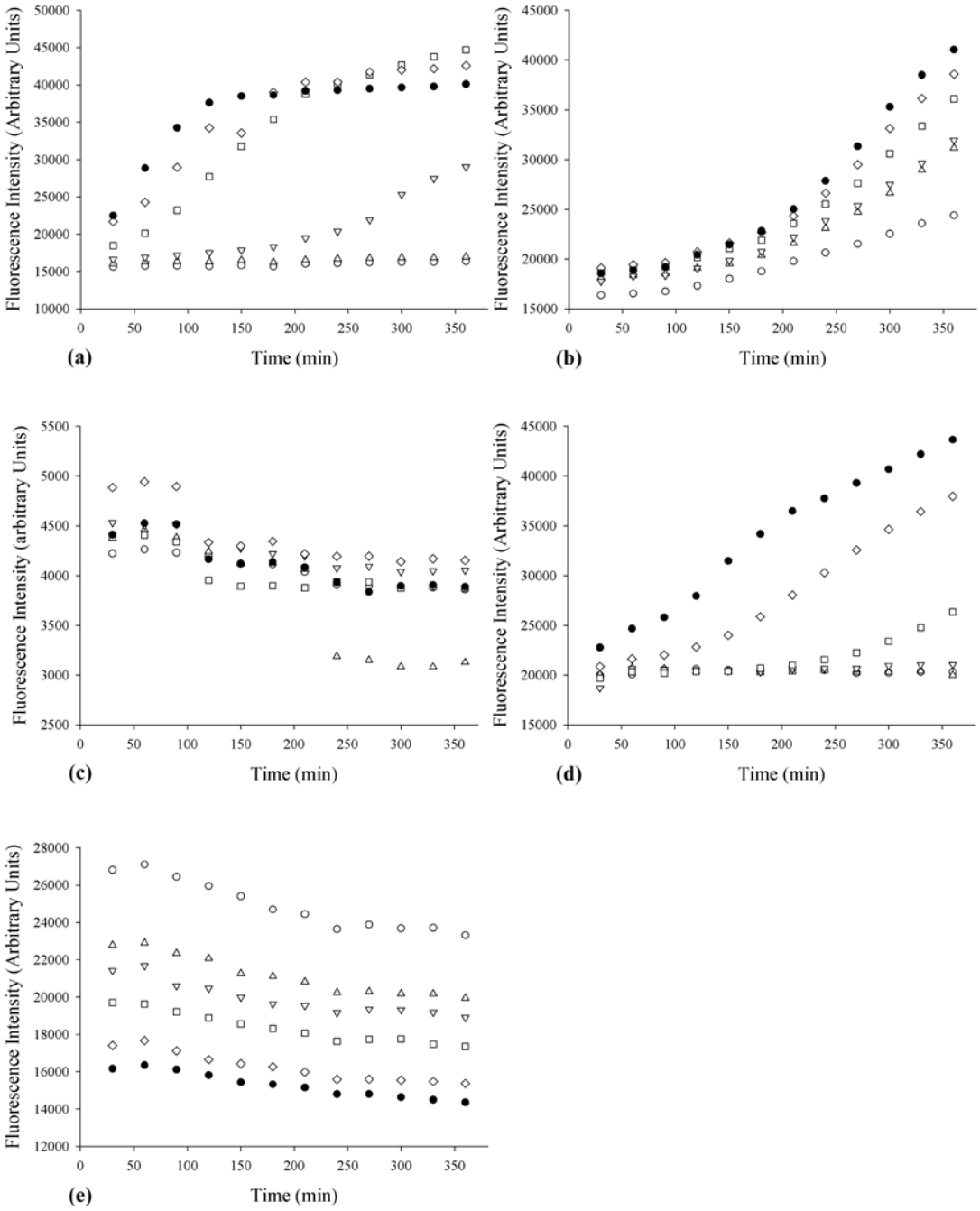

Figure 4-7 Time dependence of fluorescence intensity changes at critical solvent concentrations for holo-TK. Fluorescence intensity was measured at 340 nm with excitation at 280 nm. Holo-TK at 0.1 mg mL^{-1}, in 5 mM $MgCl_2$, 0.5 mM TPP, 25 mM Tris-HCl, pH 7.0, was measured every 30 min for 6 h at 25 °C in (○)5, (Δ)10, (▽)15, (□) 20, (◊) 25% and (●) 30% (a) acetonitrile (b) *n*-butanol (c) ethyl acetate (d) isopropanol (e) THF.

4.3.5 Particle size distributions from dynamic light scattering

Aggregation could potentially explain many of the events described above. To determine the presence of aggregates and their relative role in enzyme inactivation, we used dynamic light scattering (DLS) to measure particle size distributions in the presence of the co-solvents (Figure 4-8). Holo-TK in the absence of organic co-solvent gave a particle size of 8-9 nm (Littlechild et al., 1995) as expected for the native homodimer. At 20% (v/v) acetonitrile and 8% (v/v) *n*-butanol, holo-TK at 0.1 mg ml^{-1} contained aggregates of approximately 2000 nm. At 20% isopropanol a very small peak at 400 nm was observed, but more significantly, the monomer peak shifted to approximately 15 nm indicating the formation of a small soluble oligomer, or otherwise an extremely expanded or elongated monomer in a partially unfolded intermediate or molten globule-like state.

It should be noted that DLS is extremely sensitive to even small amounts of aggregate which can suppress the native monomer peak in proportion to the relative cubes of their diameters. Therefore, it is very possible that the 15 nm state was present also for acetonitrile or *n*-butanol, but that the smaller (400 nm) and less populated aggregate obtained with isopropanol allowed this state to be observed only in this case by DLS. However, these results are consistent with the population of aggregates in all three of these co-solvents, but in each case preceded (at lower co-solvent concentrations and/or incubation times) by the formation of an inactive state. For acetonitrile this was a partially denatured state with some loss of both secondary and tertiary structure. Aggregation of holo-TK in acetonitrile is similar to that

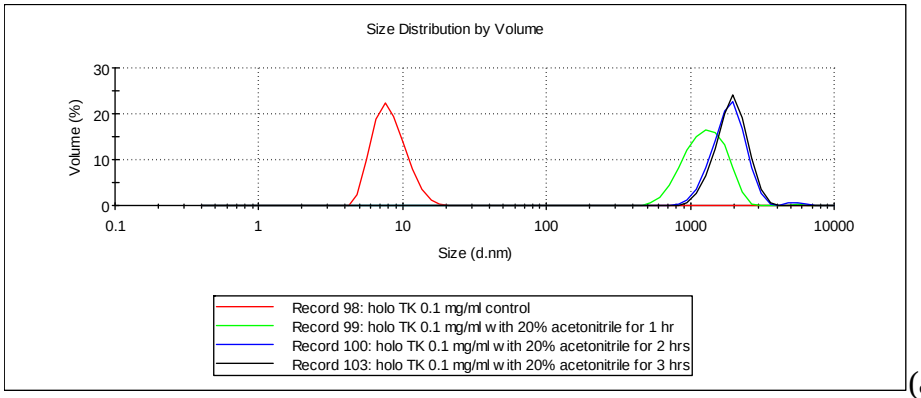

(a)

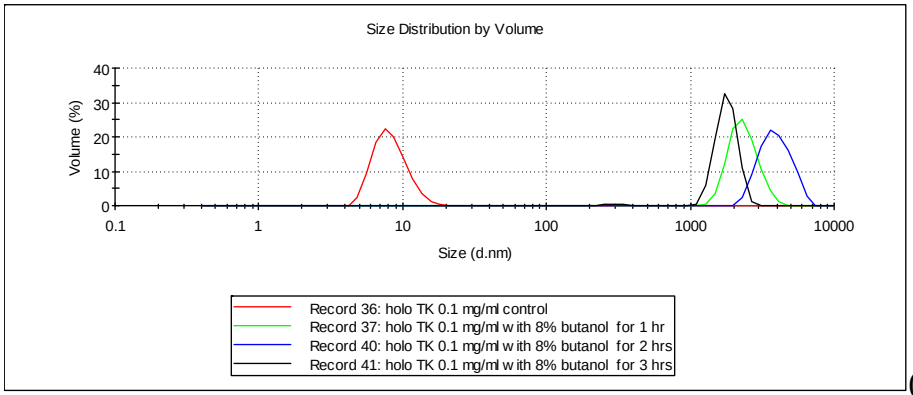

(b)

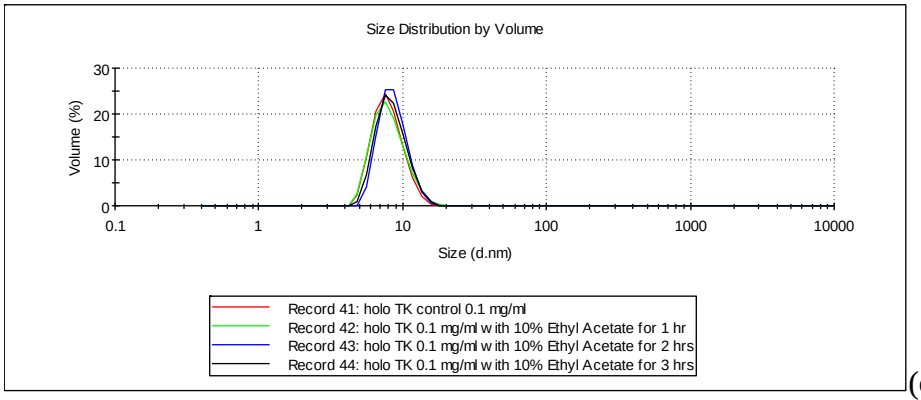

(c)

Figure 4-8 (a-c). Size distribution volume (%) of holo-TK estimated by dynamic light scattering (DLS) in the presence of organic co-solvents. Samples contained 0.1 mg mL^{-1} protein in 25 mM Tris-HCl, pH 7.0, with cofactors (0.5 mM TPP and 5 mM $MgCl_2$), and (a) 20% acetonitrile, (b) 8% *n*-butanol, or (c) 10% ethyl acetate. Samples were incubated for 1, 2 and 3 h at 25 °C before measurement.

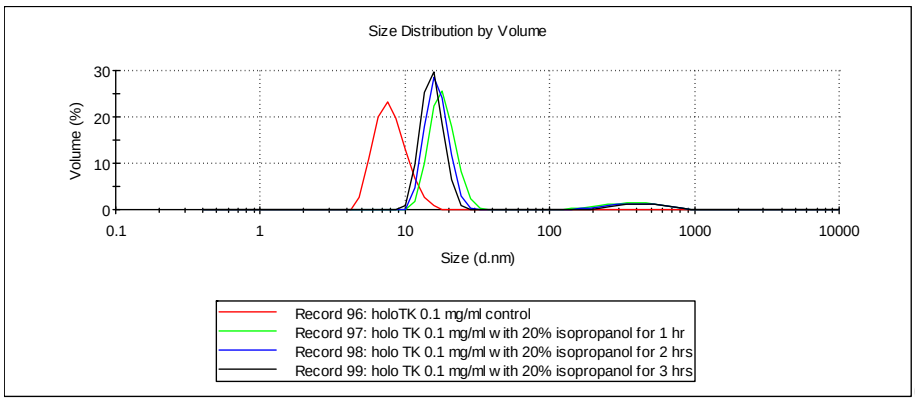

(d)

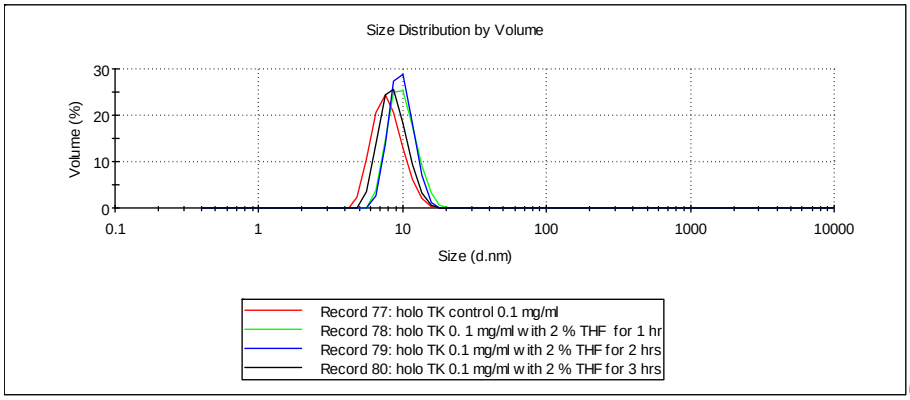

(e)

Figure 4-8 (d-e). Size distribution volume (%) of holo-TK estimated by dynamic light scattering (DLS) in the presence of organic co-solvents. Samples contained 0.1 mg mL^{-1} protein in 25 mM Tris-HCl, pH 7.0, with cofactors (0.5 mM TPP and 5 mM $MgCl_2$), and (d) 20% isopropanol or (e) 2% THF. Samples were incubated for 1, 2 and 3 h at 25 °C before measurement.

observed previously upon incubating polyethylene glycol-subtilisin with acetonitrile (Pasta et al., 1988). Their solutions became progressively turbid and after 2 h almost no protein was detectable in solution. This denaturation aggregation process was also in agreement with the half-life of the activity in acetonitrile (Pasta et al., 1988).

For *n*-butanol the first inactive state leading to aggregation was most likely a locally unfolded or molten globule-like monomer, whereas for isopropanol, it

appeared to be a small (15 nm) oligomeric state, or potentially a molten globule-like monomer. The formation of molten globules with isopropanol and *n*-butanol is consistent with previous observations that alcohols tend to disrupt tertiary structure and leave the secondary structure interactions largely undisturbed (Babu et al., 2000). This was thought to be because they have some hydrophilic component but are only moderate competitors for amide hydrogen bonds. However, the increase in holo-TK size from 9 nm to 15 nm as observed by DLS in isopropanol, is possibly too large to be due to the formation a molten globule state. However, this doesn't rule out its formation in isopropanol as such a state may instead have preceded the formation of the soluble oligomer observed at 15 nm.

At 10% v/v ethylacetate the holo-TK retained a protein with native-like dimensions of approximately 8-9 nm, and no evidence of aggregate formation was observed. This suggests that ethylacetate either retained the native structure, or formed a molten globule state that was still relatively compact. However, the CD and fluorescence intensity data showed that the secondary and tertiary structure of TK is still native-like at 10% v/v of this solvent. Inactivation by ethylacetate is therefore mainly due to non-structural mechanisms, unlike for the other solvents.

At 2% v/v THF, the size of the holo-TK molecule was observed to increase slightly to 10 nm which is consistent with this solvent causing the unfolding of both secondary and tertiary structure to form a denatured and inactive monomeric state, without leading to any aggregate formation.

4.3.6 Comparison of deactivation mechanisms for different solvents.

Overall, the solvents demonstrated several different underlying mechanisms for holo-TK inactivation which fit along a continuum that reflects the partial solvent TPSA previously weakly correlated to retained activity in Figure 4-2. A summary of the effects of solvents on various observations is summarised in Table 4-2.

Table 4-2. Effects of polar organic co-solvents on holo-TK structure and activity.

Solvent	$[S_{100}]$[a] (%v/v)	TPSA (Å^2)[b]	CD	FLI[c]	FLI(t)[d]	DLS
THF	2	9.23	Denatured	Intermediate at 1% Denatured at 2%	rapid	monomeric
iPrOH	25	20.2	Native	Increase at >20%	slow	oligomer
nBuOH	9	20.2	Native	Increase at 7-8%	slow	aggregate
AcCN	15	23.8	Denatured	Increase at >15%	slow	aggregate
EtoAc	20	26.3	Native	Native	v. slow	monomeric

[a]Concentration of solvent required for complete holo-TK enzyme inactivation. [b]Total Polar Surface Area (TPSA), calculated using the Molinsky online software tool (www.molinspiration.com). [c] Fluorescence intensity. [d] Time dependence of fluorescence intensity.

Ethylacetate was found to preserve native-like structure and has the highest TPSA of 26.3 Å^2 (Table 4-2). Acetonitrile was weakly denaturing of both secondary and tertiary structure, leading to aggregate formation, and has the next highest TPSA (23.8 Å^2). Both isopropanol and *n*-butanol have a yet lower TPSA of 20.2 Å^2, and formed molten globule-like states with retained secondary structure, but led to soluble oligomers and large aggregates respectively. Finally, THF was found to be

by far the strongest denaturant, leading to loss of secondary and tertiary structure, without forming aggregates, and has the lowest TPSA value of 9.23 $Å^2$. This trend may reflect the ability of solvents with smaller TPSA to penetrate the protein structure more rapidly, as reflected in the time dependence of the fluorescence intensity measurements. Hence, smaller TPSA solvents can fully denature the protein rapidly before slower aggregation events occur. At the other extreme, solvents with large TPSA such as ethylacetate do not readily penetrate protein structure leading to a retention of native structure and no aggregation. Solvents with intermediate TPSA penetrate protein structure, but slowly which then encourages aggregates to form from partially denatured states.

It was observed in Figure 4-2 and Table 4-1, that TPSA was correlated to the concentration of co-solvent required to achieve complete inactivation, with the exception only of isopropanol. Interestingly, isopropanol was the only solvent to form small soluble aggregates. The solvent with the same non-polar surface area, *n*-butanol, formed larger aggregates instead. This difference may be a reflection of the difference in steric bulk between the two otherwise similar solvents. Isopropanol is branched, whereas the higher molecular weight *n*-butanol is linear. The branched isopropanol may be forming a more ordered layer of solvent at the protein surface than the more flexible *n*-butanol, which could therefore limit the formation of larger aggregates.

Co-solvents that retained more native structure (eg. ethyl acetate) were found to require higher concentrations to achieve inactivation than those that were stronger denaturants (eg. THF). While this appears to be intuitive, it should be noted that

complete inactivation was also achieved upon reaching a different degree of structural denaturation for each co-solvent. This suggests a second underlying mechanism that is non-structural, which may for example be due to increasing dehydration of the active site at higher concentrations required for inactivation with the less chaotropic co-solvents. For ethyl acetate, this underlying but as yet undetermined mechanism pre-dominates, whereas at the other extreme with THF, protein denaturation is the primary cause of inactivation. Previous studies proposed that the prolonged exposure to organic solvents leads to a decrease in enzyme dynamic and active-site polarity and a reorientation of the active site residues. These affect the ionization state of the catalytic residues as well as the stability of transition states and intermediates, resulting in reduced enzyme activity (Bansal et al., 2010). However, the differences in mechanism observed for holo-TK in different solvents highlights the difficulty in finding simple explanations or correlations to individual solvent properties. Indeed it is quite likely that the mechanisms may also be dependent on the properties of the enzyme under study, making future generalisations or predictions across solvent and protein combinations extremely challenging.

4.4 Conclusions

The catalytic properties of TK varied with the % (v/v) of co-solvents and this behaviour was different across the group of polar solvents. The presence of an organic solvent constitutes a risk to enzyme inactivation during biocatalysis. It is therefore very useful to be able to conclude how organic substances interact with enzyme molecules and their effect on the enzyme in terms of stability and activity.

The reduction of enzyme activity at very high levels of dehydration by pure organic solvents was previously suggested to be explained by conformational changes that could alter the active site, consistent with the observation that enzymes display much more native structure in pure organic solvents than in aqueous organic mixture.

The results observed with transketolase in aqueous-solvent mixtures instead implied that the solvent dependence of catalytic activity cannot be simply explained by only one mechanism such as active site binding or replacement of water molecules, and the effect of different solvents on protein structure penetration, denaturation and aggregation must also be considered.

Overall, all organic co-solvents might be considered to have a denaturing tendency towards proteins. However, the total polar surface area (TPSA) of the co-solvent is a key factor which appears to affect the ability at which the solvent can penetrate and denature the protein. As the solvents be able to penetrate, for example by THF which had the lowest TPSA value, appeared to be able to penetrate and denature TK more to a fully denatured state, which avoided the formation of aggregates. Less penetration by larger TPSA solvents resulted in partial and take

longer time for denaturation which promoted the formation of aggregates or small soluble oligomers. The largest TPSA solvent, ethylacetate appeared to be unable to penetrate and denature TK, yet it still led to deactivation of the enzyme. The latter effect highlights that the solvents can inactivate the enzyme via modulation of for example active site residues or replacement of essential water molecules. An ideal solvent is therefore one that is tolerated by the enzyme active site, but also one with a high TPSA value that therefore less penetrate the protein structure and cause denaturation or aggregation.

Chapter 5

5. Mutagenesis of *E. coli* transketolase cofactor binding loops towards those of *Thermus thermophilus*: Impact on thermotolerance.

5.1 Introduction

Having characterized the factors that lead to loss of transketolase (TK) activity at extreme pH, high temperatures, and in the presence of polar organic co-solvents in previous Chapters, the aim of this Chapter was to apply that knowledge to the design of TK mutants that could improve the stability of the enzyme, particularly to high temperatures.

Enzymes are catalysts that provide high selectivity under mild conditions of pH, temperature in aqueous media. The demanding of the commercial compounds in pharmaceuticals are fast growing and become more complex and focusing more on the process friendly with the environment, therefore biocatalysts are increasingly for the demanding of being preferred over non-biological catalysts (Moore et al., 2007; Pollard and Woodley, 2007). However, a significant challenge in enzyme biotechnology is the need to maintain their stability, particularly as the reaction environment is pushed further away from physiological aqueous conditions. For example, improvement of the stability of enzymes at high temperatures would allow

them to be employed for the biotransformation of compounds not readily soluble in lower temperatures. High temperatures also increase the rate of chemical reactions, including many that occur within enzyme active sites, thus giving enzymes the potential to operate with higher efficiency at high temperatures. However, issues with enzyme instability are a major factor preventing the wide spread adoption of enzymes as synthetic catalysts.

As the structure of *E. coli* TK has been characterised (Littlechild et al., 1995), comparative structural studies of yeast apo-TK and holo-TK showed that the conformation of the cofactor binding loops 187-198 and 384-384 were different, in that they were disordered in the apo-TK (Sundstrom et al., 1992). These two loops interact with one another and with TPP in holo-TK to form the active centre in which the loops become more ordered (Nikkola et al., 1994). Deactivation, denaturation, and potentially also the aggregation of transketolase at extreme pH, high temperature and in the presence of co-solvents, characterized in previous Chapters in this thesis, appears to be strongly linked to the binding of cofactors and to the structure of the cofactor binding loops. Obtaining such knowledge is an important step for informing protein engineering or process strategies that could be used to minimise the impact on biocatalysis of non-physiological conditions such as high temperature. In this case, engineering of the cofactor binding loops of transketolase appears to be a promising potential route to improving the overall stability of the enzyme (Jahromi et al., 2011), which in turn will meet the needs arising from the directed evolution of

TK variants which accept less soluble substrates (Dalby et al., 2007; Hibbert et al., 2007).

Although the optimal temperature range for wild-type (WT) transketolase activity was previously given to be 20-40 ^{o}C, the effect of temperature on the structure, stability, aggregation and activity of *E. coli* TK has now been characterized in more detail (Chapter 3; Jahromi et al., 2011). Holo-TK lost activity at above 55 °C due to irreversible aggregation of the enzyme, which begins to occur in the 1-3 hour timeframe of a typical TK biocatalytic reaction, at 58.3 °C. Surprisingly, heating at 40-55 °C and re-cooling of the enzyme progressively increased the enzyme activity where annealing at 55 °C for 1 hour improved the activity by up to 3-fold (Jahromi et al). As aggregation occurred at a much lower temperature for apo-TK than for holo-TK, and as the disordered state of the two cofactor loops in apo-TK is the only structural difference to holo-TK, the cofactor binding loops provide an attractive target to improve the stability of the enzyme.

At high temperatures, the thermostable proteins are capable to maintain their activities and are also thermodynamically stable to denaturation or aggregation. The challenge is to be able to explain and understand all the factors that contribute to the stability of proteins from organisms living under extreme conditions. The structure of *Thermus thermophilus* (*Th. thermophilus*) TK has been characterised recently (Yoshida et al., to be published) which provides an excellent opportunity to study the differences between this enzyme and that of the *E. coli* TK structure and sequence.

In particular, this Chapter aimed to compare the respective sequences of the cofactor binding loops and the effect upon thermostability and activity of introducing *Th. thermophilus* sequence mutations into *E. coli* TK.

Thermophilus TK is a transketolase protein of length 651, compared to the 680 residues in *E. coli* TK. This shortening of sequence due to smaller loop regions, is typical in thermostable enzymes as it reduces the flexibility and therefore inherent entropy in the protein structure. The % sequence identity between *thermus thermophilus* TK and *E. coli* TK is 49% (determined using BioEdit). The two cofactor binding loops of *E. coli* TK and *Th. thermophilus* TK are similar as shown below with differences shown in bold:

E. coli TK loop 1 (185-192)	N**G**ISIDG**H**
Th. thermophilus TK loop 1	N**R**ISIDG**P**

E. coli TK loop 2 (384-394)	L**A**PSN**L**T**LWS**G
Th. thermophilus TK loop 2	L**T**PSN**N**T**KAE**G

The aim of this Chapter was to create single, double, triple and quadruple mutants, in addition to transplants of the whole of each cofactor loop from *Th. thermophilus* TK into *E. coli* TK, and then to determine the effect of cofactor binding loop sequence changes on the stability of TK to high temperatures, as measured by

catalytic activity and melting temperatures of the corresponding proteins originating from both thermophilic and mesophilic organisms.

5.2 Materials and Methods

All chemicals were obtained from Sigma-Aldrich UK.

5.2.1 Over-expression and purification of His-tagged wild-type transketolase

Transketolase was expressed with an N-terminal His_6 tag from *E. coli* XL10-Gold (Stratagene, La Jolla, CA) containing the engineered plasmid pQR791, purified as described previously (Martinez-Torres et al., 2007), dialysed for 24 hours against 25 mM Tris-HCl, pH 7.5, at 4 °C then stored at 4 °C for a maximum of two weeks without loss of activity, and with no precipitation visible. Protein concentration was determined by absorbance at 280 nm, assuming a monomeric molecular weight (MW) of 72260.82 g mol^{-1} and an extinction coefficient (ε) of 93905 L mol^{-1} cm^{-1} (Pace et al., 1995).

5.2.2 Mutant construction

All defined mutants and libraries were introduced into the tktA gene in plasmid pQR791 (includes the N-terminal His tag), using the Quikchange method as described previously (Hibbert et al., 2007), then transformed into XL10-gold cells (Stratagene, La Jolla, CA) for expression of the TK mutants. All defined mutants were confirmed by DNA sequencing. The G186R/H192P double-mutant was constructed from the G186R mutant plasmid as template and H192P mutagenic primers modified to avoid reverting R186 back to G. The triple and quadruple mutants of loop 2 were constructed directly from wild-type using primers containing

all mutations simultaneously (Table 5-1) as the positions for each mutation were sufficiently close. Colonies from each mutagenesis were picked and cultured individually, and confirmed by DNA sequencing.

Table 5-1 Mutagenic primer sequences (5' to 3')

Loop1

G186R fwd GCATTCTACGATGACAAC**CGT**ATTTCTATCGATGGTCAC

G186R rev GTGACCATCGATAGAAAT**ACG**GTTGTCATCGTAGAATGC

H192P fwd GGTATTTCTATCGATGGT**CCG**GTTGAAGGCTGGTTCACC

H192P rev GGTGAACCAGCCTTCAAC**CGG**ACCATCGATAGAAATACC

Loop2

L387N fwd

GACCTGGCGCCGTCTAAC**AAC**ACCCTGTGGTCTGGTTCTAAAGC

L387N rev

GCTTTAGAACCAGACCACAGGGT**GTT**GTTAGACGGCGCCAGGTC

W390A fwd

CCGTCTAACCTGACCCTG**GCG**TCTGGTTCTAAAGCAATCAAC

W390A rev

GTTGATTGCTTTAGAACCAGA**CGC**CAGGGTCAGGTTAGACGG

L389K/W390A/S392E fwd

GCGCCGTCTAACCTGACC**AAGGCGGAA**GGTTCTAAAGCAATCAACG

L389K/W390A/S392E rev

CGTTGATTGCTTTAGAACC**TTCCGCCTT**GGTCAGGTTAGACGGCGC

L387N/ L389K/W390A/S392E fwd

GCGCCGTCTAAC**AAC**ACC**AAGGCGGAA**GGTTCTAAAGCAATCAACG

L387N/ L389K/W390A/S392E rev

CGTTGATTGCTTTAGAACC**TTCCGCCTT**GGT**GTT**GTTAGACGGCGC

TK primer for sequencing

TKN primer for the G182P, H192P

GATCCAGAGATTTCTGA for

TK 250^{+} fwd for all loop 2 mutations.

AGCCCGAACAAGGCGGGAGGCCACGAC

5.2.3 Activity of holo-TK at 55, 60 and 65 ^{o}C.

Wild-type and mutants of *E. coli* transketolase were obtained as purified enzymes 0.1 mg mL^{-1} (1.38 μM), containing 2.4 mM TPP, 9 mM $MgCl_2$ and in 25 mM Tris-HCl, pH 7.0 and pre-incubated at 25 °C for 30 minutes. Temperature inactivation was done by placing the 100 μL samples into a water bath at the required temperature (55, 60, or 65 °C), then the reactions were initiated immediately by addition of pre-warmed 50 μL of 50 mM Li-HPA and 50 mM GA in 25 mM Tris-HCl, pH 7.0, then quenched at various times over 180 minutes with 1 vol. 0.2 % (v/v) trifluoroacetic acid (TFA). Sample temperatures were monitored using a digital

wired-thermometer (Topac, USA). Purified TK activity at standard conditions of 25 ^{o}C was also measured as a control. Samples were analysed by HPLC (Dionex, CA, USA) with 210 nm absorbance detection, a 50mm PL Hi-Plex H guard column (Polymer Laboratories Ltd, UK), 0.1 % (v/v) TFA mobile phase, and a flow rate of 0.6 mL min^{-1}.

5.2.4 Temperature inactivation of holo-TK by pre-incubation for 1 h at 55, 60 and 65 ^{o}C.

Wild-type and mutants of *E. coli* transketolase were obtained as purified enzymes 0.1 mg mL^{-1} (1.38 μM), containing 2.4 mM TPP, 9 mM $MgCl_2$, in 25 mM Tris-HCl, pH 7.0 and pre-incubated at 25 °C for 30 minutes. Temperature inactivation was initiated by placing the 100 μL samples into a water bath pre-heated at 55, 60 and 65 °C. Sample temperatures were monitored using a digital wired-thermometer (Topac, USA). Samples were removed after 1 h, immediately cooled on ice then equilibrated to 25 °C. Reactions were initiated with 50 μL of 50 mM Li-HPA and 50 mM GA in 25 mM Tris-HCl, pH 7.0, then quenched at various times over 180 minutes with 1 vol. 0.2 % (v/v) trifluoroacetic acid (TFA). Purified TK standard conditions were also measured at 25^{o}C as a control. Samples were analysed as above by HPLC.

5.2.5 Dynamic light scattering (DLS)

The thermal denaturation of purified transketolase was measured with a Zetasizer Nano S (Malvern Instruments Ltd., UK). Wild-type and mutants holo-TK at 0.1 mg mL^{-1} (1.38 μM) was prepared in 25 mM Tris-HCl, pH 7.0 with 0.5 mM TPP, 5 mM $MgCl_2$. The temperature was raised from 4 to 70 °C at 1.0 °C intervals per minute between measurements. A control sample of buffers with or without cofactors was subtracted from each recording. Data were acquired in triplicate with a low volume disposable sizing cuvette with a path length of 1 cm. The hydrodynamic diameters of each sample were calculated from the averaged-measurements using the Zetasizer Nano Series software V.4.20 (Malvern Instruments Ltd., Worcestershire, UK).

5.3 Results and discussion

5.3.1 Design of *E.coli* TK mutations

As described in the introduction (Section 5.1), the aim of this Chapter was to create single, double, triple and quadruple mutants, as well as whole cofactor loop grafts based upon the homologous *Th. thermophilus* TK sequence. These mutants could then be used to assess the relative effects of individual and combined cofactor binding loop sequence changes on the stability of TK to high temperatures, as well as the relative contribution of the two loops to thermotolerance.

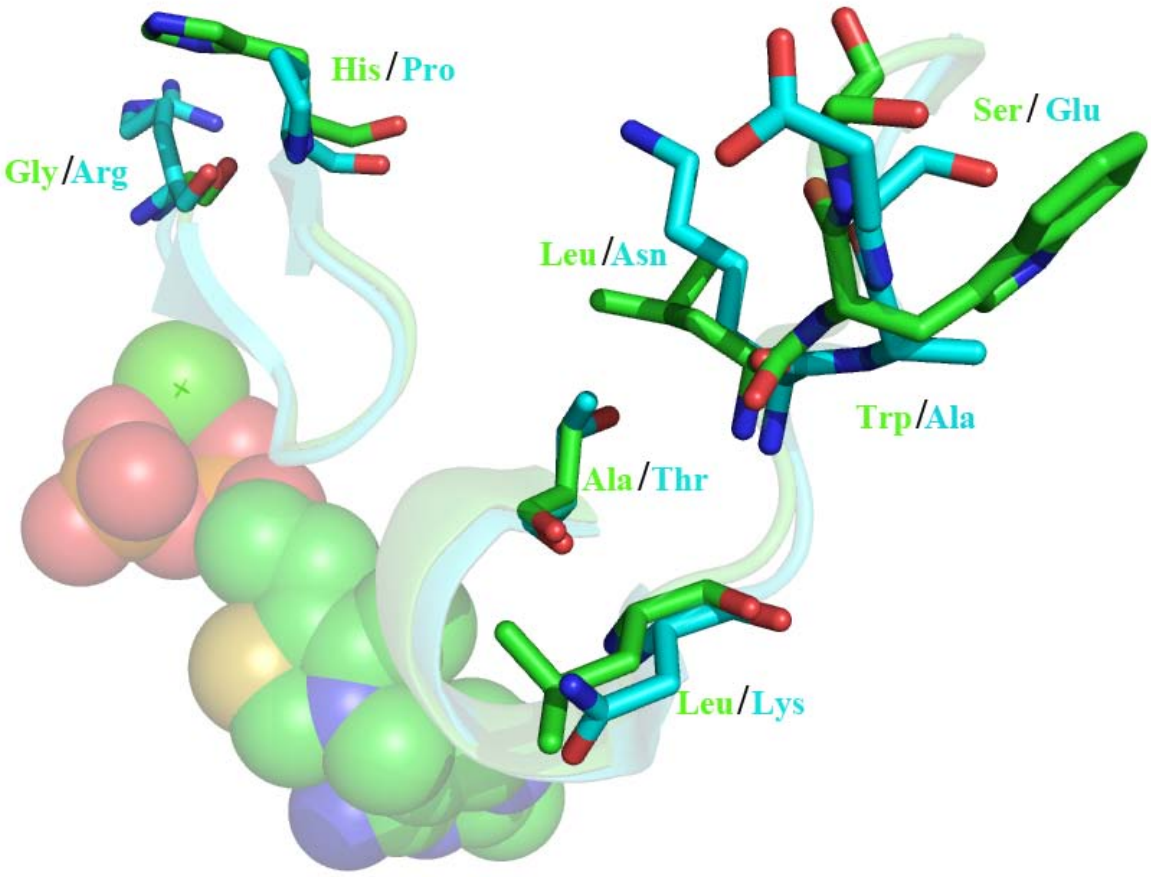

Figure 5-1 Structural comparison of the cofactor loops from wild-type *E. coli* TK, 1qgd.pdb (green) and wild-type *Thermus thermophilus* TK, 2e6k.pdb (cyan). The TPP cofactors and Mg^{2+} ion are shown as spheres. Residues that differ between the two structures are represented as sticks. Figure generated with PyMol (DeLano,W.L. (2002), The PyMOL Molecular Graphics System on World Wide Web http://www.pymol.org)

The two cofactor binding loops from available *Thermus thermophilus* and *E. coli* transketolase structures are overlaid and compared in Figure 5-1. It can be seen that the overall structure of the cofactor loops is the same for both organisms, with the backbone atoms aligning closely to form the same hairpin in loop1 and partial helix in loop2. The mutations designed to convert *E. coli* TK loops towards

those of *Th. thermophilus* were: (loop1) H192P, G186R, G186R/H192P; and (loop2) L387N, W390A, L389K/W390A/S392E, and L387N/L389K/W390A/S392E.

5.3.2 Investigating the catalytic activity of TK wild-type and mutants at 25, 55, 60 and 65 ^{o}C.

The optimum temperature range for TK enzyme activity has been previously reported as 20-40 °C (Sprenger and Pohl, 1999), although an annealing effect has also been observed for wild-type *E. coli* TK that improves activity up to approximately 55 °C (Jahromi et al., 2011). The catalytic activities of wild-type and mutant TKs at 25 °C, 55 °C and 60 °C are compared in Figures 5-2, 5-3 and 5-4 respectively. G186R in loop1 was not active under any condition (data not shown). By contrast, H192P in loop1 resulted in significant faster catalytic bioconversion than wide-type TK at 25 °C, and the double mutant G186R/H192P had similar activity to the wild type. This result suggests that the H192P mutation partly accommodates the otherwise disruptive G186R mutation, potentially by removing a steric clash between the two structurally adjacent residue side-chains (Figure 5-1),

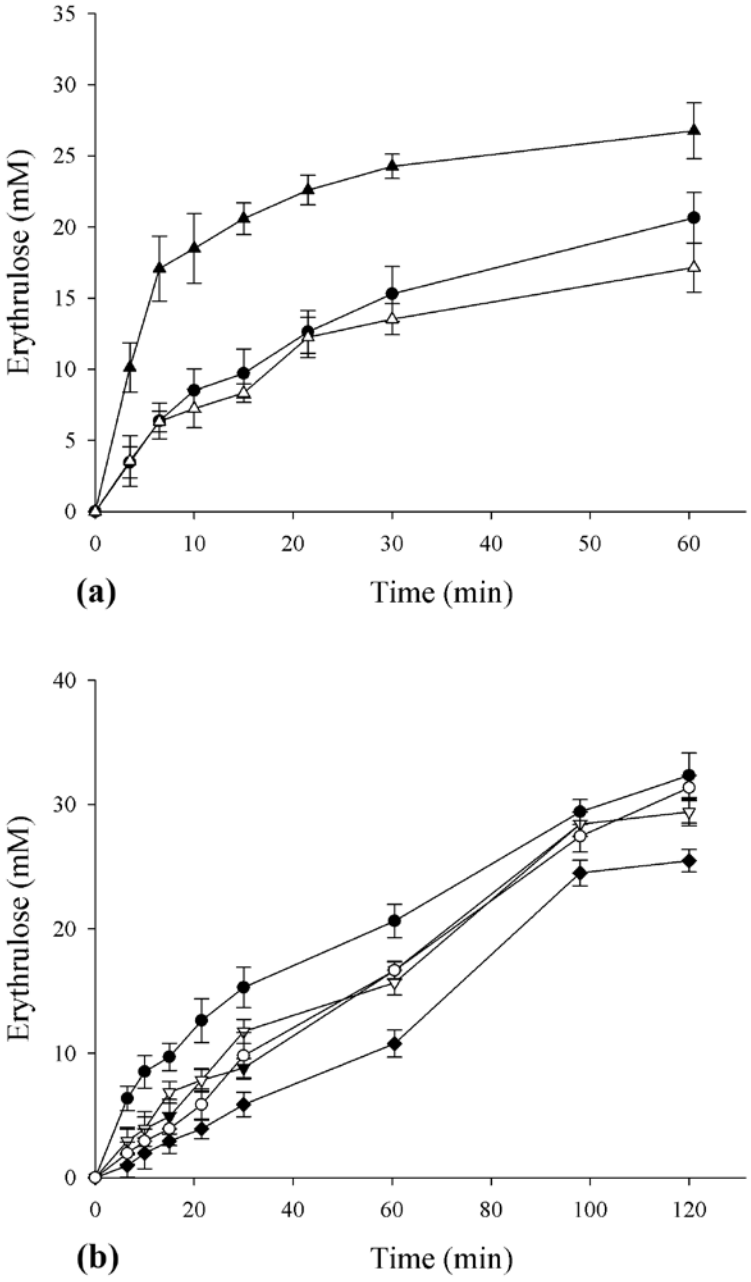

Figure 5-2 Catalytic activity of holo-transketolase mutants at 25 °C. The catalytic activity of pure wild-type compared to mutants was measured in triplicate at 25°C in 50 mM Tris-HCl, pH 7.0. (a) loop 1 (▲) H192P (Δ) G186R/H192P (b) loop 2 (▽) L387N, (○) W390A, (▼) L389K/W390A/S392E, (♦) L387N/L389K/W390A/S392E compared to (●) wild-type TK in both (a) and (b). The catalytic activity was measured using 50 mM GA and 50 mM HPA as substrates and L-erythrulose as a product.

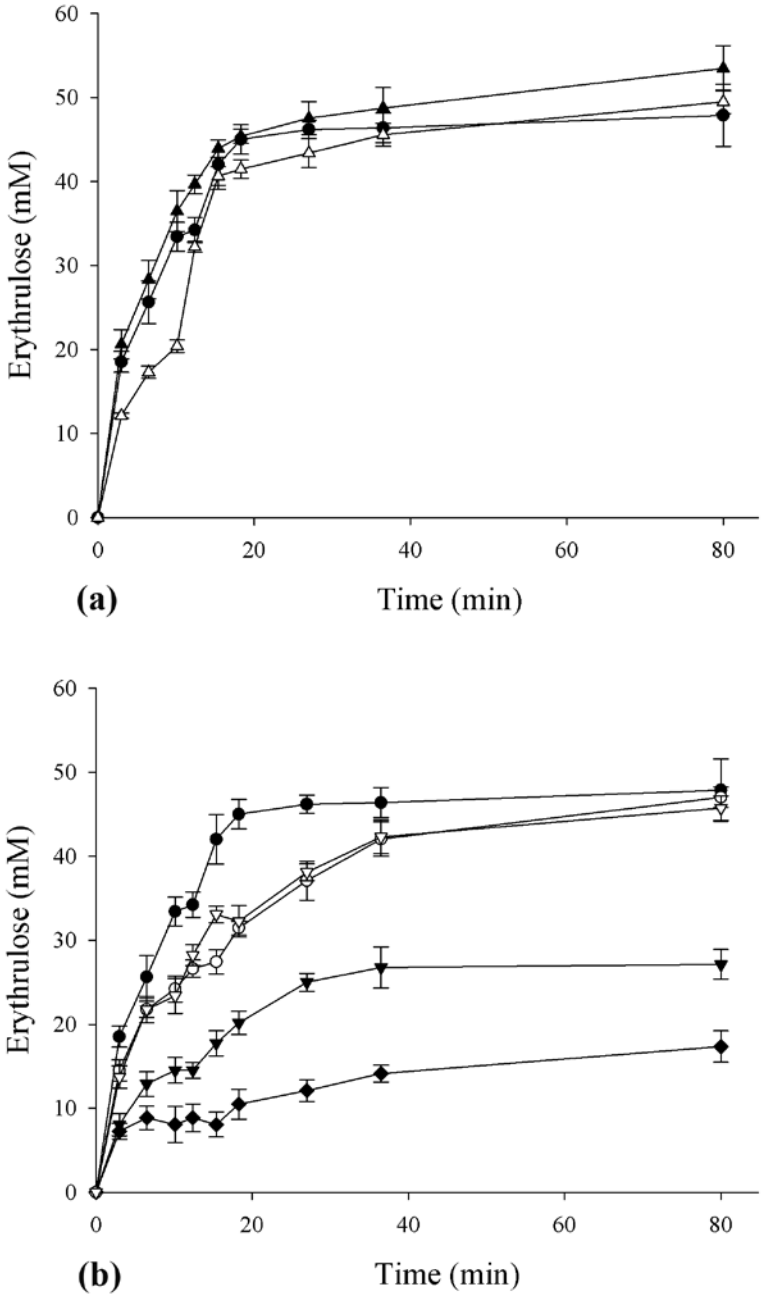

Figure 5-3 Catalytic activity of holo-transketolase mutants at 55 ^{o}C. The catalytic activity of pure wild-type compared to mutants was measured in triplicate at 55 ^{o}C in 50 mM Tris-HCl, pH 7.0. **(a)** loop 1 (▲) H192P (Δ) G186R/H192P **(b)** loop 2 (▽) L387N, (○) W390A, (▼) L389K/W390A/S392E, (♦) L387N/L389K/W390A/S392E compared to ⧫) wild -type TK in both (a) and (b). The catalytic activity was measured using 50 mM GA and 50 mM HPA as substrates and L-erythrulose as a product.

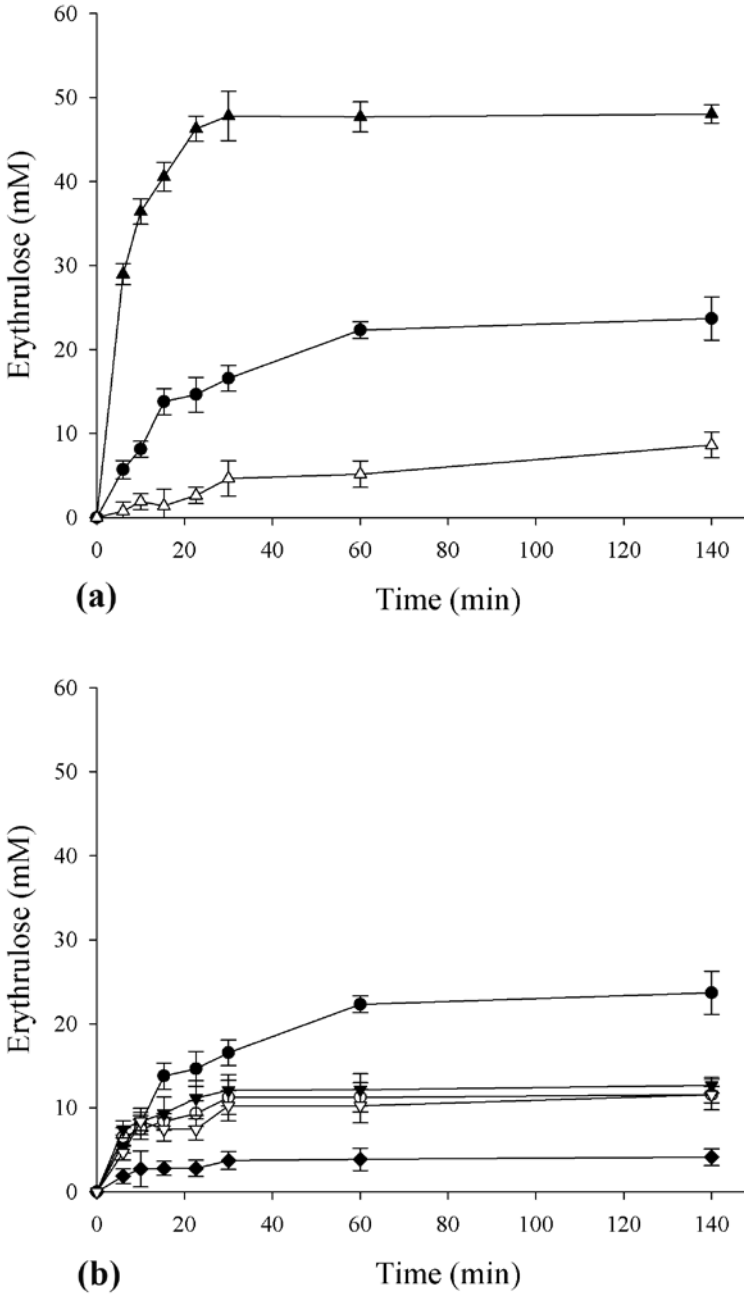

Figure 5-4 Catalytic activity of holo-transketolase mutants at 60 ^{o}C. The catalytic activity of pure wild-type compared to mutants was measured in triplicate at 60 ^{o}C in 50 mM Tris-HCl, pH 7.0. (a) loop 1 (▲) H192P (Δ) G186R/H192P (b) loop 2 (∇) L387N, (○) W390A, (▼) L389K/W390A/S392E, (♦) L387N/L389K/W390A/S392E compared to ⧫) wild -type TK in both (a) and (b). The catalytic activity was measured using 50 mM GA and 50 mM HPA as substrates and L-erythrulose as a product.

formed by inserting the large arginine residue at G186. Mutation of H192 to proline reduces the steric bulk at residue 192 and could therefore accommodate better the G186R mutation.

For loop2, all of the mutants had a lower catalytic activity than the wild type at 25 °C, particularly for the quadruple mutant which was less than 50% as active. This trend was observed with loop 2 mutants for activity at all elevated temperatures tested. At 55 ^{o}C mutants in loop 1 as well as the wild-type TK (Figure 5-3) have the same catalytic activity with full bioconversion after 30 min. The activity of H192P TK is slightly higher at 55 ^{o}C than at 25 ^{o}C, whereas wild type and G186R/H192P both increased significantly in activity at the higher temperature. Even more interestingly, at 60 ^{o}C (Figure 5-4), while H192P in loop 1 maintains the same high activity as at 55 ^{o}C, with full bioconversion after 30 min, the wild-type TK and G186R/H192P mutant activities decreased dramatically. This suggested that the mutation in cofactor binding loop 1, of the polar basic amino acid histidine 192, to a non-polar hydrophobic proline residue, which also restricts backbone rotations, improved the thermal stability and activity of TK at elevated temperatures, while also retaining higher activity at 25 ^{o}C. In other words, H192P has a much broader temperature optimum than the wild-type enzyme. It has been previously reported that thermal stability can be increased by improving hydrophobic interactions through protein engineering (Kumar and Nussinov, 2001). The behaviour of G186/H192P was similar to wild-type until activity at 60 ^{o}C was compared, at which point the

activity of the wild type was greater. Therefore, the disruptive G186R mutation, which has no activity in the single mutant at any temperature (data not shown), was not fully accommodated by the H192P mutation.

In loop 2, the triple mutant, L389K/W390A/S392E, achieved a similar degree of bioconversion as the wild type after 80 minutes at 25 ^{o}C, whereas the quadruple mutant L387N/L389K/W390A/S392E clearly had a decreased activity that led to only 80% of the wild type bioconversion level after 80 minutes. Bioconversion was not complete within 80 minutes for wild type or any of the mutants in loop 2. Only H192P in loop1 achieved this at 25 ^{o}C. At 55 ^{o}C, wild type TK, L387N, and W390A reached the complete conversion within 80 minutes, but the two mutants were slower than wild type by approximately the same degree. Neither the triple or quadruple mutants achieved complete conversion at 55 ^{o}C, and appeared to level off indicating that the enzyme had become inactive before complete bioconversion was achieved. The double and triple mutants were therefore clearly less thermostable than the wild-type or single mutants in loop2. At 60 ^{o}C, the wild type TK and mutants in loop 2 all failed to reach complete bioconversion, indicating the loss of active enzyme before the reaction was complete. Wild type TK, achieved 50% bioconversion within 140 minutes, whereas L387N, W390A and L389K/W390A/S392E achieved only 20% bioconversion, and L387N/L389K/W390A/S392E achieved less than 10% bioconversion. There was no catalytic activity of wild-type TK, or for any of the mutants in loop 1 and loop 2 when tested at 65 ^{o}C (data not shown).

5.3.3 Thermal inactivation of wild-type and mutants-TK after incubated at 55, 60 and 65 °C for 1 h and re-cooling to 25 °C

The catalytic activity of holo-TK was also investigated after a 1 hour incubation at 55-60 °C followed by re-cooling of the samples and measurement of activity at 25 °C (Figure 5-5, 5-6). After incubation at 55°C for 1 h and re-cooling to 25 °C, H192P showed a faster bioconversion than wild-type TK and G186R/H192P. Interestingly, the wild-type and G186R/H192P both showed an increase in activity to a level similar to that actually measured at 55 °C (Figure 5-3). This indicates that the annealing effect seen previously for wild-type TK (Jahromi et al., 2011) was confirmed here also for the G186R/H192P double mutant, but that H192P already had the higher activity when measured immediately at 25 °C, without the need for a 55 °C pre-incubation.

For loop2 mutants, after pre-incubation at 55 °C L387N, W390A and L389K/W390A/S392E all achieved 50% bioconversion after 2 hours, but L387N/L389K/W390A/S392E achieved only approximately 1% bioconversion after 2 hours. Interestingly, the bioconversion did not level off indicating that the enzymes retained their activity, but they did not show the annealing effect which increased the activity of wild-type TK and G186R/H192P.

Table 5-2 summarises the specific activities of wild-type and mutant TKs for all temperature conditions and the experiments performed. This clearly shows the improved stability of the H192P mutation in cofactor binding loop1, to elevated

temperatures. The activity of H192P was 3 times higher than that for wild-type TK at 60 ^{o}C, and also after re-cooling from the pre-incubation at 55 ^{o}C for 1 h. However, at room temperature H192P already showed 2 times greater specific activity than wild-type TK. Comparing loop 1 and loop 2 mutants in general reveals their relative effects on the thermal stability of wild type TK. Given that H192P in loop1 was able to eliminate the need for temperature annealing at 55 °C, whereas the loop2 mutations removed any annealing effect, the annealing phenomenon clearly appears to be linked to both cofactor loops. Potentially, the annealing involves the formation of stable structure in loop1 which is inherently formed in the H192P mutant due to the more rigid backbone flexibility induced by the proline. The loss of stability in loop2 in mutations of that loop could also interfere with the formation of a stable structure in loop1, hence leading to the loss of annealing capability. Alternatively, the loss of stability in loop2 may lead simply to a loss of activity that cannot be rescued by an annealing of loop1.

Increasing the 1 hour pre-incubation temperature further to 60 and 65 ^{o}C was sufficient to knock out all enzyme activity at 65 ^{o}C (data not shown), and all except some residual activities in wild-type, G186R/H192P and H192P (Figure 5-6), where H192P again showed the greater activity. The enzyme inactivation at elevated temperatures is known to be due to protein aggregation, as evidenced also by a lag phase in the time dependence of inactivation for wild-type TK at 60 °C and 65 °C as studied previously (Jahromi et al., 2011). The lag phase accompanied enzyme

deactivation at 60 °C, but at 65 °C, no lag phase was observed due to the more rapid formation of denatured protein or an aggregation nucleus.

Enzyme	Specific Activity (μmol.min^{-1}.mg^{-1})						
	Rx at Temperature (^{o}C)				Rx after incubated at temperature (^{o}C) for 1 hr and re-cooling at 25^{o}C		
	25	55	60	65	55	60	65
Wild-type	8.5	37.5	15.8	0.2	18.7	0.4	0
Loop 1							
H192P	18.5	43.3	48.2	3.8	50.6	1.7	0
G186R/H192P	7.2	18.4	1.4	0.94	21.3	0.3	0
Loop 2							
L387N	4.7	18.5	7.4	0	4.9	0	0
W390A	3.1	15.1	7.4	0	2.3	0	0
L387N/W390A/S392E	4.2	9.4	8.3	0	2.8	0	0
L387N/L389K/W390A/S392E	1.9	4.8	1.1	0	0.6	0	0

Table 5-2 Specific activity of wild-type and mutants TK in loop 1 and 2 at room temperature (25^{o}C) , 55,60 and 65^{o}C and after incubated 1 h at 55,60and 65^{o}C before re-cooling at 25^{o}C. The specific activities were measure by the initial rate of the reaction (chapter 2 section 2.2.7) divided by the concentration of enzyme in the reaction.

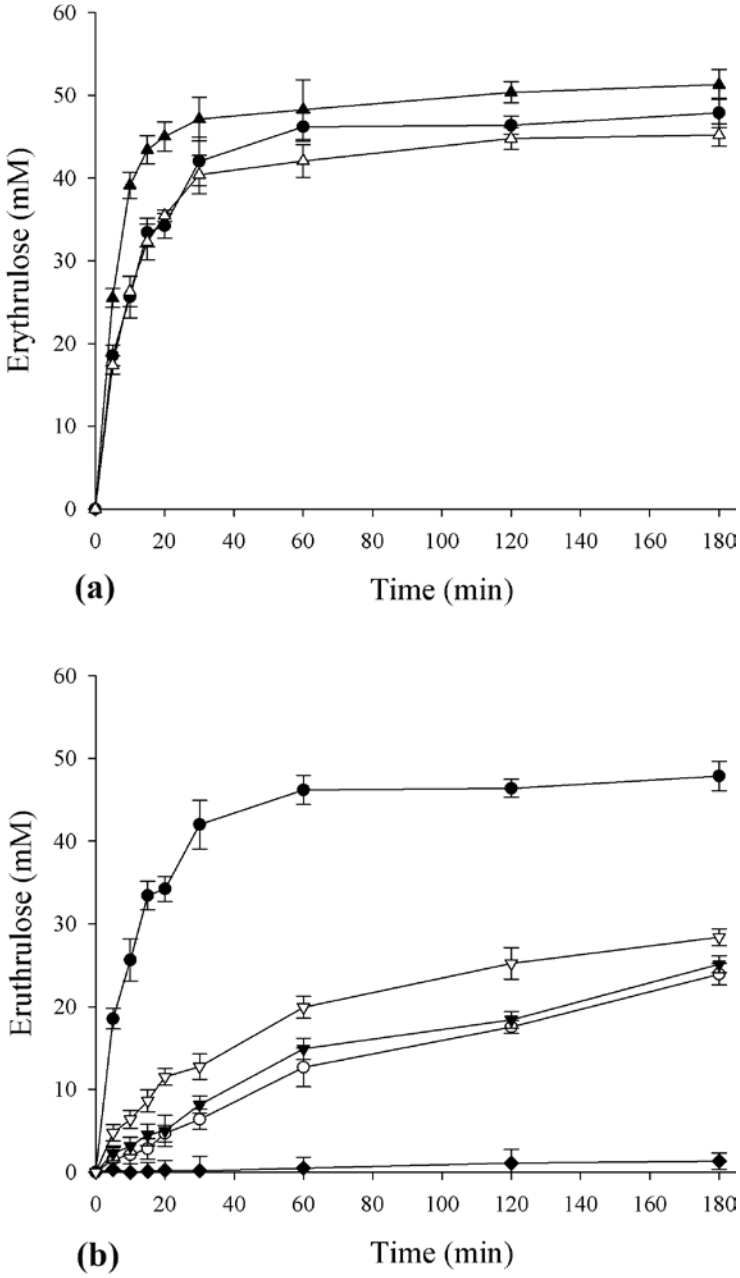

Figure 5-5 Catalytic activity of holo-transketolase after pre-incubation at 55 °C for 1 hour. The catalytic activity of pure wild-type compared to mutants was measured in triplicate after incubation at 55 °C in 50 mM Tris-HCl, pH 7.0 for 1 h and re-cooling for reactions at 25 °C. (a) loop 1 mutants (▲) H192P (Δ) G186R/H192P; and (b) loop 2 mutants (∇) L387N, (○) W390A, (▼) L389K/W390A/S392E, (♦) L387N/L389K/W390A/S392E are compared to (●) wild-type TK in both (a) and (b). The catalytic activity was measured using 50 mM GA and 50 mM HPA as substrates and L-erythrulose as a product.

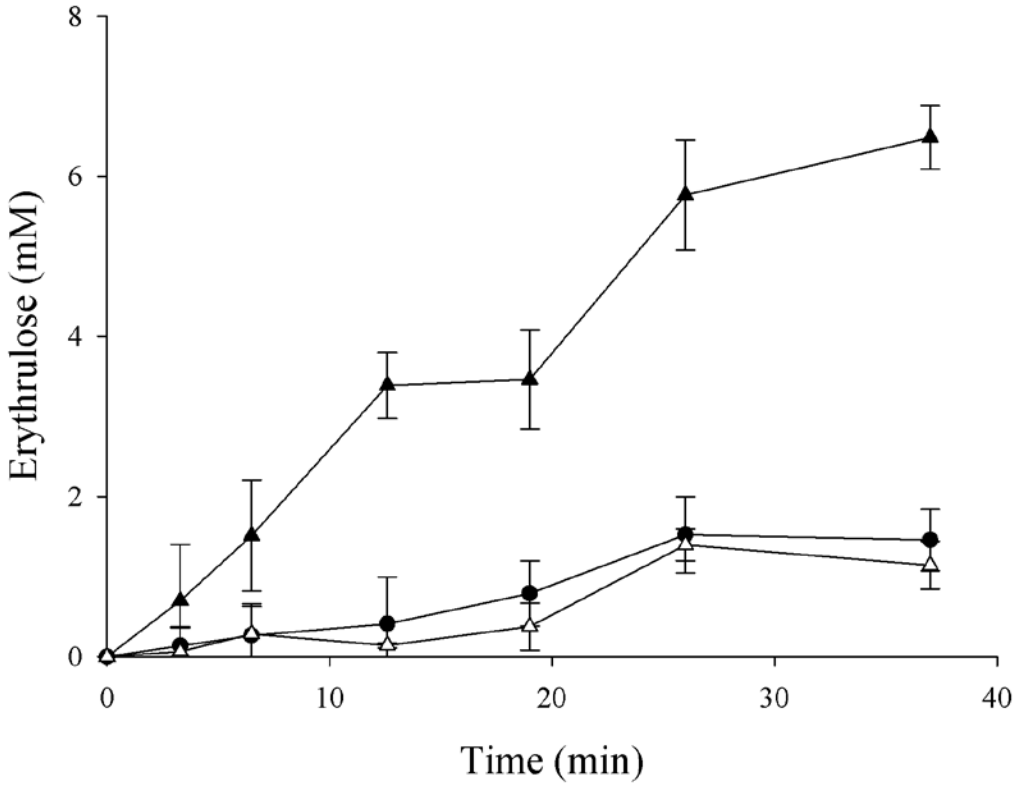

Figure 5-6 Catalytic activity of holo-transketolase after incubation at 60 ^{o}C for 1 hour. The catalytic activity of pure wild-type compared to mutants was measured in triplicate after incubation at 60 ^{o}C in 50 mM Tris-HCl, pH 7.0 for 1 h and re-cooling for reactions at 25 ^{o}C. Loop 1 mutants (▲) H192P (Δ) G186R/H192P are compared to (●) wild-type TK. The catalytic activity was measured using 50 mM GA and 50 mM HPA as substrates and L-erythrulose as a product.

Perhaps surprising is that the introduction of mutations based upon the cofactor loops of *Thermus thermophilus*, did not generally improve thermostability or activity at higher temperatures, with the exception of H192P. This is interesting given that thermophiles are thought to improve their stability often through better packing, rigidification, deletion or shortening of loops (Russell et al., 1997). None of

the mutations led to deletion or shortening of loops, probably because the loops are critical for cofactor binding, and there is little room for their shortening. Better packing may not have been achieved with the mutations made, although it could be argued that complete grafting of both loops is required to achieve the optimal packing effect, potentially also requiring other surrounding mutations. Interestingly, the one mutation that improved the stability of TK was H192P which introduces a rigidifying proline mutation. This rigidifies loops due to the formation of a covalent bond from the side chain back to the backbone amine, thus removing free rotation about the N-Cα bond. Improving the thermal stability of enzymes by protein engineering has been reported elsewhere by other mechanisms, and among the prominent reasons given are the introduction of greater hydrophobicity (Haney et al., 1997), or improved hydrophobic interactions within proteins (Kumar and Nussinov, 2001). This effect may also have contributed to the improved thermostability of H192P.

5.3.4 Particle-size distribution of wild-type and cofactor loop mutants during thermal denaturation

The effect of temperature on the Z-average hydrodynamic radius of holo-TK was determined by DLS from the particle size distributions (Figure 5-7,5-8). The Z-average for the H192P homodimer remained constant above 20 °C, then started to increase at above 55 °C, forming large aggregates (>1,000 nm) at 61.5 ^{o}C which

correlated to the stable activity at 55 and 60 ^{o}C for this mutant. For wild-type, a growth in the particle size began already at 46 ^{o}C, and larger aggregates (> 1,000 nm) were detected at above 55 ^{o}C. G186R/H192P holo-TK retains the native size until 55 ^{o}C, and then increased to > 1000 nm at 59.4 ^{o}C (Table 5-3). These data indicate that H192P is more resistant to aggregation at elevated temperatures than for wild-type TK, and G186R/H192P, consistent with their activities after pre-incubations or actually at the elevated temperatures. The data also confirm that the primary mechanism of inactivation for the mutants is aggregation as found previously for wild type.

In loop 2, the quadruple mutant L387N/L389K/W390A/S392E which showed a decrease in catalytic activity at > 55 ^{o}C, also gave a significant appearance of aggregate at 53.7 ^{o}C. This link was similar for the triple mutant L389K/W390A/S392E for which aggregates appeared at 54 ^{o}C. For the single mutants in loop 2, L387N and W390A, the large particle size of more than 1000 nm was detected at 55.2 ^{o}C and 55 ^{o}C respectively. Presumably, a number of weakly stabilised structural elements such as ordered loops become partially denatured as the temperature increases, and eventually induces the formation of the aggregates observed. These results show that the cofactor binding loops play a significant role in this partial denaturation and aggregation, and that engineering them can improve their stability to temperature denaturation, as found for H192P.

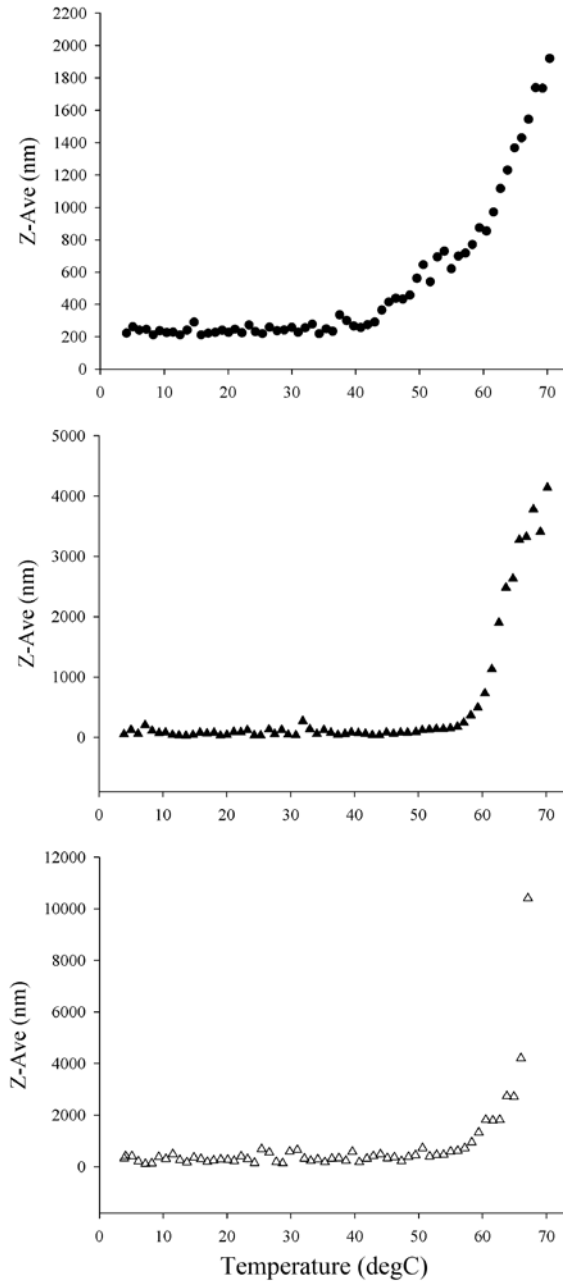

Figure 5-7 Temperature dependence of average particle size for (●) wild type and mutants in loop 1 (▲) H192P and (Δ) G186R/H192P holo-TK determined by dynamic light scattering. TK at 0.1 mg mL^{-1} (1.38 μM) was incubated at 25 °C for 1 h in 25 mM Tris–HCl, pH 7.0, 5 mM $MgCl_2$, 0.5 mM TPP prior to measurements. Temperature was increased at 1.0 °C per minute from 4 to 70 °C for each measurement of particle size distribution. Mean diameter (Z-ave) was calculated from the % intensity distribution at each temperature.

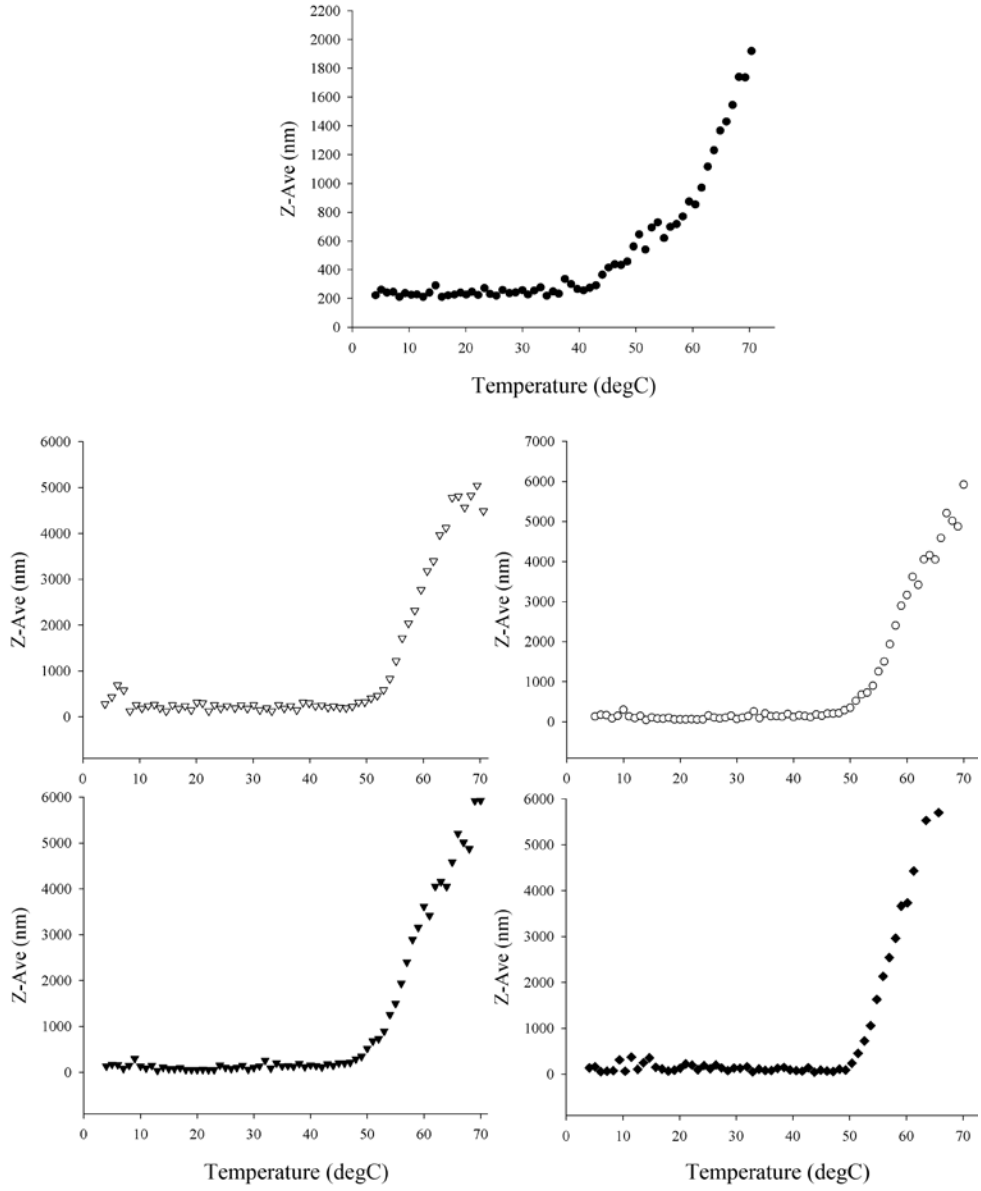

Figure 5-8 Temperature dependence of average particle size for (●) wild type and mutants in loop 2 (▽) L387N, (△) (W390A, (▼) L387N/W390A/S392E, (♦) L387N/L389K/W390A/S392E holo-TK determined by dynamic light scattering. TK at 0.1 mg mL^{-1} (1.38 μM) was incubated at 25 °C for 1 h in 25 mM Tris–HCl, pH 7.0, 5 mM $MgCl_2$, 0.5 mM TPP prior to measurements. Temperature was increased at 1.0 °C per minute from 4 to 70 °C for each measurement of particle size distribution. Mean diameter (Z-ave) was calculated from the % intensity distribution at each temperature.

Enzyme	Temperature (^{o}C) giving an average particle size of >1,000 nm for holo TK
Wild-type	55.0
Loop 1	
H192P	61.5
G186R/H192P	59.4
Loop 2	
L387N	55.2
W390A	55.0
L387N/W390A/S392E	54
L387N/L389K/W390A/S392E	53.7

Table 5-3 Temperature dependent particle size > 1,000 nm for wild type and mutants in loop1 H192P, G186R/H192P and loop 2 L387N, W390A, L387N/W390A/S392E, L387N/L389K/W390A/S392E holo-TK determined by dynamic light scattering. TK at 0.1 mg mL^{-1} (1.38 μM) was incubated at 25 °C for 1 h in 25 mM Tris–HCl, pH 7.0, 5 mM $MgCl_2$, 0.5 mM TPP prior to measurements. Mean diameter (Z-ave) was calculated from the % intensity distribution at each temperature.

5.4 Conclusions

In this study, mutagenesis was targeted to cofactor binding loops to probe their role in the loss of thermal stability in the wild-type enzyme. Mutants of TK based upon the sequence of TK from the thermostable organism *Thermus thermophilus* were designed and examined for their impact upon stability and activity at elevated temperatures. The thermal stability of TK was successfully improved by mutation of cofactor binding loop1, but not for loop2. H192P in loop1 resulted in improved stability at elevated temperatures which correlated with the critical onset of aggregation occurring at higher temperatures. The specificity activity of H192P was 3 times higher than that for wild-type at 60 ^{o}C, and their particle size distributions show significantly improved tolerance to aggregation at elevated temperatures, with wild type and H192P becoming aggregated to >1000 nm on average, at 55 ^{o}C and 61.5 ^{o}C respectively. The double, triple and quadruple mutants in loop2 did not improve the specific activity at elevated temperatures, indicating that this loop was less critical than loop1 to thermostability or thermotolerance. However, it would be interesting to introduce rigidifying proline mutations into loop2 to compare this effect to that observed in loop1 with H192P. The information gained by further changing amino acids around the cofactor binding loops will impact further studies designed to improve the stability of the enzyme.

Chapter 6

6. Overall conclusions and future recommendations

Following the conclusions from each chapter in this thesis, the ultimate aim of the project was achieved in that the deactivation mechanisms of TK at extremes of pH, temperature and the presence of co-solvent were revealed in greater structural detail. This has led to a greater understanding of the critical mechanisms for *E. coli* TK deactivation in terms of catalytic activity, structural stability and the formation of aggregates at various pH, elevated temperatures and addition of polar organic co-solvents. When compared to previous work on TK using urea to denature the enzyme, it became clear that deactivation at extreme pH, high temperature or in the presence of solvents occurred through a wide range of mechanisms with few common overlaps across the conditions. For example, in urea previously, TK denatured by unfolding to form a homodimeric but inactive intermediate state prior to any further denaturation and dissociation to unfolded monomers. No aggregates were observed. Denaturation by heating however, led to the formation of aggregates which appeared to be strongly linked to the structured state of the cofactor binding loops. By contrast, low pH led to an aggregation-linked deactivation, whereas high pH led to partial structural denaturation and loss of cofactor binding, again pointing to the stability of the cofactor binding loops as critical. Finally, organic solvents

exerted different deactivation mechanisms dependent largely on the polarity of the co-solvent. For example, THF led to simple protein denaturation without aggregation, whereas co-solvents with greater polar surface area promoted aggregation. However, the largest solvent, ethylacetate, did not denature the enzyme at all, or cause aggregation, yet it still led to enzyme deactivation, presumably by inhibition in the active site, or by removal of critical waters in the active site.

These findings underpinned the rationale for targeting mutagenesis to the cofactor loops to improve the stability of TK under industrial bioprocess conditions. Furthermore, conditions are now known for *E. coli* TK in which it is reasonably tolerant to limited quantities of organic co-solvents. These have recently been successfully used to increase the solubility of a substrate to get a greater % yield of bioconversion by a collaborating PhD student Lydia Crago (data not shown). The successful improvement of wild-type TK thermal stability or activity at higher temperatures will lead to the application of this mutant at larger scale for the synthesis of more non-polar substrates. The results presented in chapter 4 will be submitted for publication.

In summary, possible extensions to this project for further gain of understanding or for improved enzymes includes:

- Further rational or directed evolution mutagenesis to improve thermostability and tolerance to low pH, targeted toward regions of protein predicted to have high propensity for aggregation using available online tools.

- For retention of biocatalytic activity at high pH, stabilisation of the cofactor binding loops in their native holo-TK structure would be an attractive target also for further rational mutagenesis or directed evolution.

- Exploration into alternative new substrates such as aromatic aldehdydes, that have poor solubility in aqueous media using the organic solvents optimal for *E. coli* transketolase stability.
- Investigation of the stability of the H192P new mutant which increased the thermostability, to see whether this also increases the tolerance to organic solvent mixtures due to the frequently observed correlation of high thermostability and the tolerance of enzymes in non-aqueous media.
- Combine the H192P mutant with D469T and D469E which have already been found to increase catalytic activity towards non-polar substrates, and yet also lead to poor thermostability. Collaboratory for D469T and D469E, Rios-Solis et al., 2011 (published as presented in appendix2; Strafford et al (in progress).

References

Arnold, F.H. (1990). Engineering enzymes for nonaqueous solvents. *TIBTech* 8, 244-249.

Aucamp,J.P., Cosme, A.M., Lye,G.J., Dalby,P.A. (2005). High-throughput measurement of protein stability in microtiter plates. *Biotechnology and Bioengineering*, 89(5), 599-607.

Babu, K.R., Moradian, A., Douglas, D.J. (2000) The methanol-induced conformational transitions of beta-lactoglobulin, cytochrome c, and ubiquitin at low pH: a study by electrospray ionization mass spectrometry. *J. Am. Soc. Mass Spectrom.* 12, 317–328.

Badoei-Dalfard,A., Khosro,K., Mohsen, A.S., Ranjbar,B., Hamid,K.H.R.(2010) Enhanced activity and stability in the presence of organic solvents by increased active site polarity and stabilization of a surface loop in a metalloprotease, *Journal of Biochemistry*. 148(2),231-238.

Bansal,V., Delgado,Y., Fasoli,E., Ferrer, A.A., Griebenow, K., Secundo, F., Barletta, G.L. (2010). Effect of prolonged exposure to organic solvents on the active site environment of subtilisin Carlsberg. *J of Molecular Catalysis B:Enzymatic*. 64(1-2), 38-44.

Benov,L., Irwin,F. (1998). Why Superoxide Impose an Aromatic Amino Acid Auxotrophy on Escherichia coli. The Transketolase Connection. *J Biological Chemistry* 274,4202-4206.

Boer,H., Koivula,A. (2003). The relationship between thermal stability and pH optimum studied with wild-type and mutant Trichoderma reesei cellobiohydrolase Cel7A. *Eur. J. Biochem.* 270(5), 841-848.

Bongs, J., Hahn, D., Schorken, U., Sprenger, G. A., Kragl, U., Wandrey, C., (1997). Continuous production of erythrulose using transketolase in a membrane reactor. Biotechnol. *Letts.* 19, 213-215.

Brocklebank,S., Woodley,J.M., & Lilly,M.D. (1999). Immobilised transketolase for carbon-carbon bond synthesis: biocatalyst stability. *J.Molec.Catal.B: Enzymatic*, 7, 223-231.

Butler,L.G. (1979). Enzymes in nonaqueous solvents. *Enzyme Microb.Technol*. 1, 253-259.

Cazares,A., Galman,J.L., Crago,L.G., Smith,M.E., Strafford,J., Rios-Solis,L., Lye,G.J., Dalby,P.A., Hailes,H.C. (2010). Non-alpha-hydroxylated aldehydes with evolved transketolase enzymes. *Org. Biomol. Chem*. 8, 1301-1309.

Cooney,C.L., Hueter,J. (1974). Enzyme catalysis in the presence of nonaqueous solvents using chloroperoxidases. *Biotech and Bioeng*. 16,1045-1053.

Costelloe,S., Ward,J., Dalby,P. (2008). Evolutionary Analysis of the TPPDependent Enzyme Family. *Journal of Molecular Evolution*, 66(1), 36-49.

D'Souza,V.T., Lu,X.L., Ginger,R.D., Bender,M.L. (1987). Thermal and pH stability of "f8-benzyme" (artificial enzyme/chymotrypsin). *Proc. Nati. Acad. Sci.USA*. 84, 673-674.

Dalby,P.A. (2007). Engineering enzymes for biocatalysis. *Recent Patents Biotechnol*. 1 (1), 1-9.

Dalby,P.A., Baganz,F., Lye,G.J., Ward,J.M. (2009). Protein and pathway engineering in biocatalysis. *Chim. Oggi*. 27, 18.

Daniel,R.M., Danson,M.J., Eisenthal,R. (2001). The temperature optima of enzymes: a new perspective on an old phenomenon. *Trends in Biochemical Sciences*, 26(4), 223-225.

Danson,M.J., Hough,D.W., Russell,R.J.M., Taylor,G.L., Pearl,L. (1996). Enzymethermostability and thermoactivity. *Protein Engineering Design and Selection*, 9(8), 629-630.

Datta,A.G., Racker,E. (1961). Mechanism of Action of Transketolase .1. Properoperties of Crystalline Yeast Enzyme. *J.Biol.Chem.*, 236(3), 617-623.

de la Haba,G., Leder,I.G., Racker,E. (1955). Crystalline transketolase from bakers' yeast: isolation and properties. *J.Biol.Chem.*, 214, 409-426.

Domagk G.F., Horecker B.L. (1965) Fructose and erythrose metabolism in *Alcaligensis faecalis*, *Arch. Biochem. Biophys.* 109, 342–349.

Dong,A., Meyer,J.D., Kendrick,B.S., Manning,M.C., Carpenter,J.F. (1996). Effect of secondary structure on the activity of enzymes suspended in organic solvents. Archives of Biochemistry and Biophysic. 334(2), 406-414.

Dordick,S.J. (1991). Non-aqueous enzymology. *Curr Opinion in Biotech*. 2, 401-407.

Dordick,S.J. (1991). Non-aqueous enzymology. *Curr Opinion in Biotech*. 2,401-407.

Eijsink,V.G., Gaseidnes, S., Borchert, T. V., van den Burg, B. (2005) Directed evolution of enzyme stability. *Biomol. Eng.* 22, 21-30.

Eijsink,V.G.H., Bj°rk,A., Gsseidnes,S., Sirevsg,R., Synstad,B.r., Burg,B.v.d., Vriend,G. (2004). Rational engineering of enzyme stability. *Journal of Biotechnology*, 113(1-3), 105-120.

Esakova,O.A., Meshalkina,L.E., Kochetov,G.A. (2005). Effects of transketolase cofactors on its conformation and stability. *Life Sci*. 78(1), 8–13.

Galman,J.L., Steadman,D., Bacon,S., Morris,P., Smith,M.E., Ward,J.M., Dalby,P.A., Hailes,H.C. (2010). alpha,alpha'-Dihydroxyketone formation using aromatic and heteroaromatic aldehydes with evolved transketolase enzymes. *Chem. Commun*. 46, 7608-7610.

Gandhi,N.N. (1997). Applications of Lipase. *JAOCS, Journal of the American Oil Chemists' Society* 74(6), 621-634.

Gupta,M.N. (1992). Enzyme function in organic solvents. *Eur. J Biochem*. 203, 25-32.

Haney,P., Konisky, J., Koretke, K.K., Luthey-Schulten, Z., Wolynes,P.G. (1997). Structural basis for thermostability and identification of potential active site residues for adenylate kinases from the archaeal genus *Methanococcus*. *Proteins* 28,117-130.

Hecquet,L., Bolte,J., Demuynck,C. (1996). Enzymatic synthesis of "naturallabeled" 6-deoxy-L-sorbose precursor of an important food flavor. *Tetrahedron*,52(24), 8223-8232.

Hecquet,L., Lemaire,M., Bolte,J., Demuynck,C. (1994). Chemoenzymatic Synthesis of Precursors of Fagomine and 1,4-Dideoxy-1,4-Imino-D-Arabinitol. *Tetrahedron Lett.*, 35(47), 8791-8794.

Heinrich,P.C., Wiss,O. (1971) Transketolase from human erythrocyte: purification and properties, *Helv. Chim. Acta.* 54, 2658–2668.

Hibbert EG, Senussi T, Smith MEB, Costelloe SJ, Ward JM, Hailes HC, Dalby PA. Directed evolution of transketolase substrate specificity towards an aliphatic aldehyde. *J. Biotechnol.* 2008,134,240.

Hibbert,E.G., Senussi,T., Costelloe,S.J., Lei,W., Smith,M.E.B., Ward,J.M., Hailes,H.C., Dalby,P.A. (2007). Directed evolution of transketolase activity on non-phosphorylated substrates. *Journal of Biotechnology*, 131(4), 425-432.

Himmo,S.D., Thomson,M.,Gu bler,C.J. (1988). Isolation of transketolase from human erythrocytes. *Prep.Biochem.*, 18(3), 261-276.

Horecker B.L., Smyrniotis P.Z., Hurwitz J. (1956) The role of xylulose 5-phosphate in the transketolase reaction, *J. Biol. Chem.* 223, 1009–1019.

Illanes,A. (2008). Enzyme Biocatalysis: Principles and Applications. USA; Springer.

Ingram,C.U., Bommer,M., Smith,M.E., Dalby,P.A., Ward,J.M., Hailes,H.C., Lye,G.J. (2007). One-pot synthesis of amino-alcohols using a de-novo transketolase and beta-alanine: pyruvate transaminase pathway in Escherichia coli. *Biotechnol. Bioeng*. 96, 559-569.

Ishige,T., Honda,K., Shimizu,S. (2005). Whole organism biocatalysis. Curr. Opin. Chem. Biol. 9, 174-180.

Jahromi,R.R.F., Morris,P., Martinez-Torres,R.J., Dalby,P.A., (2011) Structure stability of E.coli transketolase to temperature and pH denaturation. *Journalof Biotechnology*. 155, 209-216.

Kiely,M.E., Tan,E.L., Wood,T. (1969) The purification of transketolase from *Candida utilis, Can. J. Biochem.* 47, 455–460.

Klibanov,A.M, Wescott, C.R. (1994). The solvent dependence of enzyme specificity. *Biochi et Biophy Acta*. 1206,1-9.

Klibanov,A.M., (1997). Why are enzymes less active in organic solvents than in water? *Trends Biotecnol*. 15, 97-101.

Kochetov, G. A., Philippov, P. P., Razjivin, A. P., Tikhomirova, N. K. (1975). Kinetics of reconstruction of holo-transketolase. *FEBS Lett.* 53, 211-212.

Kochetov,G.A. (2001). Functional flexibility of the transketolase molecule. *Biochem.(Mosc.).*, 66(10), 1077-1085.

Koeller, K. M., Wong, C. H. (2001). Enzymes for chemical synthesis. *Nature.* 409, 232-240.

Kovina,M.V, Bykoya,I.A., Solovjeva,O.N., Meshalkina, L.E., Kochetov,G.A. (2002). The origin of the absorption band induced through the interaction between apotransketolase and thiamine diphosphate. *Biochemical and Biophyssical Research Communications.* 294,155-160.

Krishna, S.H. (2000). Developments and trends in enzyme catalysis in nonconventional media. *Biotechnol Adv*. 20-34.

Kumar,S., Nussinov, R. (2001). How do thermophilic proteins deal with heat? *Cellular and Molecular Life Sciences*. 58(9), 1216 – 1233.

Li, Y., Ogunnaike, B.A., Roberts, C.J. (2010). Multi-variate approach to global protein aggregation behavior and kinetics: Effects of pH, NaCl, and temperature for α-chymotrypsinogen A. *J of Pharmaceutical Sciences*. 99(2), 645-662.

Liebeton, K., Zonta, A., Schimossek, K., Nardini, M., Lang, D., Dijkstra, B.W., Reetz, M.T., Jaeger, K.E. (2000) Directed evolution of an enantioselective lipase. Chem. Biol. 7(9), 709-718.

Lilly, M. D., Woodley, J. M. (1985). Biocatalytic reations involving waterinsoluble organic compounds. In: *Biocatalysts in Organic Syntheses.* Amsterdam; Elsevier.

Lindqvist,Y., Schneider,G., Ermler,U., Sundstrom,M. (1992). 3-Dimensional Structure of Transketolase, A Thiamine Diphosphate Dependent Enzyme, at 2.5 Angstrom Resolution. *Embo Journal*, 11(7), 2373-2379.

Littlechild,J.A., Turner,N.J., Hobbs,G.R., Lilly,M.D., Rawas,A., Watson,H. (1995).Crystallization and preliminary-X-ray crystallographic data with *Escherichia-coli* transketolase. *Acta Crystallogr., Sect D: Biol.Crystallogr.*, 51, 1074-1076.

Martinez-Torres, R. J., Aucamp, J. P., George, R., Dalby, P. A., (2007). Structural stability of E-coli transketolase to urea denaturation. *Enzym. Microb. Technol.* 41, 653-662.

Masri,S.W., Ali,M., Gubler,C.J. (1988). Isolation of transketolase from rabbit liver and comparison of some of its kinetic properties with transketolase from other sources. *Comp Biochem.Physiol B*, 90(1), 167-172.

Matsuyama, A., Yamamoto, H., & Kobayashi, Y. (2002). Practical Application of Recombinant Whole-Cell Biocatalysts for the Manufacturing of Pharmaceutical Intermediates Such as Chiral Alcohols. *Org. Proc. Res. Dev* 6 (4),558–561.

Mitra,R.K., Woodley,J.M., Lilly,M.D. (1998). *Escherichia coli* transketolasecatalyzed carbon-carbon bond formation: biotransformation characterization for reactor evaluation and selection. *Enzyme Microb.Technol.*, 22(1), 64-70.

Mocali,A, Paoletti,F. (1989) Transketolase from human leukocytes. Isolation, properties and induction of polyclonal antibodies, *Eur. J. Biochem.* 180, 213–219.

Moore,J., Arnold,F.H. (1996). Directed Evolution of a para-Nitrobenzyl Esterase for Aqueous-Organic Solvents. *Nature Biotechnology*. 14, 458-467.

Moore,J., Arnold,F.H. (1997). Optimizing Industrial Enzymes by Directed Evolution. *Advances in Biochemical Engineering*. 58,1-14.

Morris, K.G., Smith, M.E.B, Turner, N.J., Lilly, M.D., Mitra, R.K., Woodley, J.M. (1996). Transketolase from *Escherichia coli*: a practical procedure for using the biocatalyst for asymmetric carbon–carbon bond synthesis. *Tetrahedron: Asymmetry* 7(8), 2185–2188.

Nakagawa, Y., Hasegawa, A., Hiratake, J., Sakata, K. (2007). Engineering of *Pseudomonas aeruginosa* lipase by directed evolution for enhanced amidase activity: mechanistic implication for amide hydrolysis by serine hydrolases. *Protein Engineering, Design and Selection.* 20 (7), 339-346.

Nestl, B., Nebel, B.A., Hauer, B. (2011). Recent progress in industrial biocatalysis. *Curr. Opin. Chem. Biol* 15(2),187-193.

Nikkola,M., Lindqvist,Y., Schneider,G. (1994). Refined structure of transketolase from *Saccharomyces cerevisiae* at 2.0 A resolution. *J.Mol.Biol.*, 238(3), 387-404.

Nilsson, U., Meshalkina, L., Lindqvist, Y., Schneider, G.(1997). Examination of substrate binding in thiamin diphosphate-dependent transketolase by protein crystallography and site-directed mutagenesis. *J. Biol. Chem.* 272, 1864-1869.

Pace, C.N., Vajdos, F., Fee, L., Grimsley, G., Gray, T. (1995). How to measure and predict the molar absorption coefficient of a protein. *Prot Sci*. 4,2411–2423.

Pasta, P., Riva, S., Carrea, G. (1988) Circular dichroism and fluorescence of polyethylene glycol-subtilisin in organic solvents. *FEBS Letters*. 236(2), 329-332.

Patel,R.N. (2008). Synthesis of chiral pharmaceutical intermediates by biocatalysis. *Coordination Chemistry Reviews*. 252, 659–701

Peterson,M.E., Eisenthal,R., Danson,M.J., Spence,A., Daniel,R.M. (2004). A New Intrinsic Thermal Parameter for Enzymes Reveals True Temperature Optima. *Journal of Biological Chemistry*, 279(20), 20717-20722.

Philippov,P.P., Shestakova,I.K., Tikhomirova,N.K., Kochetov,G.A. (1980). Characterization and properties of pig liver transketolase. *Biochim Biophys Acta*, 613(2), 359-369.

Polastro, E. (1989). Enzymes in the fine-chemicals industry: dreams and realities. *Bio/Technology* 7:1238-1241.

Pollard, D.J., Woodley, J.M. (2006). Biocatalysis for pharmaceutical intermediates: the future is now**.** *Trends in biotechnology* 25(2), 66-73**.**

Prasad, B.V., Suguna, K. (2002). Role of water molecules in the structure and function of aspartic proteinases. *Acta Crystallogr. D: Biol. Crystallogr*. 58,250–259.

Racker,E. (1961) Transketolase. In: Boyer P.D., Lardy H., Myrbõck K. The Enzymes, *Academic Press* (New York, USA).

Richardson, T.H., Tan, X., Frey, G., Callen, W., Cabell, M., Lam, D., Macomber, J., Short, J.M., Robertson, D.E., Miller, C. (2002). A Novel, high performance enzyme for starch liquefaction. Discovery and optimization of a low pH, thermostable á-amylase. *J Biol Chem*. 277, 26501-26507.

Rios-Solis, L., Halim, M., Cázares, A., Ward, J.M., Hailes, H.C., Dalby, P.A., Baganz, F., Lye, G.J. (2011). Biocatalysis and Biotransformation. A microscale toolbox for rapid evaluation of multi-step enzymatic syntheses comprising a mix and match *E. coli* expression system. *In press*

Russell,R.J.M., Ferguson,J.M.C., Hough,D.W., Danson,M. J., Taylor,G.L. (1997). The crystal structure of citrate synthase from the hyperthermophilic Archaeon Pyrococcus furiosus at 1.9 angstrom resolution. Biochemistry. 36(33), 9983-9994.

Saxena, R.K., Gosh, P.K., Gupta, R., Davidson, W.S., Bradoo, S., & Gulati, R. (1999). Microbial lipases: potential biocatalysts for the future industry. *Current Science* 77(1),101-115.

Schaefer, M., Sommer, M., Karplus, M. (1997). pH-Dependence of Protein Stability: Absolute Electrostatic Free Energy Differences between Conformations. *J. Phys. Chem.* 101(9),1663-1683.

Schenk,G., Duggleby,R.G., Nixon,P.F. (1998). Properties and functions of the thiamin diphosphate dependent enzyme transketolase. *Int.J.Biochem.Cell Biol.*, 30(12), 1297-1318.

Schmid, A., Dordick, J.S., Hauer, B., Kien, A. (2001). Industrial biocatalysis today and tomorrow. Nature 2001;409:258-68.

Schoemaker, H.E., Mink, D., Wubbolts, M. (2003). Dispelling the Myths--Biocatalysis in Industrial Synthesis. *Science* 299(5613),1694-1697.

Schorken, U., Sprenger, G. A., (1998). Thiamin-dependent enzymes as catalysts in chemoenzymatic syntheses. *Biochim. Biophys. Acta.* 1385, 229-243.

Shaeri,J., Wohlgemuth,R., Woodley,J.M. (2006). Semiquantitative process screening for the biocatalytic synthesis of D-xylulose-5-phosphate. *Org. Proc. Res. Dev*. 10, 605-610.

Simon, L.M., Kotormán, M., Szabó,A., Nemcsók,J., Laczkó I. (2007). The effects of organic solvent/water mixtures on the structure and catalytic activity of porcine pepsin. *Process Biochemistry*. 42(5),909-912.

Simpson F. (1960) Preparation and properties of transketolase from pork liver, *Can. J. Biochem. Physiol.* 38, 115–124.

Smith,M.E.B., Chen,B.H., Hibbert,E.G., Kaulmann,U., Smithies,K., Galman,J.L., Baganz,F., Dalby,P.A., Hailes,H.C., Lye,G.J., Ward,J.M., Woodley,J.M., Micheletti,M. (2010). A Multidisciplinary Approach Toward the Rapid and Preparative-Scale Biocatalytic Synthesis of Chiral Amino Alcohols: A Concise Transketolase-/omega-Transaminase-Mediated Synthesis of (2S,3S)-2-Aminopentane-1,3-diol. *Org. Proc. Res. Dev*. 14, 99-107.

Smith,M.E.B., Hibbert,E.G., Jones,A.B., Dalby,P.A., Hailes,H.C. (2008). Enhancing and Reversing the Stereoselectivity of Escherichia coli Transketolase via Single-Point Mutations. *Adv. Synth. Catal*. 350, 2631-2638.

Sprenger, G.A. (1991) Cloning and preliminary characterization of the transketolase gene from *Escherichia coli* K12. In: Bisswanger H., Ullrich J. (eds.) Biochemistry and physiology of thiamin diphosphate enzymes, Weinheim, Germany,*VCH*.

Sprenger,G.A., Pohl,M., (1999). Synthetic potential of thiamin diphosphate-dependent enzymes. *J. Mol. Catal. B: Enzym* 6, 145-159.

Sprenger,G.A., Schorken,U., Sprenger,G., Sahm,H. (1995). Transketolase A of *Escherichia coli* K12. Purification and properties of the enzyme from recombinant strains. *Eur.J.Biochem.*, 230(2), 525-532.

Sundstrom,M., Lindqvist,Y., Schneider,G. (1992). 3-Dimensional structure of apotransketolase - flexible loops at the active-site enable cofactor binding. *FEBS Lett.*, 313(3), 229-231.

Takeuchi,T., Nishino,K., Itokawa,Y. (1986). Purification and characterization of, and preparation of an antibody to, transketolase from human red blood cells. *Biochim.Biophys Acta*, 872(1-2), 24-32.

Tittmann, K., Golbik, R., Uhlemann, K., Khailova, L., Schneider, G., Patel, M., Jordan, F., Chipman, D. M., Duggleby, R. G., Hu¨bner, G. (2003) NMR analysis of covalent intermediates in thiamin diphosphate enzymes, *Biochemistry 42*, 7885-7891

Torossian, K., & Bell. (1991). Purification and characterization of acid resistant triacylglycerol lipase from *Aspergillus niger*. *Biotechnology and Applied Biochemistry* (13), 205-211.

Villafranca, J.J.,Axelrod,B. (1971). Heptulose Synthesis from Nonphosphorylated Aldoses and Ketoses by Spinach Transketolase. *J.Biol.Chem.*, 246(10), 3126-3131.

Walsh,C. (2001). Enabling the chemistry of life. *Nature*, 409(6817), 226-231.

Wang, L.j., Kong, X.d., Zhang, H.y., Wang, X.p., Zhang, J. (2000). Enhancement of the Activity of -Aspartase from Escherichia coli W by Directed Evolution. *Biochemical and Biophysical Research Communications*, 276(1), 346-349.

Woodley,J.M., Mitra,R.K., & Lilly,M.D. (1996). Carbon-carbon bond synthesis - reactor design and operation for transketolase catalyzed biotransformations. *Ann.N.Y.Acad.Sci.*, 799, 434-445.

Yoshida,H., Kamitori, S., Agari,Y., Iino, H., Kanagawa, M., Nakagawa,N., Kuramitsu, S., Yokoyama S, Riken. X-ray structure of thermus thermophilus hb8 tt0505. To be published.

Zak,A., Klibanov, A.M. (1985). Enzyme-catalyzed in organic solvents. *Proc. Natl Ac. Sci. USA*. 82, 3192-3196.

Zaks, A. (2001). Industrial biocatalysis. *Curr Opin Chem Biol* 5(2)130-136.

Appendix 3 HPLC profile for HPA and Erythrulose